PACIFIC EARTHQUAKE ENGINEERING RESEARCH CENTER

Seismic Qualification and Fragility Testing of Line Break 550-kV Disconnect Switches

Shakhzod M. Takhirov
University of California, Berkeley

Gregory L. Fenves
Univerity of California, Berkeley

and

Eric Fujisaki
Pacific Gas & Electric Co.

Sponsor:
California Energy Commission

PEER 2004/08
FEB. 2005

Seismic Qualification and Fragility Testing of Line Break 550-kV Disconnect Switches

Shakhzod M. Takhirov
University of California, Berkeley

Gregory L. Fenves
Department of Civil and Environmental Engineering
University of California, Berkeley

Eric Fujisaki
Pacific Gas and Electric Company
Oakland, California

Sponsor:
California Energy Commission

PEER Report 2004/08
Pacific Earthquake Engineering Research Center
College of Engineering
University of California, Berkeley

February 2005

ABSTRACT

The objective of the study was to conduct seismic qualification and fragility testing of a single pole of a 550-kV porcelain disconnect switch. Due to clearance limitations above the shake table, the switch with the main blade in the open position could not be tested in a typical field installation; therefore, several switch configurations were developed for testing. The 550-kV disconnect switch was tested in three configurations: mounted on typical 14-ft-tall supports, mounted on a short 4-in. spacer to simulate flexibility of the top plates of the supports, and rigidly fixed to the earthquake simulation platform. In the latter two configurations the switch was tested with the main blade in the open and closed positions, and these configurations were used for seismic qualification testing of the open-blade switch and in the experimental study for the estimation of the amplification factor.

Triaxial tests of a single pole of the porcelain disconnect switch mounted on elevated supports were conducted by means of an IEEE-compatible time history to determine the dynamic properties and to qualify the switch at the high performance level. The feasibility of seismic qualification testing of tall electrical equipment with supports removed by introducing an amplification factor due to the supports was also studied experimentally. Triaxial time history tests of a single pole of a porcelain disconnect switch mounted without the tall supports on the simulator platform were conducted to determine the dynamic properties of the pole and to evaluate its seismic response. A seismic qualification test for the switch in the open-blade position on the earthquake simulator platform (mounted without the tall supports) was performed by using the amplification factor.

The main objectives of the study included static and dynamic testing of switch components (the tall supporting legs and the insulator posts) and determining the feasibility of replacing the blade with an equivalent shorter blade or a concentrated mass for seismic qualification testing of tall electrical equipment that cannot clear the table. The component testing also included static cantilever tests on the ceramic insulator posts to determine equivalent cantilever loads in failure.

ACKNOWLEDGMENTS

This project was sponsored by the Pacific Earthquake Engineering Research Center's Program of Applied Earthquake Engineering Research of Lifeline Systems supported by the California Energy Commission, California Department of Transportation, and the Pacific Gas & Electric Company. This financial support is gratefully acknowledged.

This work made use of the Earthquake Engineering Research Centers Shared Facilities supported by the National Science Foundation under award number EEC-9701568 through the Pacific Earthquake Engineering Research (PEER) Center. Any opinions, findings, and conclusion or recommendations expressed in this material are those of the author(s) and do not necessarily reflect those of the National Science Foundation.

This report was prepared as a result of work sponsored by the California Energy Commission ("the Commission"). It does not necessarily represent the views of the Commission, its employees, or the State of California. The Commission, the State of California, its employees, contractors, and subcontractors make no warranty, express or implied, and assume no legal liability for the information in this report; nor does any party represent that the use of this information will not infringe upon privately owned rights. This report has not been approved or disapproved by the Commission nor has the Commission passed upon the accuracy or adequacy of the information in this report.

The authors would like to acknowledge Southern States, Inc., (Hampton, Georgia) for donating the 550-kV switch. The authors wish to thank the following individuals of the company for their extremely valuable technical contributions to the project: Mr. Cary Ahrano and the Southern States staff for rapid assembly and disassembly of the switch on the shake table and for providing constant technical support at all stages of the experimental study. Special thanks are due to NGK-Locke, Inc. (Baltimore, Maryland) for donating a number of insulator posts to be used in the final fragility tests and for valuable technical support and discussion of fragility tests results. The authors would also like to thank Valmont Industries, Inc., (Omaha, Nebraska) for donating the steel supports. Mr. Don Clyde, of EERC, University of California, Berkeley, made significant contributions to the experimental program. Thanks are also due to Mr. Wesley Neighbour of and Mr. David MacLam of EERC for their help in the shaking table testing, and to Ms. Janine Hannel of PEER for editing this report. The authors would also like to acknowledge

Mr. Craig Riker of SDG&E, Mr. Philip Mo of Southern California Edison, Dr. Anshel Schiff, and members of the Utility Consortium for active participation in the test plan development, discussion of the test results, and for observing the testing procedure.

CONTENTS

LIST OF FIGURES

LIST OF TABLES

1 Introduction

1.1 OVERVIEW

Disconnect switches are key components of power transmission and distribution (T&D) systems. These switches are used to control the flow of electricity between substation equipment and to isolate substation equipment for maintenance. Figure 1.1 shows an elevated three-phase (pole) vertical-break disconnect switch. At each terminal, the switch is connected to stiff aluminum bus tubes that are attached to bus supports consisting of insulators and steel tube structures. The aluminum bus tubes and their supports can also be seen in the figure.

Typically, disconnect switches consist of three poles (or phases), each consisting of two or three insulator posts. The insulators are either porcelain or composite polymers. Cast or extruded aluminum is used for most of the live (current-carrying) parts. Base and operation-mechanism hardware is generally manufactured from structural or alloy steel or ductile iron. Disconnect switches are typically mounted on support structures to provide sufficient clearance of the ground, and to integrate them into the design of the substation.

For the single-pole switch tested as part of this study, the pole consists of three insulator posts that are mounted on the switch base, which is in turn attached to 14-ft-tall tapered steel supports. The pole's main blade mounted on top of the posts provides control of the electrical connection. In addition to the main blade, each pole of a grounding switch is grounded by a grounding blade during maintenance procedures. A crank and interpole linkages operate the main and grounding blades and synchronize the operation of the three poles. Typically, the mechanical operation of the switch is achieved by means of a motor mechanism that provides remote-control-powered operation of disconnect switches in large switchyards. Gang-operated, manually controlled switches are also used by some utilities. The main blade of the pole tested as part of this study opens in-plane of the pole, so the switch is termed a "vertical-break line switch."

There are limitations on the size of a test specimen intended for seismic qualification testing on an earthquake simulator. In order to accommodate these limitations, only one pole of the switch is used for the experimental study and is referenced further in the discussion simply as "the switch."

Fig. 1.1 Typical field installation of 500-kV disconnect switch consisting of three poles

Recent major earthquakes in the United States (Northridge, California, 1994) and other parts of the world (Taiwan 1999) have demonstrated that the reliability of a power transmission and distribution system in a seismically active region is dependent upon the seismic response of its individual components. Porcelain disconnect switches have frequently suffered two types of failures in past earthquakes: structural damage (fracture of brittle components) and loss of functionality (blades not operating correctly), although numerous other types of failures have also been observed. Additional information on the seismic performance of disconnect switches may be found in Schiff, 1999. Since disconnect switches form an important part of power T&D

systems, their structural and electrical integrity are critical to maintaining operation of the electrical power grid after a major earthquake.

To mitigate the vulnerability of new disconnect switches and other electrical substation equipment in the United States, the Institute for Electrical and Electronics Engineers (IEEE) developed guidelines for seismic testing and qualification of substation equipment, including disconnect switches. These guidelines are described in *IEEE Recommended Practices for Seismic Design of Substations, IEEE 693-1997*. The key IEEE 693-1997 requirements for seismic qualification tests and new recommendations developed in a companion study (Takhirov, et al., 2004) are summarized in Appendix A.

1.2 REVIEW OF PREVIOUS RESEARCH

The literature contains limited information on the seismic performance of disconnect switches and their response to strong motion time histories compatible with the IEEE spectra, including tests on switches mounted on full-size supports replicating field installations. This section summarizes the available literature relating to dynamic testing of disconnect switches.

Seismic qualification testing of 500-kV switch at Wyle. Seismic qualification testing conducted in 1984 on a 500-kV vertical break disconnect switch is discussed in a report from Wyle Laboratories (Wyle Laboratories, 1993). The switch was subjected only to resonance-search and sine beat testing using the Wyle biaxial seismic simulator and with a relatively stiff supporting system. The specimen was subjected to input motions along its longitudinal axis, and for subsequent tests the specimen was rotated 90 degrees in the horizontal plane. The sine-beat tests consisted of 10 simultaneous horizontal and vertical oscillations per beat with a time pause of approximately 2 sec between each of five beats.

The switch had the lowest resonant frequency in the transverse direction with the switch in the open position, estimated as 1.25 Hz, with a damping ratio of about 6%. The second resonant frequency in the transverse direction was 3.2 Hz (3.4 Hz in the parallel direction) with the blade open and a damping ratio of about 3% (4% damping in the parallel direction). The lowest frequency in the parallel direction was 1.4 Hz (blade) with damping ratios around 7% (blade-open configuration). The fundamental frequencies in the closed-blade configuration were around 3.0 Hz for both the transverse and parallel directions, with damping ratios around 4%.

Seismic qualification testing of 230-kV switch at Wyle. The experimental study of the qualification of a 230-kV switch is presented in another report by Wyle Laboratories (Thornberry and Hardy 1997). The scope was limited to switch testing and qualification. No fragility data were collected and no conclusions were drawn regarding the seismic performance of the switch. The elevated switch was attached to the biaxial simulator using bolted connections. The specimen was tested initially along its longitudinal and vertical axes. It was then rotated 90 degrees and tested along its lateral and vertical axes. Resonant-search, sine-beat, and bidirectional seismic simulation tests were conducted to characterize the dynamic properties of the switch. Spectrum-compatible random motions rather than earthquake histories were used for the earthquake simulation tests. The switch had a fundamental frequency of between 5–6 Hz and a damping ratio of between 2–4 % of critical.

Seismic testing of 230-kV switches by PEER. A comprehensive experimental study of 230-kV disconnect switches was conducted by the Pacific Earthquake Engineering Research (PEER) Center at the University of California, Berkeley, Richmond Field Station (Gilani, et al. 2000). The study focused on seismic qualification testing of the 230-kV switches subjected to the IEEE-compatible strong motion time histories. The poles were tested in two configurations: mounted directly on the earthquake simulator, and on a low-profile braced stiff frame. Sine-sweep and white-noise tests were used to calculate the modal frequencies and damping ratios for the poles in both configurations.

The earthquake histories used for the qualification and fragility testing of the 230-kV bushings were developed using a three-component set of near-field earthquake motions recorded during the 1978 Tabas, Iran, earthquake. Two independent sets of three-component earthquake histories (Tabas-1 and Tabas-2) were generated to envelop the entire IEEE spectrum over two frequency bands. Since it is impractical to qualify the switches on all possible mounting frames, a low-profile braced frame was used for testing. The process of qualification therefore involved the use of two sets of earthquake histories and two blade positions (open and closed).

Five disconnect switches were evaluated by analysis and experimentation in this study. One type was the ABB Type DR9 porcelain horizontal-break 230-kV switch. The insulator posts were bolted to ductile iron rotor-bearing housings bolted to a double-channel beam. The second type was ABB Type TTR-8 vertical-break 230-kV switch with variations in design details and insulator material: porcelain insulators mounted on aluminum spacers, the cast aluminum spacers replaced by welded steel spacers, and composite polymer insulators with a single hollow core with both aluminum and steel spacers.

The vertical-break switches mounted on the welded steel spacers survived tests with earthquake histories whose spectral ordinates equaled or exceeded the IEEE 693-1997 spectrum for high seismic performance level (PL) qualification (peak acceleration equal to 1.0g). Because the test frame was of similar stiffness to the low-profile braced frame proposed for new construction at PG&E, it was concluded that the switches be considered qualified to the high level for use on the PG&E braced frame.

1.3 OBJECTIVES OF STUDY

The study described in this report was motivated by the lack of information on triaxial seismic qualification and fragility testing of 500-kV disconnect switches. The objectives of the study are:

(1) to conduct resonant-search and triaxial time history tests of a single pole of a porcelain disconnect switch mounted on elevated supports to determine the dynamic properties, to qualify the switch to the high PL if possible, or to determine the failure modes;

(2) to study the feasibility of seismic qualification testing of tall electrical equipment with supports removed by use of an amplification factor, and experimentally and theoretically investigate a technique to estimate the amplification factor;

(3) to conduct resonant-search and triaxial time history tests of a single pole of a porcelain disconnect switch mounted directly on the simulator platform to determine the dynamic properties of the pole and to evaluate its seismic response; to conduct a seismic qualification test for the switch in the open-blade position on the earthquake simulator platform by using the amplification factor;

(4) to conduct comprehensive testing and calibration of switch components, including supporting legs and insulator posts;

(5) to conduct a detailed study of seismic qualification testing for the switch with the main contact open, and the feasibility of replacing the blade with an equivalent shorter blade or concentrated mass; and

(6) to conduct in case the switch passes the high PL test, a cantilever test on the insulator posts to determine the failure modes and failure-equivalent cantilever loads for the ceramic insulators.

1.4 REPORT ORGANIZATION

This report is organized as follows. Chapter 2 provides information on the seismic qualification testing procedure used during the study, including test setup and instrumentation, switch configurations tested, experimentation program, and input strong motion time histories that accommodate the capacity of the earthquake simulator (shake table) at the University of California, Berkeley. The report focuses on the response and performance of the switch to strong earthquake motions. Qualification activities include activities required by IEEE 693-1997, which is the version of the standard currently in force, as well as practices recommended for use in Takhirov, et al., 2004, which deals with the development of input motions for testing. It should be noted that the practices recommended in the latter reference do not, at present, constitute a part of the IEEE 693 standard. Qualification of the switch is discussed in greater detail in a separate report to be developed by the switch manufacturer.

Chapter 3 discusses the results of an experimental study conducted on the components of the switch before and after the seismic qualification tests. The typical 14-ft-tall supports are tested with and without leveling rods. Based on experimental data, an elastic stiffness of the support from a static pull-back test, and a natural frequency and a damping from a free-vibration test are estimated. A similar procedure is followed for the insulator posts. The stiffness before and after the qualifications tests and the natural frequency and damping after the tests are computed based on porcelain post and section testing. The component-testing program is concluded by static cantilever tests of all insulator posts used in the switch assembly during the qualification tests.

Chapter 4 discusses the test results for the “original switch,” a switch with an unreinforced base. The tests are conducted only at low level up to 0.25g PGA. Since the equivalent cantilever loads in the insulator posts at 0.25g PGA appeared to be greater than the allowable loads, the base of the switch is reinforced in order to proceed to more severe dynamic testing and to seismically qualify the switch at the higher level. Most of the experimental study is conducted for the “modified switch,” the switch with a reinforced base. The test results are discussed in the next chapters.

Chapter 5 follows the requirements of IEEE 693 (IEEE, 1998) on qualification testing of electrical equipment by means of an earthquake simulator and presents results of seismic qualification of the modified switch mounted on supports. Seismic qualification testing of the disconnect switch mounted on the supporting structure is conducted with the main blade in the closed position due to clearance limitations above the simulator platform.

Chapter 6 presents results and discussions related to estimation of the amplification factor due to the supporting structure, and to seismic qualification testing of the disconnect switch in the open position. To qualify the disconnect switch in the open-blade position, the switch is tested without the supports by introducing an amplification factor to represent an elevated mounting. The qualification testing of the switch in the open-blade position is conducted with the switch mounted on short spacers and subjected to a time history scaled by the amplification factor.

Chapter 7 presents results and discussions related to a feasibility study of replacing the blade with an equivalent mass or a shortened blade. The switch with an equivalent mass is tested in the support-mounted configuration, and the spacer-mounted configuration is used for a switch with a shortened blade. The tests are conducted on the modified switch with the grounding blade in both the closed and open positions.

Chapter 8 includes a summary of the key findings and conclusions drawn from the research project.

The IEEE 693-1997 recommended practice for earthquake testing of disconnect switches and new recommendations developed in a companion study (Takhirov, et al., 2004) are summarized in Appendix A. Appendix B presents a complete list of all test steps undertaken. Resonance-search results for two configurations of the switch used for the qualification study are presented in Appendix C. Raw data and video images from all earthquake tests have been supplied to Pacific Gas & Electric, Southern California Edison, San Diego Gas & Electric, and Southern States Inc. (manufacturer of the switch) under separate cover.

2 Testing Procedure for Seismic Qualification

This chapter presents information on the seismic qualification testing procedure used during the study, including test setup and instrumentation, switch configurations tested, experimental program, and input strong motion time histories.

2.1 SWITCH CONFIGURATIONS AND EXPERIMENTAL SETUP

The 550-kV disconnect switch was tested in three configurations: mounted on typical 14-ft-tall supports, mounted on short 4-in. spacers to simulate flexibility of the top plates of the supports, and rigidly attached to the earthquake simulator platform. The switch was tested dynamically on the earthquake simulator platform (shake table) by means of random, sweep, and IEEE-compatible time histories. Some component testing was conducted before and after the major dynamic testing.

2.1.1 Major Components of Single-Pole Switch and Experimental Setup

The experimental study used a single-pole “EV-1” switch with electrical ratings: 550-kV and 4000A. The switch was manufactured, supplied, and assembled on the earthquake simulator platform by Southern States, Inc.

The pole was assembled from several major components as shown in Figure 2.1 that presents a typical field installation: the switch, typically installed on tall supports, comprises an assembly consisting of a base, insulator posts, and a main blade. The insulator posts were assembled on the base of the switch and named “rigid,” “rotating,” and “jaw,” respectively. The porcelain insulators used in the study were manufactured and supplied by NGK-Locke, Inc., and were rated at 2900 lbs cantilever strength. Each insulator post consists of three sections: bottom, middle, and top with decreasing cross section from bottom to top. The switch is installed in an elevated position on a support structure that consists of two steel tapered legs. The support columns, manufactured and supplied by Valmont Industries, Inc., have tubular sections. The leveling of the whole structure in a field installation is typically achieved by the use of leveling nuts on threaded rods embedded in the foundation under the pole. The configuration of the anchor bolts at the column bases is intended to represent the case in which base plates are left ungrouted, which is a frequent utility practice.

In addition to the main blade, the switch tested has a grounding blade located at the jaw post. The grounding switch and the main blade are operated by the motor mechanism mounted on the support under the rigid post, as shown in Figure 2.2.

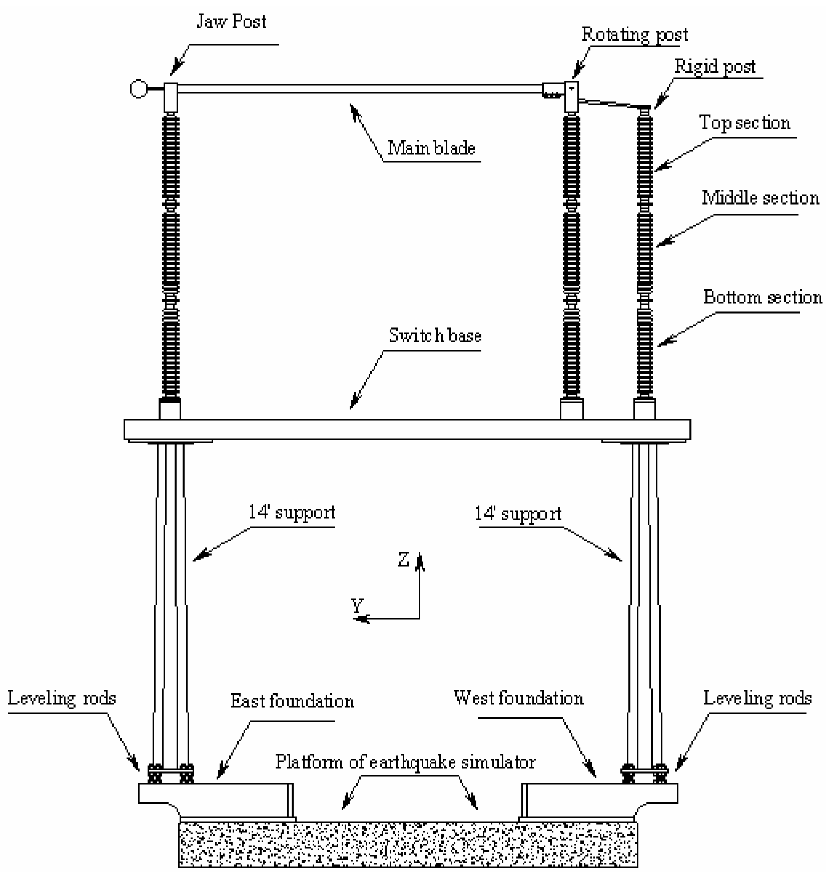

Fig. 2.1 Major components of single-pole switch assembled on earthquake simulator platform

2.1.2 Switch Configurations Tested in the Study

The switch was tested in three configurations, configuration 1, configuration 2, and configuration 3. The footprints of the switch base and support legs exceeded the size of the earthquake

Fig. 2.2 Configuration 1: support-mounted configuration of switch (main blade closed)

simulator platform; therefore two relatively rigid foundations were designed and built to extend the size of the shake table and attach the switch to it. Configuration 1 represents a typical field mounting as shown in Figure 2.2: the switch is mounted on 14-ft-tall supports attached to the foundations by means of the leveling threaded rods. The details of the attachment to the foundation are shown in Figure 2.3. In the case of configuration 2, the switch is mounted on short 4-in. spacers designed to simulate the flexibility of the top plates in the 14-ft-tall supports. The switch is tested with the main blade open and closed in configuration 2 as presented in (Figs. 2.4–2.5). The details of the attachment to the foundations are presented in Figure 2.6. The switch attached directly to the foundations represents configuration 3.

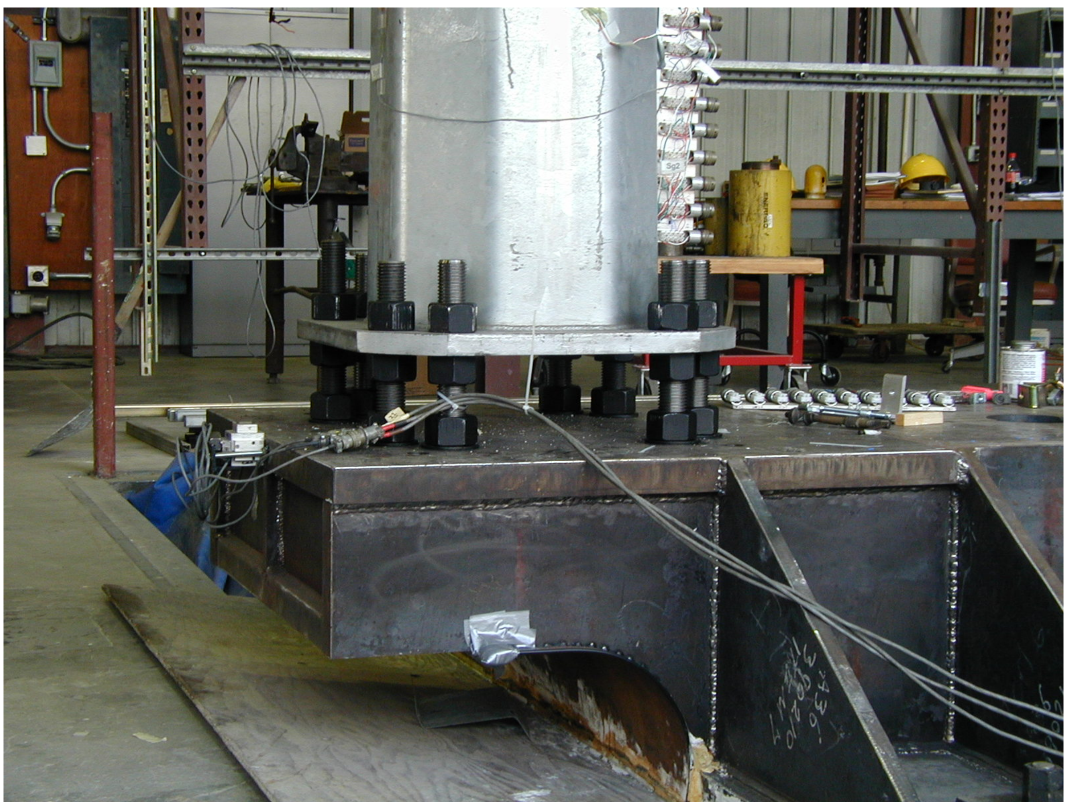

Fig. 2.3 Details of attachment to the rigid foundation for configuration 1

2.1.3 Instrumentation

The 550-kV disconnect switch was extensively instrumented by strain gages, accelerometers, and displacement transducers installed at the most critical locations. A list of the instrumentation used is presented in Table 2.1.

Table 2.1 Instrumentation list

No.	Quantity	Device No.	Location/ID	Blade Closed	Blade Open
Displacements of table					
1	Displacement		Horizontal in N-S direction (SE Actuator)	X	X
2	Displacement		Horizontal in E-W direction (NE Actuator)	Y	Y
3	Displacement		Horizontal in N-S direction (NW Actuator)	X	X
4	Displacement		Horizontal in E-W direction (SW Actuator)	Y	Y
5	Displacement		Vertical Displacement (SE Actuator)	Z	Z
6	Displacement		Vertical Displacement (NE Actuator)	Z	Z
7	Displacement		Vertical Displacement (NW Actuator)	Z	Z
8	Displacement		Vertical Displacement (SW Actuator)	Z	Z
Accelerations of table					
9	Acceleration		Horizontal in N-S direction (SE Actuator)	X	X
10	Acceleration		Horizontal in E-W direction (NE Actuator)	Y	Y
11	Acceleration		Horizontal in N-S direction (NW Actuator)	X	X
12	Acceleration		Horizontal in E-W direction (SW Actuator)	Y	Y
13	Acceleration		Vertical Acceleration (SE Actuator)	Z	Z
14	Acceleration		Vertical Acceleration (NE Actuator)	Z	Z
15	Acceleration		Vertical Acceleration (NW Actuator)	Z	Z
16	Acceleration		Vertical Acceleration (SW Actuator)	Z	Z
Accelerations at top of rigid foundation					
17	Acceleration	Acc1	West foundation	X	X
18	Acceleration	Acc2	West foundation	-Y	-Y
19	Acceleration	Acc3	West foundation	Z	Z
20	Acceleration	Acc4	East foundation	X	X
21	Acceleration	Acc5	East foundation	-Y	-Y
22	Acceleration	Acc6	East foundation	Z	Z
Displacements at top of 14-ft-tall support					
23	Displacement	Wp1	West support	X	X
24	Displacement	Wp2	West support	Y	Y
25	Displacement	Wp3	East support	X	X
26	Displacement	DCDT1	East to West support	Y	Y
Flexural displacement of rigid foundation					
27	Displacement	DCDT2	West foundation	Z @ X-	Z @ X-
28	Displacement	DCDT3	West foundation	Z @ X+	Z @ X+

Table 2.1 ***(continued)***

No.	Quantity	Device. No.	Location/ID	Blade Closed	Blade Open
Switch base accelerations (at top of 14-ft-tall support)					
29	Acceleration	Acc7	West support	X	X
30	Acceleration	Acc8	West support	-Y	-Y
31	Acceleration	Acc9	West support	Z	Z
32	Acceleration	Acc10	East support	X	X
33	Acceleration	Acc11	East support	-Y	-Y
34	Acceleration	Acc12	East support	Z	Z
35	Acceleration	Acc13	Pipe under rotating post	X	X
36	Acceleration	Acc14	Pipe under rotating post	-Y	-Y
37	Acceleration	Acc15	Pipe under rotating post	Z	Z
Displacements at top of rigid foundation					
38	Displacement	Wp4	East foundation	X	X
39	Displacement	Wp5	West foundation	X	X
40	Displacement	Wp6	West foundation	Y	Y
Displacements at base of rotating post					
41	Displacement	Wp7	Pipe under rotating post	X	X
42	Displacement	Wp8	Pipe under rotating post	X	X
43	Displacement	DCDT4	Pipe under rotating post	Z @ X+	Z @ X+
44	Displacement	DCDT5	Pipe under rotating post	Z @ X-	Z @ X-
Accelerations at top of insulator posts					
45	Acceleration	Acc16	Rigid post	X	X
46	Acceleration	Acc17	Rigid post	-Y	-Y
47	Acceleration	Acc18	Rigid post	Z	Z
48	Acceleration	Acc19	Rotating post	X	X
49	Acceleration	Acc20	Rotating post	-Y	-Y
50	Acceleration	Acc21	Rotating post	Z	Z
51	Acceleration	Acc22	Jaw post	X	X
52	Acceleration	Acc23	Jaw post	-Y	-Y
53	Acceleration	Acc24	Jaw post	Z	Z
Displacements at top of insulator posts					
54	Displacement	Wp9	Rigid post	X	X
55	Displacement	Wp10	Rigid post	Y	Y
56	Displacement	Wp11	Rotating post	X	X
57			empty channel		
58	Displacement	Wp12	Jaw post	X	X
59	Displacement	Wp13	From jaw post to rotating post	Y	Y
Tip of blade accelerations					
60	Acceleration	Acc25	Tip of blade	X	-Y
61	Acceleration	Acc26	Tip of blade	-Y	Z
62	Acceleration	Acc27	Tip of blade	Z	X
63-64			empty channels		

Table 2.1 ***(continued)***

No.	Quantity	Device. No.	Location/ID	Blade Closed	Blade Open
Strains in support legs (@20" from base plate)					
65	Strain	R11	East support	X @Y-	
66	Strain	R12	East support	@45toZ@Y-	
67	Strain	R13	East support	Z @Y-	
68	Strain	R21	East support	Y @X-	
69	Strain	R22	East support	@45toZ @X-	
70	Strain	R23	East support	Z @X-	
71	Strain	Sg3	East support	Z @Y+	
72	Strain	Sg4	East support	Z @X+	
73	Strain	Sg5	West Support	Z @Y+	
74	Strain	R61	West Support	Y @X+	
75	Strain	R62	West Support	@45toZ@X+	
76	Strain	R63	West Support	Z @X+	
77	Strain	R71	West Support	X @Y-	
78	Strain	R72	West Support	@45toZ @Y-	
79	Strain	R73	West Support	Z @Y-	
80	Strain	Sg8	West Support	Z @X-	
Porcelain strains (base of bottom porcelain section)					
81	Strain	Sg9	Rigid post	Z @X-	Z @X-
82	Strain	Sg10	Rigid post	Z @Y-	Z @Y-
83	Strain	Sg11	Rigid post	Z @X+	Z @X+
84	Strain	Sg12	Rigid post	Z @Y+	Z @Y+
85	Strain	Sg13	Rotating post	Z @X-	
86	Strain	Sg14	Rotating post	Z @Y-	
87	Strain	Sg15	Rotating post	Z @ X+	
88	Strain	Sg16	Rotating post	Z @Y+	
89	Strain	Sg17	Jaw post	Z @X-	Z @X-
90	Strain	Sg18	Jaw post	Z @Y-	Z @Y-
91	Strain	Sg19	Jaw post	Z @X+	Z @X+
92	Strain	Sg20	Jaw post	Z @Y+	Z @Y+
Porcelain strains (base of middle porcelain section)					
93	Strain	Sg21	Jaw post	Z @X-	Z @X-
94	Strain	Sg22	Jaw post	Z @Y-	Z @Y-
95	Strain	Sg23	Jaw post	Z @X+	Z @X+
96	Strain	Sg24	Jaw post	Z @Y+	Z @Y+
97	Strain	Sg25	Rigid post	Z @X-	Z @X-
98	Strain	Sg26	Rigid post	Z @Y+	Z @Y+
99	Strain	Sg27	Rigid post	Z @X+	Z @X+
100	Strain	Sg28	Rigid post	Z @Y-	Z @Y-
Porcelain strains (base of top porcelain section)					
101	Strain	Sg29	Rigid post	Z @X-	Z @X-
102	Strain	Sg30	Rigid post	Z @Y+	Z @Y+
103	Strain	Sg31	Rigid post	Z @X+	Z @X+
104	Strain	Sg32	Rigid post	Z @Y-	Z @Y-

Table 2.1 ***(continued)***

No.	Quantity	Device No.	Location/ID	Blade Closed	Blade Open
Porcelain strains (top of top porcelain unit)					
105	Strain	Sg33	Rigid post	Z @X+	Z @X+
106	Strain	Sg34	Rigid post	Z @Y-	Z @Y-
Strain at bottom of blade (4.5" from root)					
107	Strain	Sg35	Top of blade pipe	Y @Z+	Z @X-
108	Strain	Sg36	North side of blade pipe	Y @X-	Z @X+
109	Strain	Sg37	Bottom of blade pipe	Y @Z-	Z @Y+
110	Strain	Sg38	South side of blade pipe	Y @X+	Z @Y+
Electrical connectivity test (closed switch)					
111	Current	Voltmeter			
Load cell for static pull-back tests					
112	Load	Load cell			

Fig. 2.4 Configuration 2: spacer-mounted configuration of switch (main blade closed)

Fig. 2.5 Configuration 2: spacer-mounted configuration of switch (main blade open)

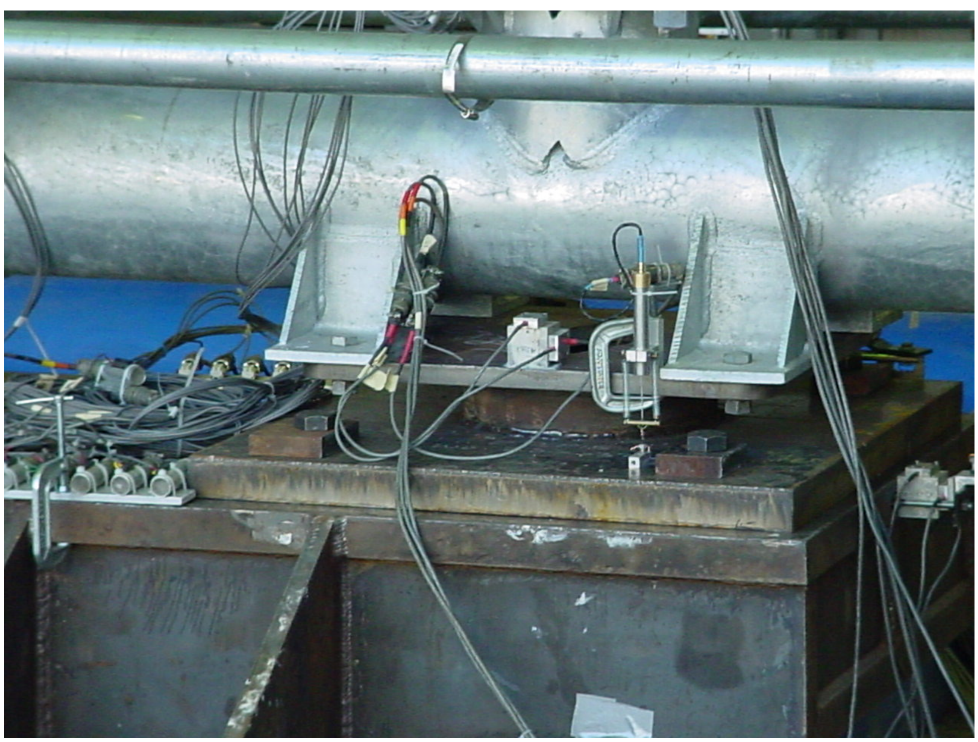

Fig. 2.6 Details of attachment to the foundation for configuration 2

Strain gages. Strain gages were installed on the most critical parts of the switch. The insulator posts were instrumented by unidirectional strain gages to measure a bending strain at several levels along the height of the insulator posts. For redundancy, the strain gages were installed 90 degrees apart along the section's circumference at each level. The details of the strain gages location on the porcelain insulator posts are presented in Figure 2.7.

The second major component instrumented by the strain gages was a support structure. The gages were installed and placed in 90-degree increments around the circumference of the support section. The strain gages consisted of unidirectional strain gages and rosettes to be used for computing the equivalent cantilever loads, bending moments, and principal strains in the legs. The blade of the switch was instrumented by the unidirectional strain gages only. Four strain gages were installed near the root of the blade in 90-degree increments around the blade's circumference. The strain gages were used to estimate the cantilever loads and bending moments during the tests. The locations of the strain gages with the dimensions are presented in Figure 2.8, and a typical strain gage installation on the porcelain insulator is shown in Figure 2.9. A strain gage installation located close to the root of the blade is presented in Figure 2.10.

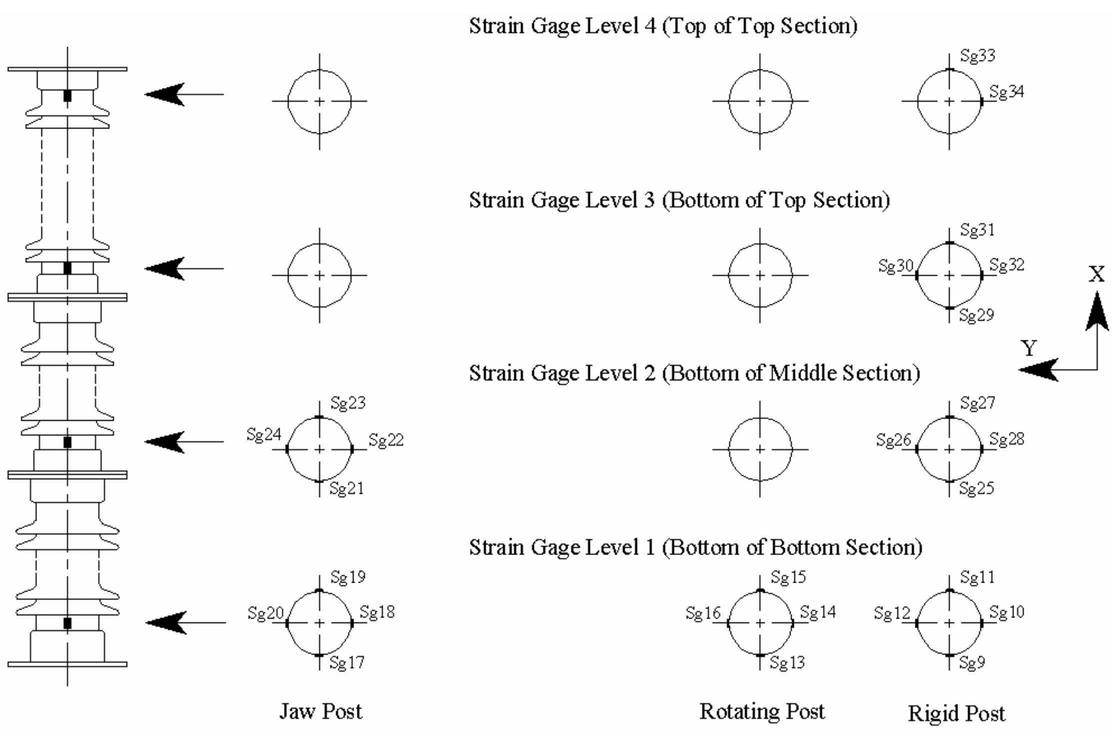

Fig. 2.7 Strain gage locations on insulator posts

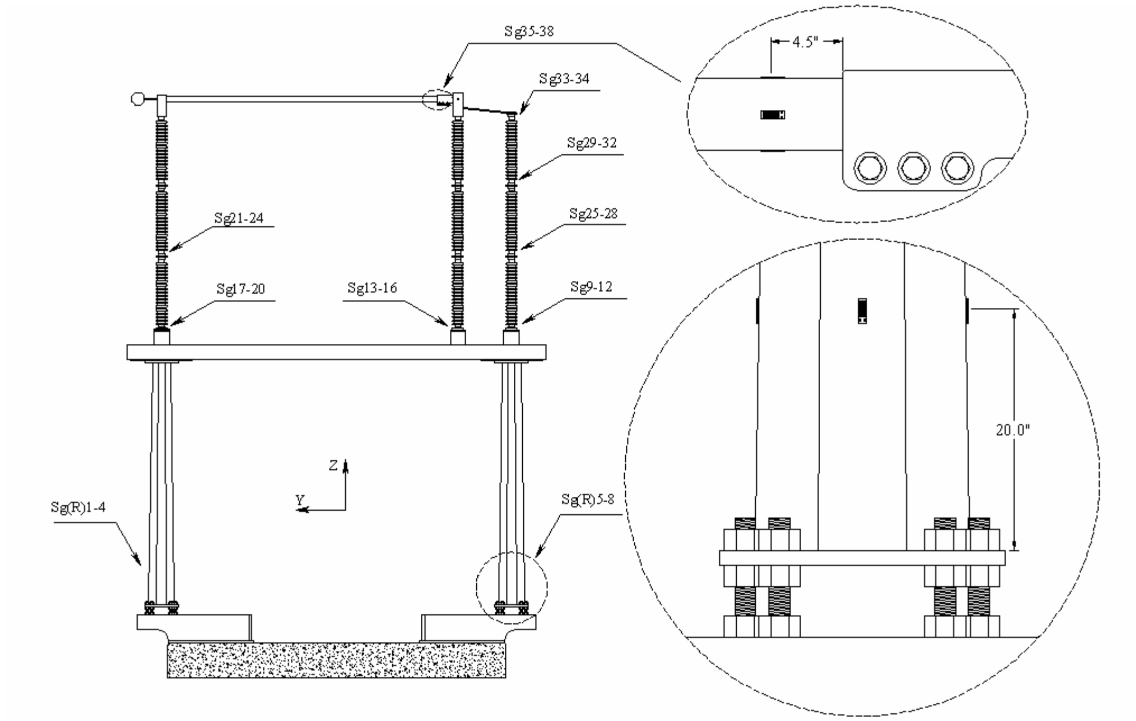

Fig. 2.8 Strain gage locations on steel supports and switch blade

Accelerometers. The switch was instrumented by accelerometers to record three-component acceleration data at the tops of the foundation, the support legs, insulator posts, and at the tip of the blade. The accelerometer locations for the switch in two configurations (with and without supports) are shown in Figure 2.11. A photo of a typical installation of accelerometers (Fig. 2.12) shows the accelerometers on the top of the rigid post.

Displacement transducers. Displacement transducers were used to measure the horizontal displacements at the major locations. Most of the transducers measure a horizontal displacement of the switch parts relative to two stiff instrumentation frames located near the earthquake simulator platform. In addition, two sets of the displacement transducers were used to measure a vertical displacement of the switch components. One set was installed to measure the rotation of the pipe at the base of the switch and the vertical displacement of the pipe relative to the platform. A second set confirmed that the vertical displacements of the cantilevered part of the stiff foundation were negligible. The displacement transducer locations are presented in Figure 2.13, which shows the support-mounted configuration of the switch. Also shown are the horizontal displacements measured at three levels. For the configuration with no supports, the displacements were recorded at two levels (Fig. 2.14). The displacement at the tip of the blade was estimated from the acceleration data.

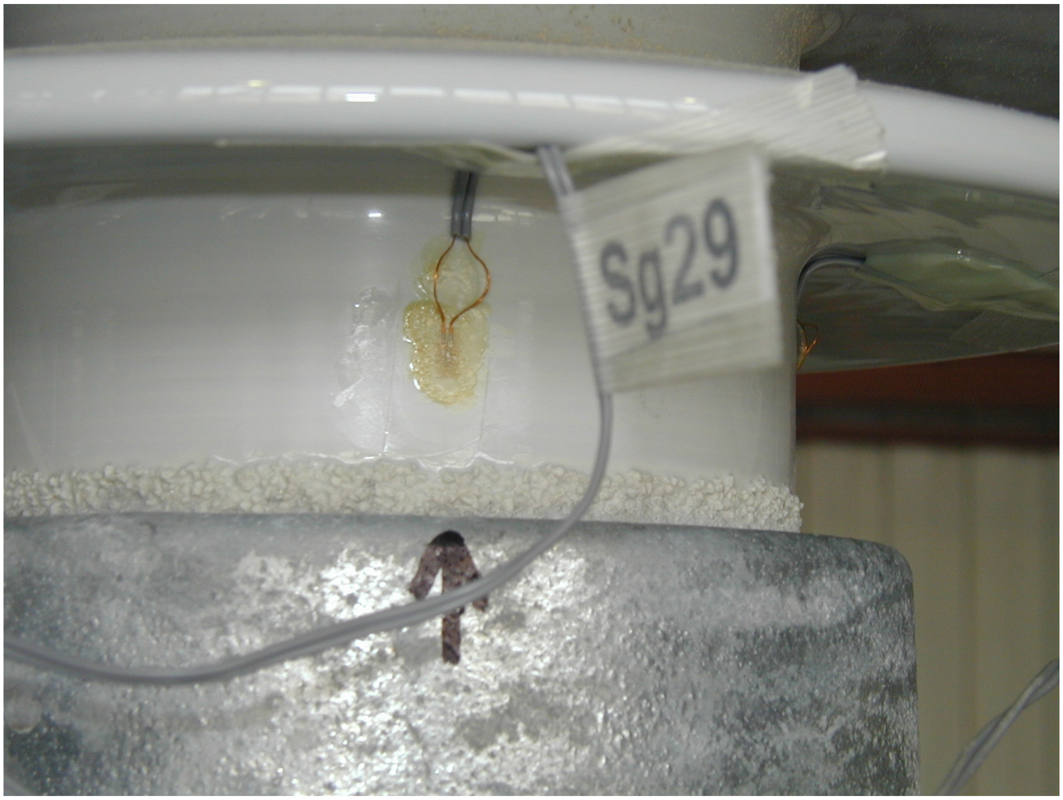

Fig. 2.9 Sample of typical strain gage installation on insulator post

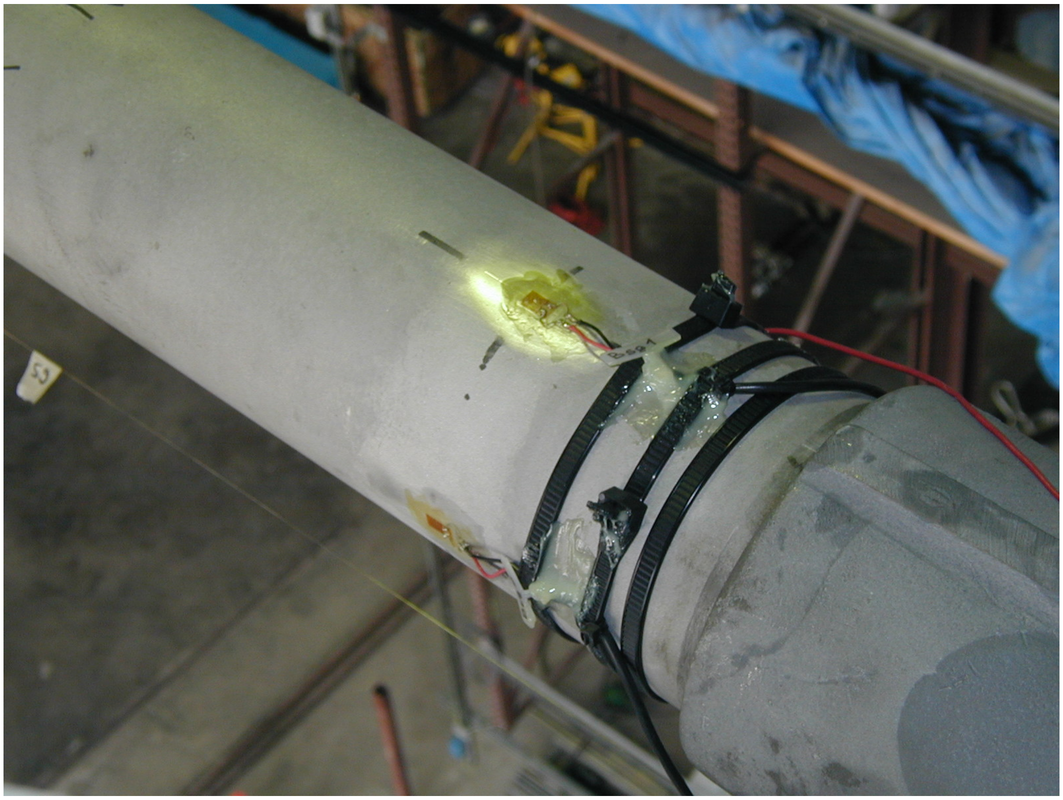

Fig. 2.10 Strain gage location on switch blade

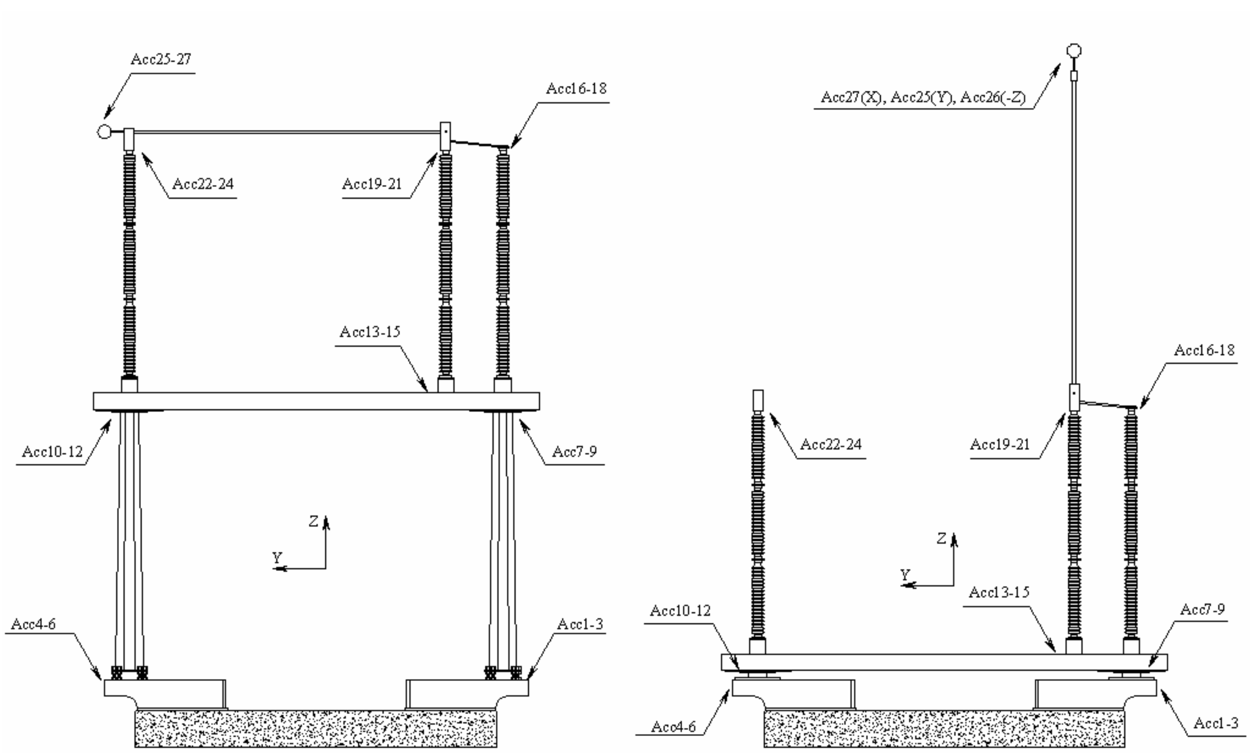

Fig. 2.11 Accelerometer locations for switch in two configurations

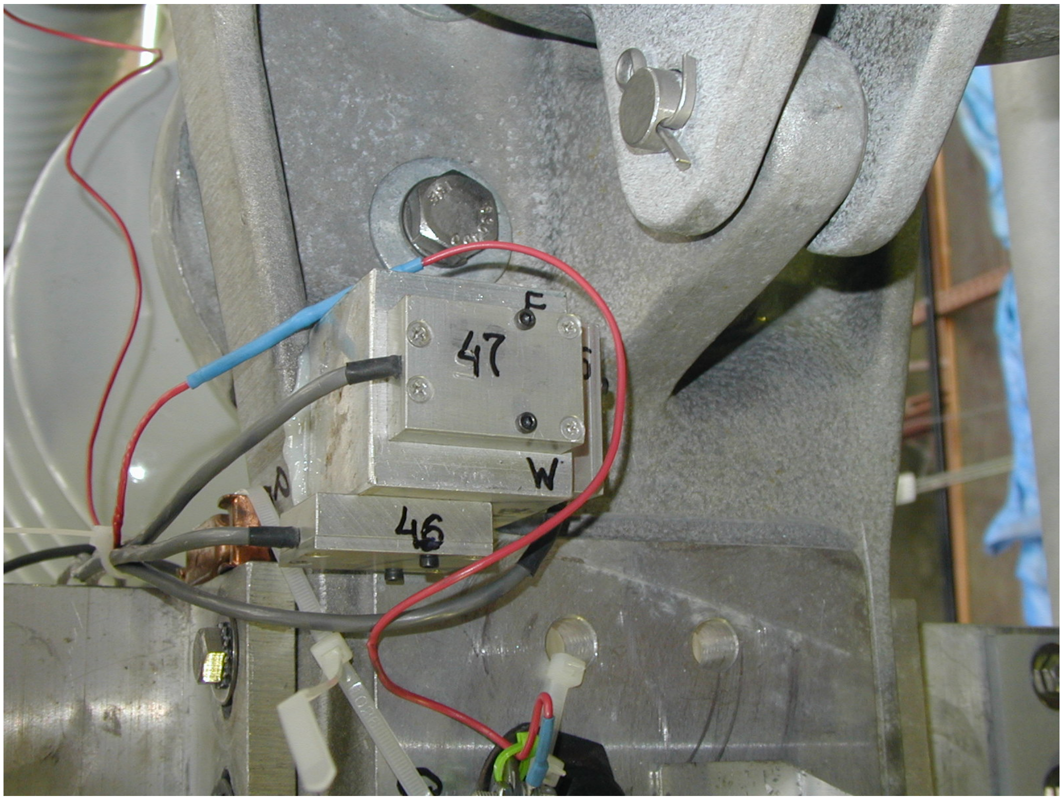

Fig. 2.12 Sample of typical accelerometer installation (top of rigid post)

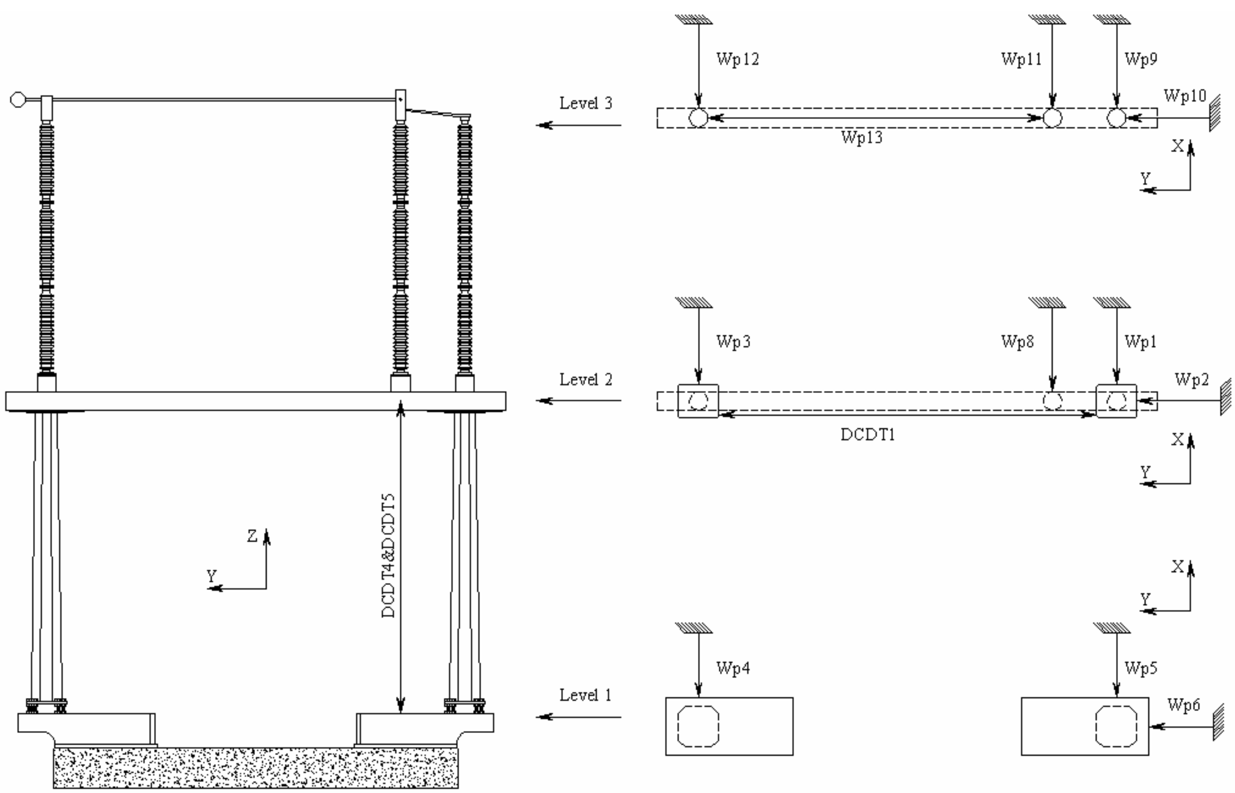

Fig. 2.13 Displacement transducer locations for support-mounted configuration

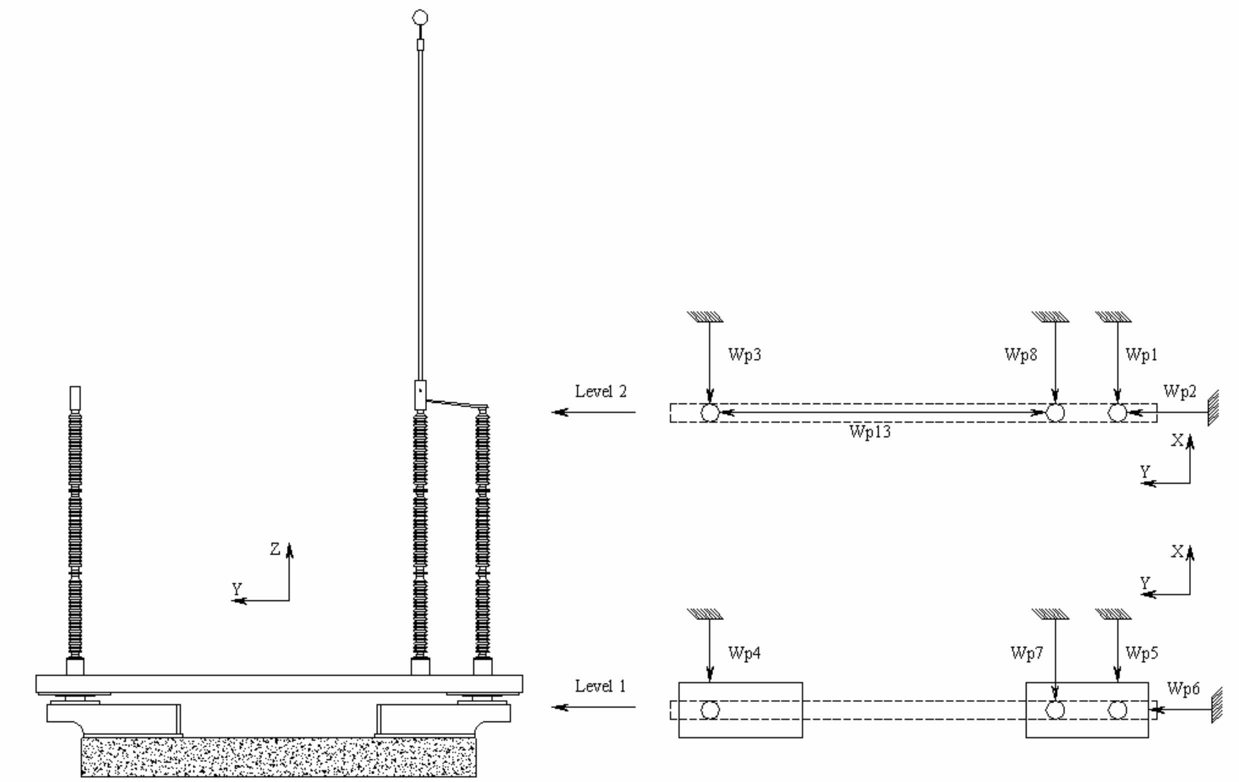

Fig. 2.14 Displacement transducer locations for configuration without support structure

2.2 EXPERIMENTAL PROGRAM

The experimental program included (1) seismic qualification testing of the switch under the IEEE 693 requirements and (2) an assessment of the feasibility of testing tall electrical equipment with components and supports removed or replaced by equivalent ones. A list of test steps conducted during the experimental study is presented in Appendix B.

2.2.1 Qualification Testing

The primary objective of the study was to conduct a seismic qualification test of a 550-kV switch in a typical field installation in accordance with the IEEE 693-1997 (IEEE, 1998) requirements. Due to size limitations of the earthquake simulator platform, only a single-pole switch could be subjected to the required stages of testing.

The IEEE 693 document provides two options for seismic qualification testing at the high performance level: the test specimen should be subjected to a strong motion time history with the test response spectrum (TRS) that envelops the IEEE required response spectra (RRS) at 0.5g PGA or the TRS should envelop the IEEE PL spectrum (twice the RRS) anchored at 1.0g PGA. Input motions used in this project are intended to conform to the new recommended requirements for the development of input motions summarized in Appendix A. The new recommended requirements include various computational checks intended to assure robustness of the input motion, and new matching/enveloping requirements to supplement the requirements of IEEE 693-1997. It should be noted that the new recommended requirements, summarized in Appendix A at present, do not constitute a part of IEEE 693.

In the first option the stresses at the most critical components of the electrical equipment should be less than the allowable stresses, and the equipment must remain functional and sustain no structural damage. In the second option, qualified equipment is expected to perform acceptably up to the PL loading, although some minor structural damage may occur.

Dynamic testing. Dynamic testing by means of the earthquake simulator platform involves random noise testing, sine-sweep testing, and testing with the IEEE-compatible strong motion time history. Because of the limited clearance above the earthquake simulator platform, three configurations of the switch were tested for qualification purposes. Configuration 1 was tested up to the high seismic PL, whereas the other two were tested to the high RRS qualification level. For configurations 2 and 3, an amplification factor due to the support structure was introduced, as estimated from the combined experimental study of all three configurations. The input strong motion for the earthquake simulator platform was amplified by this factor to represent the effect of the omitted support structure.

The IEEE 693 standard requires conducting a low-level resonance search (e.g., sine sweep or white noise vibration test) before the earthquake time history test for estimating the natural frequencies and damping values of the equipment. To calibrate the strain gages installed on the switch, the instrumented switch components were statically tested at low levels of loading. The stiffness of the switch configuration was estimated during static pull-back tests, and the natural frequency and damping value for each configuration were estimated from a free-vibration test. All of these test steps are included in the experimental program presented in Table 2.2 (part 2).

Experimental program for major components of switch. An experimental study of the major components of the switch included tests before and after the seismic qualification tests. The component testing consisted of calibration tests of insulator sections, calibration tests for support legs with and without leveling bolts, and low-level calibration and cantilever strength tests for assembled insulator posts. A free-vibration test was conducted for the support legs and the insulator posts to estimate their natural frequencies and damping values. The list of experimental steps related to the component testing is also presented in Table 2.2 (part 1).

2.2.2 Experimental Study on Feasibility of Testing without Support Structure

An experimental study on the feasibility of the switch testing without a support structure was one of the most important objectives of the study. A number of tests were conducted to assess this approach. A list of tests under strong motion time history excitation is presented in Table 2.3. Two tests related to this part of the study are included in the list for seismic qualification testing, namely Tests 60 and 84 in Table 2.2.

Table 2.2 Experimental program for seismic qualification testing of 550-kV switch

Part 1: Static Component Testing

No.	Test No.	File Name	Signal name/Test	Component	Date
1	1–4	*	Static pull-back tests in X and Y	Both 14-ft-tall supports	3/25/03
2	5–14	*	Static pull-back tests in X and Y	Insulator posts and sections	3/31&4/01/2003
3	171–172	030523105635	Free-vibration and static pull-back test	West 14-ft-tall Support (no leveling bolts)	5/23/03
4	173–181	030523111547	Free-vibration and static fragility test	Insulator posts	5/27&5/28/2003

Part 2: Dynamic and Static Tests of Modified Switch

No.	Test No.	File Name	Signal name/Test	Mounting	Main Blade	Ground Switch	Date
5	51–58	*	Free-vibration and resonance-search	4" spacer	Closed	Open	4/24/03
6	61–66	*	Free-vibration and resonance-search	4" spacer	Open	Open	4/24/03
7	73–74	*	Static pull-back tests in X and Y	14′ Support	Closed	Open	5/6/03
8	75–82	*	Free-vibration and resonance-search	14′ Support	Closed	Open	5/06&5/07/2003
9	60	030424161120	Landers5L@0.25g	4" spacer	Closed	Open	4/24/03
10	84	030507144116	Landers5L@0.25g	14′ Support	Closed	Open	5/7/03
11	119	030515102324	Landers5L@0.125g	14′ Support	Closed	Open	5/15/03
12	120	030515103702	Landers5L@0.25g	14′ Support	Closed	Open	5/15/03
13	121	030515120814	Landers5L@0.5g	14′ Support	Closed	Open	5/15/03
14	122	030515124835	Landers5H@0.75g	14′ Support	Closed	Open	5/15/03
15	123	030515150039	Landers5H@1.0g (PL)	14′ Support	Closed	Open	5/15/03
16	124–129, 132–133	*	Free-vibration and resonance-search	4" spacer	Closed	Open	5/19/03
17	134–135, 148–153	*	Free-vibration and resonance-search	4" spacer	Open	Open	5/19/03
18	136–147, 158–160	*	Free-vibration and resonance-search	4" spacer	Open	Closed	5/19&5/20/2003
19	161	030520123032	Landers5H@0.5g	4" spacer	Open	Closed	5/20/03
20	162	030520125337	Landers5H@0.85g	4" spacer	Open	Closed	5/20/03
21	163	030520132259	Landers5H@1.0g	4" spacer	Open	Closed	5/20/03
22	164	030520141531	Landers5H@1.17g	4" spacer	Open	Closed	5/20/03
23	165–170	*	Free-vibration and resonance-search	4" spacer	Open	Closed	5/20/03

Notes: Tests 60 and 84 used for amplification factor calculation; tests 171–181 were conducted after the major dynamic tests.

Table 2.3 List of tests used in amplification factor assessment study

Part 1: Tests for Modified Switch Rigidly Mounted to Table; main blade closed: 04/15–04/16 and 04/18/2003

Test	File Name	Signal name/Test	Mounting	Main Blade	Ground Switch
28–29	*	Manual excitation in X and Y directions	Rigid	Closed	Open
34–36	*	Random in X, Y, Z directions	Rigid	Closed	Open
37–39	*	Sweep24 in X, Y, Z directions	Rigid	Closed	Open
40	030416135700	Amplified Landers5L@0.25g; scale 1/4	Rigid	Closed	Open
41	030416144312	Amplified Landers5L@0.25g; full scale	Rigid	Closed	Open
42	030416151618	Amplified Landers5L@0.25g; scale 2	Rigid	Closed	Open
50	030419150732	Landers5L@0.25g	Rigid	Closed	Open

Part 2: Tests for Modified Switch Mounted on 4-in Spacer; main blade closed: 04/24 and 05/19/2003

Test	File Name	Signal name/Test	Mounting	Main Blade	Ground Switch
53–55	*	Random in X, Y, Z directions	4" spacer	Closed	Open
56–58	*	Sweep24 in X, Y, Z directions	4" spacer	Closed	Open
59	030424160518	Amplified Landers5L@0.25g; full scale	4" spacer	Closed	Open
60	030424161120	Landers5L@0.25g	4" spacer	Closed	Open
130	030519111046	Landers5L@0.25g	4" spacer	Closed	Open
131	030519104714	Landers5L@0.5g	4" spacer	Closed	Open
156	030519163549	Landers5H@0.5g	4" spacer	Closed	Open

Part 3: Tests for Modified Switch Mounted on 14-ft-tall Supports; main blade closed: 05/06–05/08 and 05/15/2003

Test	File Name	Signal name/Test	Mounting	Main Blade	Ground Switch
73–74	*	Pull-back test in X&Ydirections@500lbs	14′ Support	Closed	Open
75–76	*	Manual excitation in X&Y directions	14′ Support	Closed	Open
77–79	*	Random in X, Y, Z directions	14′ Support	Closed	Open
80–82	*	Sweep24 in X, Y, Z directions	14′ Support	Closed	Open
83	030507142414	Landers5L@0.125g	14′ Support	Closed	Open
84	030507144116	Landers5L@0.25g	14′ Support	Closed	Open
85	030508122001	Landers5L@0.125g	14′ Support	Closed	Open
86	030508124144	Landers5L@0.5g	14′ Support	Closed	Open
119	030515102324	Landers5L@0.125g	14′ Support	Closed	Open
120	030515103702	Landers5L@0.25g	14′ Support	Closed	Open
121	030515120814	Landers5L@0.5g	14′ Support	Closed	Open

2.2.3 Experimental Study on Feasibility of Testing with Blade Removed or Shortened

Table 2.4 presents a list of experimental steps used in the study to assess the feasibility of testing the switch with the main blade removed or replaced by an equivalent mass or equivalent shortened blade. The purpose of the program is to develop recommendations for the qualification testing procedure of a support-mounted switch with the main blade in an open position that cannot be tested on some major U.S. earthquake simulators because of the clearance limitations above the simulator.

Table 2.4 Tests of modified support-mounted switch; main blade replaced by dummy mass or removed (05/09 and 05/12/2003)

Test No.	File Name	Signal name\Test	Mounting	Main Blade	Ground Switch
88–91	*	Stiffness in X&Y directions	14′ Support	Dummy mass	Open
92–97	*	Manual excitation in X&Y directions	14′ Support	Removed	Open
98–100	*	Random in X&Y directions	14′ Support	Removed	Open
101–103	*	Sweep24 in X&Y directions	14′ Support	Removed	Open
104–106	*	Random in X&Y directions	14′ Support	Removed	Closed
107–109	*	Sweep24 in X&Y directions	14′ Support	Removed	Closed
110	030512124245	Landers5L@0.125g	14′ Support	Removed	Open
111	030512142536	Landers5L@0.25g	14′ Support	Removed	Open
112	030512143921	Landers5L@0.5g	14′ Support	Removed	Open
113	030512151835	Landers5L@0.125g	14′ Support	Removed	Closed
114	030512152035	Landers5L@0.25g	14′ Support	Removed	Closed
115	030512152232	Landers5L@0.5g	14′ Support	Removed	Closed

2.3 INPUT TIME HISTORIES FOR EARTHQUAKE SIMULATOR

Two types of earthquake-simulator testing identified in the IEEE 693 (IEEE, 1998) document and required for the seismic qualification of disconnect switches are: (1) earthquake ground motions and (2) resonant frequency search. The earthquake ground motion tests (termed "time-history shake table tests" in IEEE 693) and the resonant frequency search tests are mandatory. Before the time-history shake table tests, the resonance-search test was conducted by means of two different input motions imposed in three principal directions, a broadband white noise time history and a sine-sweep time history.

The three-component IEEE-compatible Landers strong motion time history (Takhirov et al., 2004) was used as an input signal for the earthquake simulator platform for the qualification testing. The signal was developed in a companion project (PEER/PG&E Lifelines Program, Task

408). The signal is filtered to accommodate the displacement and velocity limits of the shake table at the University of California's Richmond Field Station, the headquarters of PEER. The signal consisted of two versions named Landers5L and Landers5H. The first version is for high RRS spectra testing up to 0.5g PGA, whereas the second is for testing at high seismic PL with the target spectrum anchored at 1.0g PGA. A limited number of tests were conducted with a synthetic IEEE-compatible strong motion obtained from the U.S. Army Construction Engineering Research Laboratory (CERL), and a few tests were conducted with Landers3 delivered from the IEEE-compatible Landers by using slightly different filtering parameters.

2.3.1 Resonance-Search Tests

Resonance-search tests were conducted with the PGA at 0.05g in all three principal directions as required by IEEE 693, section A.1.3 (IEEE, 1998). Sine-sweep and broadband white noise tests were used to determine the resonant frequencies and damping ratios of the switch. Free-vibration tests were also used but limited to manual excitation and release tests only.

Broadband white noise. The history for the broadband white-noise tests was prepared using a random signal generator commonly used in qualification testing of electrical equipment (Gilani, et al., 1998; Gilani, et al., 1999; Gilani, et al., 2000).

Sine-sweep. For the sine-sweep test, IEEE 693 specifies that the resonance search should be conducted at a rate not exceeding one octave per minute in the range for which the equipment has resonant frequencies but at least at 1 Hz; frequency searching above 33 Hz is not required. Modal damping was calculated using the half-power bandwidth method. The history for the sine-sweep test was developed using a rate of two octaves per minute (the excitation frequency doubles every 30 sec). A continuous frequency function of the form

$$f(t) = 2^{t/30} \tag{2.1}$$

where t is time in seconds, was used to develop the sine-sweep function

$$x(t) = x_0 \sin(2\pi\,(30/\log 2)2^{t/30}) \tag{2.2}$$

where x is the displacement, and x_0 is the maximum displacement.

Free-vibration tests. In addition to the two test techniques used to assess natural frequency and critical damping of the switch in various configurations and its components, free-vibration tests were also added into the test program. The simplicity of the tests and the reliable data reduction procedure associated with it are two main reasons for inclusion. Due to adequate flexibility of the switch, a manual excitation was enough to bring the switch into a decaying cyclic motion. The natural frequency of the switch or its components was estimated by power spectral density analysis, whereas a critical damping was determined by the decay method for the free-vibration tests (Chopra, 1995).

2.3.2 Time History Shake Table Tests

Two filtered versions of the IEEE-compatible Landers records developed in the companion project (Takhirov et al., 2004) were used for the time history tests. The strong motion input signals for the earthquake simulator are represented by three-component time histories with the vertical direction at 80% of that for the two horizontal directions.

High IEEE RRS level (Landers5L). The earthquake simulator at the University of California, Berkeley, is limited to –5 in. to +5 in. horizontally and from –2 in. to +2 in. vertically with velocity up to 30 in./sec. The IEEE-compatible Landers was filtered to accommodate these limitations up to 0.5g PGA. The elastic response spectra for this input signal in the $1/12^{th}$ octave frequency resolution are presented in Figure 2.15. For a table PGA of less than 0.5g, the three-component strong motion was scaled down by a factor in all three principal directions.

The number of high cycles in the SDOF system response with 2% damping is presented in Figure 2.16. The number of high cycles does not fall below 1 cycle at any frequency of the SDOF system, and the plot has less than 5 isolated valleys to 1 cycle count as recommended in the companion study (Takhirov et al., 2004) and rephrased in Appendix A.

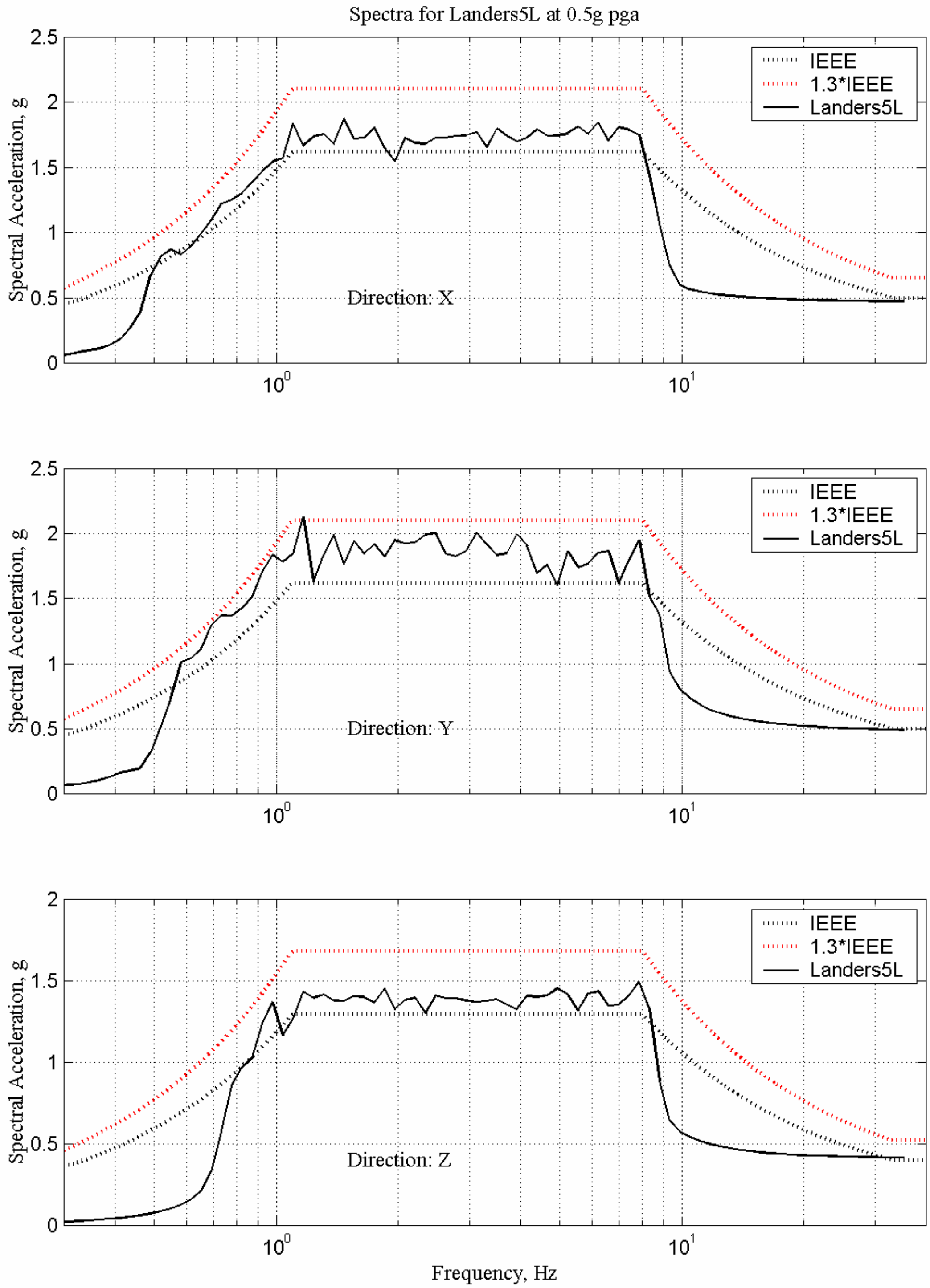

Fig. 2.15 Spectra for Landers5L designed for high RRS test at 0.5g PGA

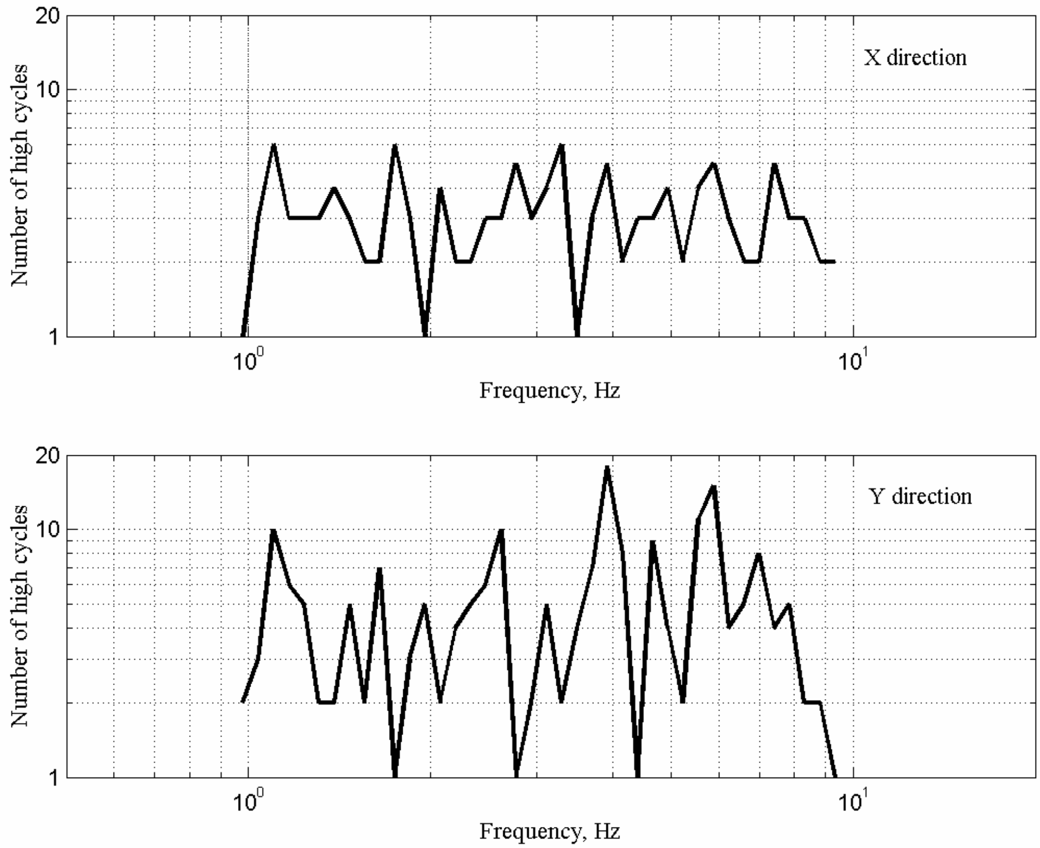

Fig. 2.16 High cycle count in SDOF system response for Landers5L anchored at 0.5g PGA

High IEEE performance level (Landers5H). Landers5H is intended for a seismic qualification testing at the high performance level; therefore it is designed to accommodate the simulator's capacity at 1.0g PGA. The elastic response spectra for this input signal in 1/12th octave frequency resolution are presented in Figure 2.17. The number of high cycles in the SDOF system response with 2% damping is presented in Figure 2.18. Similar to the Landers5L, the number of high cycles does not fall below 1 cycle at any frequency of the SDOF system, and the plot has less than 5 isolated valleys to 1 cycle count as recommended.

Both the Landers5L and Landers5H substantially satisfy the requirements for input motion developed in the companion theoretical study (Takhirov et al., 2004) and rephrased in Appendix A.

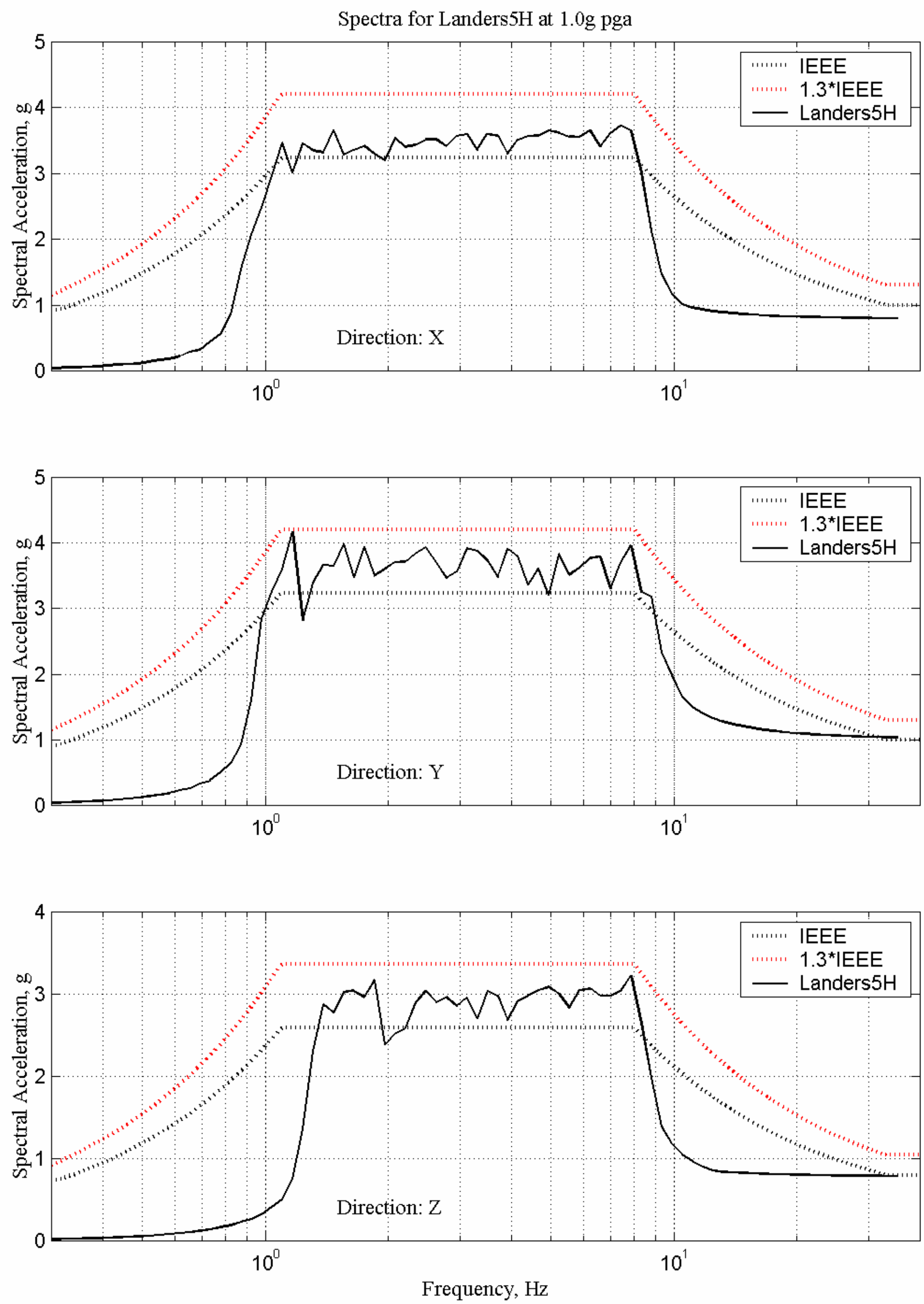

Fig. 2.17 Spectra for Landers5H developed for high PL test at 1.0g PGA

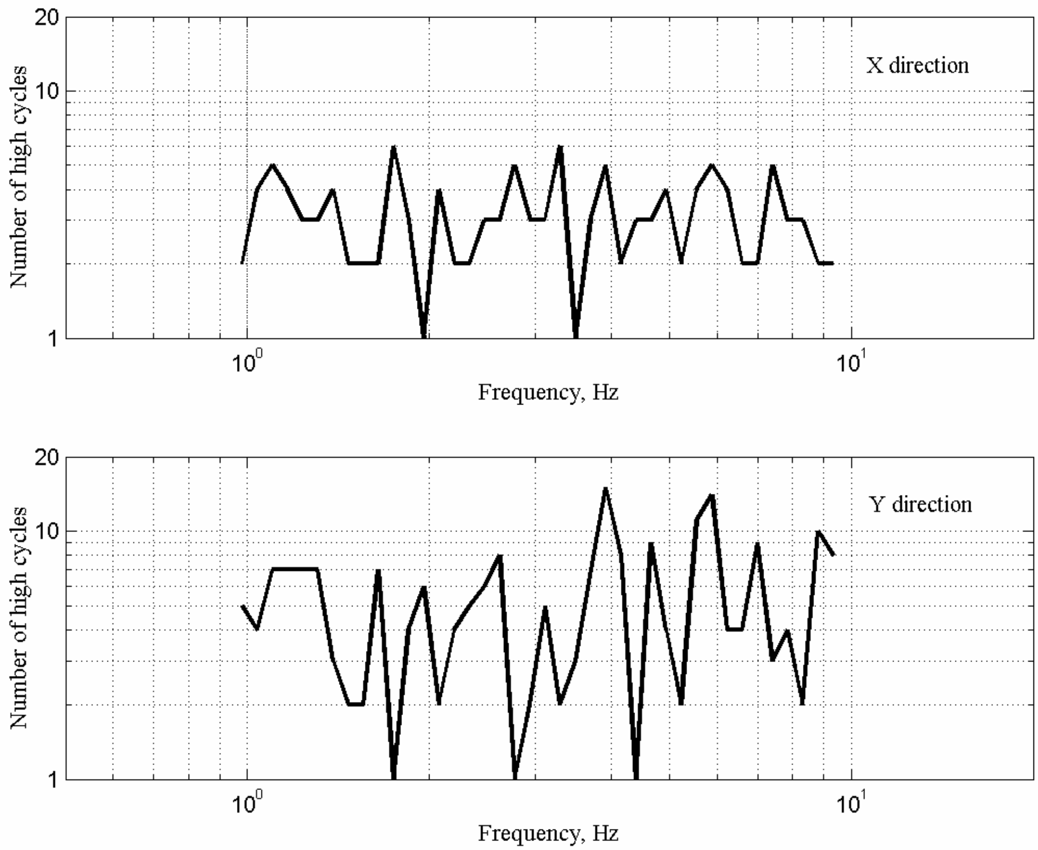

Fig. 2.18 High cycle count in SDOF system response for Landers5H anchored at 1.0g PGA

3 Disconnect Switch Component Testing

Experimental tests were conducted on components of the switch before and after the seismic qualification tests. The typical 14-ft-tall supports were tested with and without leveling rods, and the elastic stiffness of the support from a static pull-back test, and natural frequency and damping from a free-vibration test were estimated. A similar procedure was followed for the insulator posts. The component-testing program concluded with static cantilever strength tests of all insulator posts used in the switch assembly during the qualification tests. The typical setup for tests of the support and the insulator post is shown in Figures 3.1–3.2.

3.1 STATIC AND FREE-VIBRATION TESTS FOR 14-FT-TALL SUPPORTS

3.1.1 Stiffness Test for Support with Leveling Rods

The main objective of the support testing was to calibrate the strain gages, to calculate stiffness of the support, and to estimate the dynamic characteristics of the supports with and without leveling rods.

Test setup. The 14-ft-tall supports were attached to two very stiff platforms that extended the size of the shake table. The attachment simulates a common field installation that simplifies the leveling procedure with 1-¾ x 13 in. A193 B7 threaded rods (8 for each support) and washers and nuts holding the support in an elevated position as shown in Figure 2.3. This arrangement simulates the common utility practice of leaving column base plates ungrouted to introduce additional flexibility at the column base. A load was applied horizontally to reproduce a cantilever loading. The monitoring instrumentation is limited to a load cell that records a horizontal load, a displacement transducer that measures tip displacement of the support, and strain gages that record deformations of the support. The test setup for the

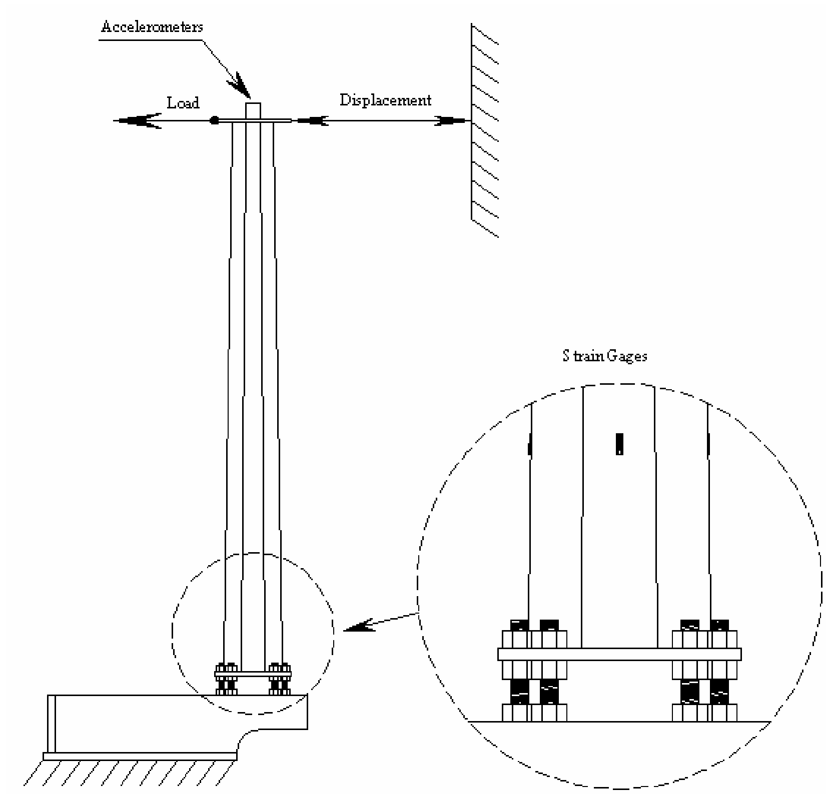

Fig. 3.1 Experimental setup for 14-ft-tall support testing

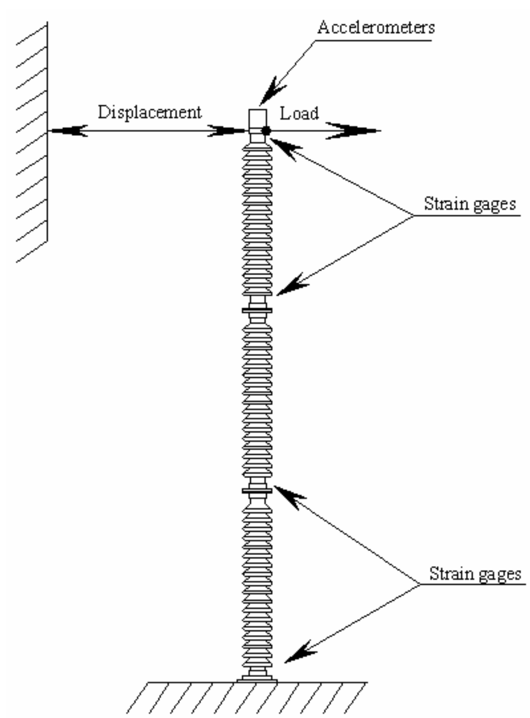

Fig. 3.2 Test setup for insulator post testing: drawing (left) and test in progress (right)

experimental study of the support is shown in Figure 3.1. The horizontal load is limited to 300 lbs to remain within the elastic range of deformation in the supports.

Test results. Test results for 14-ft-tall supports attached to the foundation by leveling rods are presented in Table 3.1. The average stiffness for both supports in two horizontal directions is estimated as 4.55 kips/in.

Table 3.1 Stiffness test for supports mounted on leveling rods

No.	File Name	Support	Signal name	Direction	Stiffness, kips/in.
1	030325092908	West	Pull-back test up to 300 lbs	Y	4.44
2	030325111853	West	Pull-back test up to 300 lbs	X	4.70
3	030325140725	East	Pull-back test up to 300 lbs	Y	4.61
4	030325142832	East	Pull-back test up to 300 lbs	X	4.44

3.1.2 Stiffness and Free-Vibration Tests for Support without Leveling Rods

The elastic stiffness of the support with no leveling rods (i.e., column base plate bolted directly to foundation blocks) was estimated after accomplishing the seismic qualification testing of the switch assembly. The strains in the steel supports monitored during the highest level dynamic tests of the switch revealed that the plastic deformation had not occurred in the supports. Therefore, the comparison of tests between two mounting configurations of the support (with and without leveling rods) is valid. The test setup was similar to that conducted before the dynamic testing except that the leveling rods were removed and the support was attached directly to the support platform.

Testing was conducted only for one support (installed on the west side in the switch assembly under the rigid post) and only in the X direction. The 14-ft-tall support was attached to the essentially rigid foundation, extending the size of the shake table. The test results for both static and free-vibration tests are presented in Table 3.2. The average cantilever stiffness of the support with no leveling rods is greater than that with leveling rods at 5.55 kips/in. The frequency and critical damping are consistent for two free-vibration tests and are estimated as 15.4 Hz and 0.5%, respectively.

The stiffness of the support with leveling rods is less than that without the rods, as expected, by about 20% and the resonant frequency is about 90% of that of the installation without leveling rods.

Table 3.2 Stiffness test for supports mounted with no leveling rods

No.	File Name	Support	Testing	Stiffness, kips/in.	Frequency, Hz	Damping, %
1	030523105635	West	Pull-back test @ 300 lbs	5.50		
2	030523105951	West	Pull-back test @ 300 lbs	5.60		
3	030523111547	West	Free vibration		15.4	0.5
4	030325141605	West	Free vibration		15.4	0.5

3.2 STATIC AND FREE-VIBRATION TESTS FOR INSULATORS

3.2.1 Calibration and Stiffness Tests for Porcelain Sections and Assembled Posts

Low-level calibration and stiffness tests for porcelain sections and completely assembled posts were conducted before the dynamic testing of the switch. The cantilever tests for insulator posts are very important because they are used for rating an insulator's structural strength. The insulator posts were manufactured and supplied by NGK-Locke, Inc., and consisted of three ceramic sections for each post. The fully assembled posts are rated at 2900 lbs of cantilever load. The cantilever strength rating is a very conservative representation of the breaking strength of the insulator.

Test setup. A separate experimental setup was designed to conduct low-level tests on insulator sections and assembled posts. The test setup was intended to measure a cantilever stiffness of the sections and the posts, and calibrate all strain gages installed at multiple locations throughout the insulator sections. The test setup is presented in Figure 3.2.

Experimental results for sections and assembled posts. The horizontal load versus horizontal deflection diagram for all insulator posts is quite close to linear as shown in Figure 3.3. The stiffness of the various posts for all directions of testing is consistent with some minor variation from the mean of 9.26 kips/in. as presented in Table 3.3. The free-vibration test revealed an estimate for a natural frequency of posts that was around 8.3 Hz. The low-level static tests conducted for all instrumented sections showed consistent gage calibration.

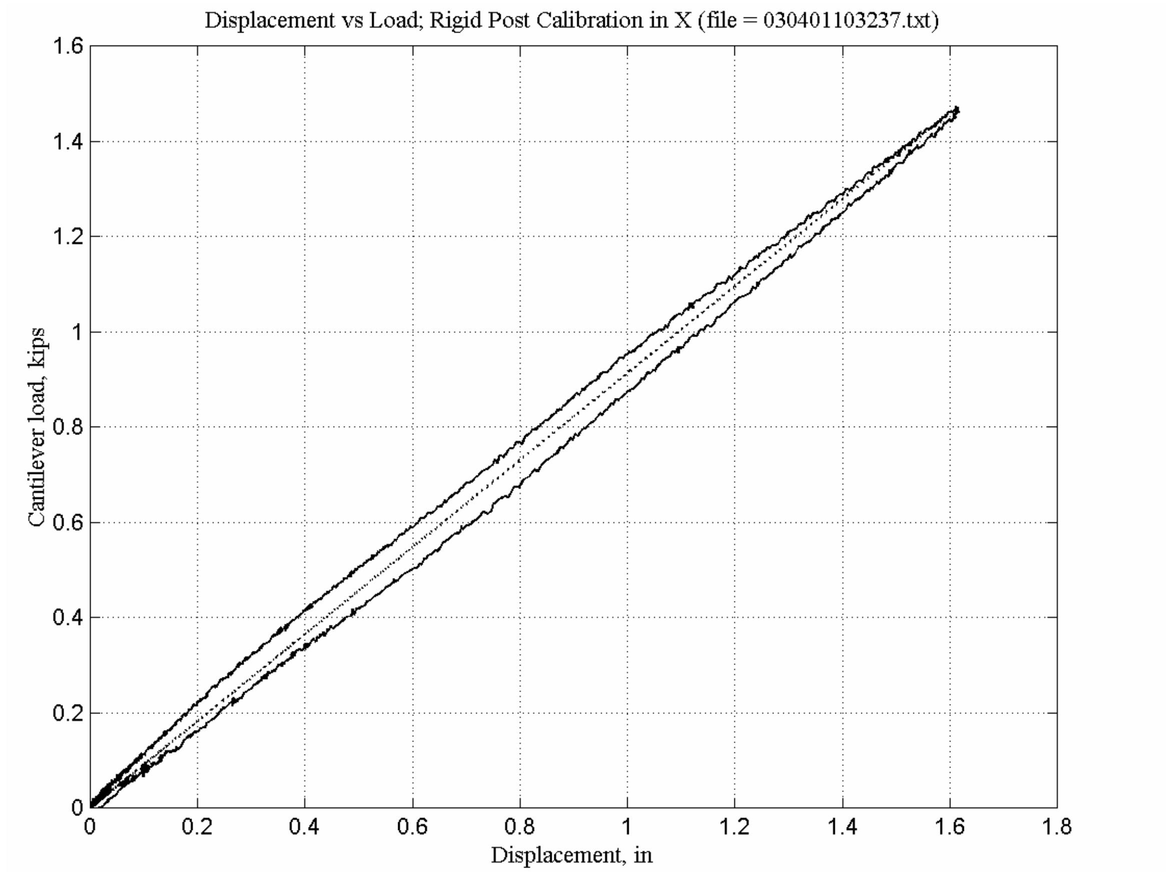

Fig. 3.3 Typical load-deflection diagram for low-level calibration test (rigid post in X direction)

An interesting phenomenon was observed for the strains in the insulator sections and posts. Since the gages were installed at 90 degrees apart, some gages were in tension and others (180 degrees apart) in compression during the cantilever testing. The horizontal load versus strain relationship is very close to linear, but the slope of the plots is different for positive (compression) and negative (tension) strain. This observation was consistent for all tests on insulator sections and assembled posts. Typical plots for horizontal load versus strain diagrams at three levels of rigid post are presented in Figure 3.4. A similar difference in slopes of load vs. strain for tension and compression was also noticed during dynamic tests as shown in (Fig. 3.5.) The relation between the compression and tension strains does not follow the dashed line that represents a case when tension strain would be equal to compression strain with opposite sign.

Table 3.3 Summary for low-level calibration and stiffness tests for insulator posts

No.	File/Direction	Post	Section	Slope T, lbs/ms	Slope C, lbs/ms	Load, kips	Stiffness, kips/in.
1	030401103237/X	Rigid	Bottom	4.12	3.54	1.47	0.91
			Middle	4.21	3.67		
			Top	3.92	3.39		
2	030401112117/Y	Rigid	Bottom	3.88	3.36	1.45	0.94
			Middle	4.41	NA		
			Top	3.90	3.46		
3	030331121137/X	Rotating	Bottom	3.92	3.52	1.49	0.89
4	030331114650/Y	Rotating	Bottom	3.99	3.38	1.45	0.97
5	030401140151/X	Jaw	Bottom	4.15	3.47	1.45	0.98
			Middle	4.12	3.87		
6	030331114650/Y	Jaw	Bottom	4.18	3.54	1.44	0.93
			Middle	4.56	3.84		

A summary of the calibration tests is presented in Table 3.3, which shows the difference in the slopes of negative (Slope T) and positive strains (Slope C). The difference in the slope values varies from about 7%–20%, depending on a particular level of the post. The average slope in tension is estimated as 4.37 lbs/ms ("ms" stands for microstrain), whereas the mean of a slope in compression is estimated as 3.69 lbs/ms; therefore, the difference between the two slope means is about 20%. This difference in strain reading may be due to the difference in displacement of the bolted joints in tension compared to compression. The tension side of a bolted joint is expected to displace more than the compression side, which results in reduction of the tensile strain, hence a higher calculation for the slope. The difference in behavior of the grouted joint, or effects related to the nonuniformity of the cross section (e.g., end effects) may also be involved.

It is noteworthy that the values of the load-strain slopes for the strain gages installed at the bottom sections are used extensively during the qualification testing in estimating the equivalent cantilever load; therefore, it is important to conduct the strain gage calibration test before the qualification test.

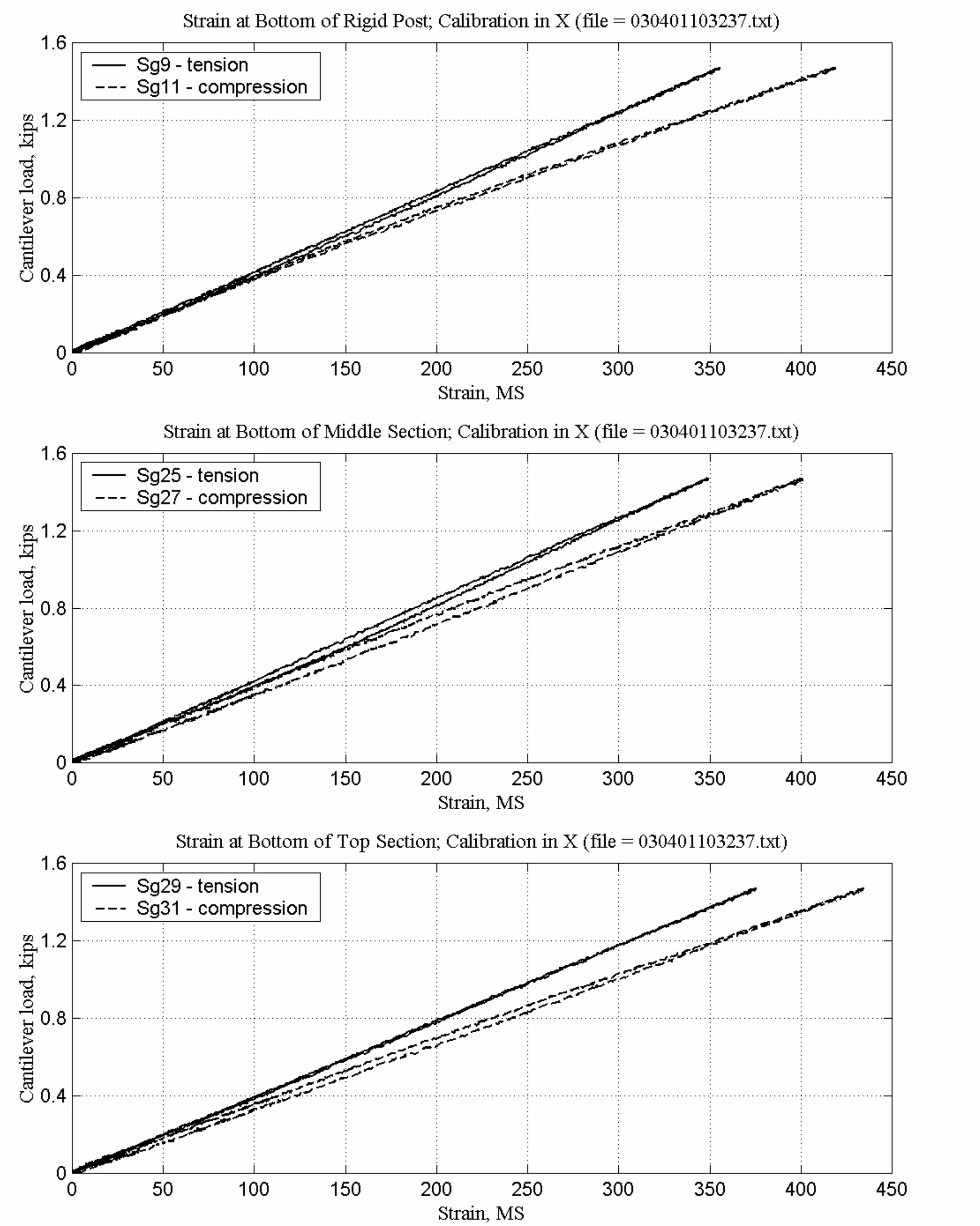

Fig. 3.4 Typical load-strain diagrams for low-level calibration test (rigid post in X axis)

3.2.2 Static Cantilever Strength Tests for Insulator Posts

The static cantilever strength tests for the insulator posts were conducted after the completion of all dynamic testing of the switch. The test setup was similar to that used for calibration testing, and the testing procedure follows the requirements of the IEC 60168 standard (IEC, 2001). The horizontal load was slowly applied until failure at the tip of the vertically mounted post. All three posts were tested. Before the cantilever strength tests, free-vibration tests were conducted on the posts to estimate the natural frequency and critical damping. A summary of the static cantilever strength tests is presented in Table 3.4.

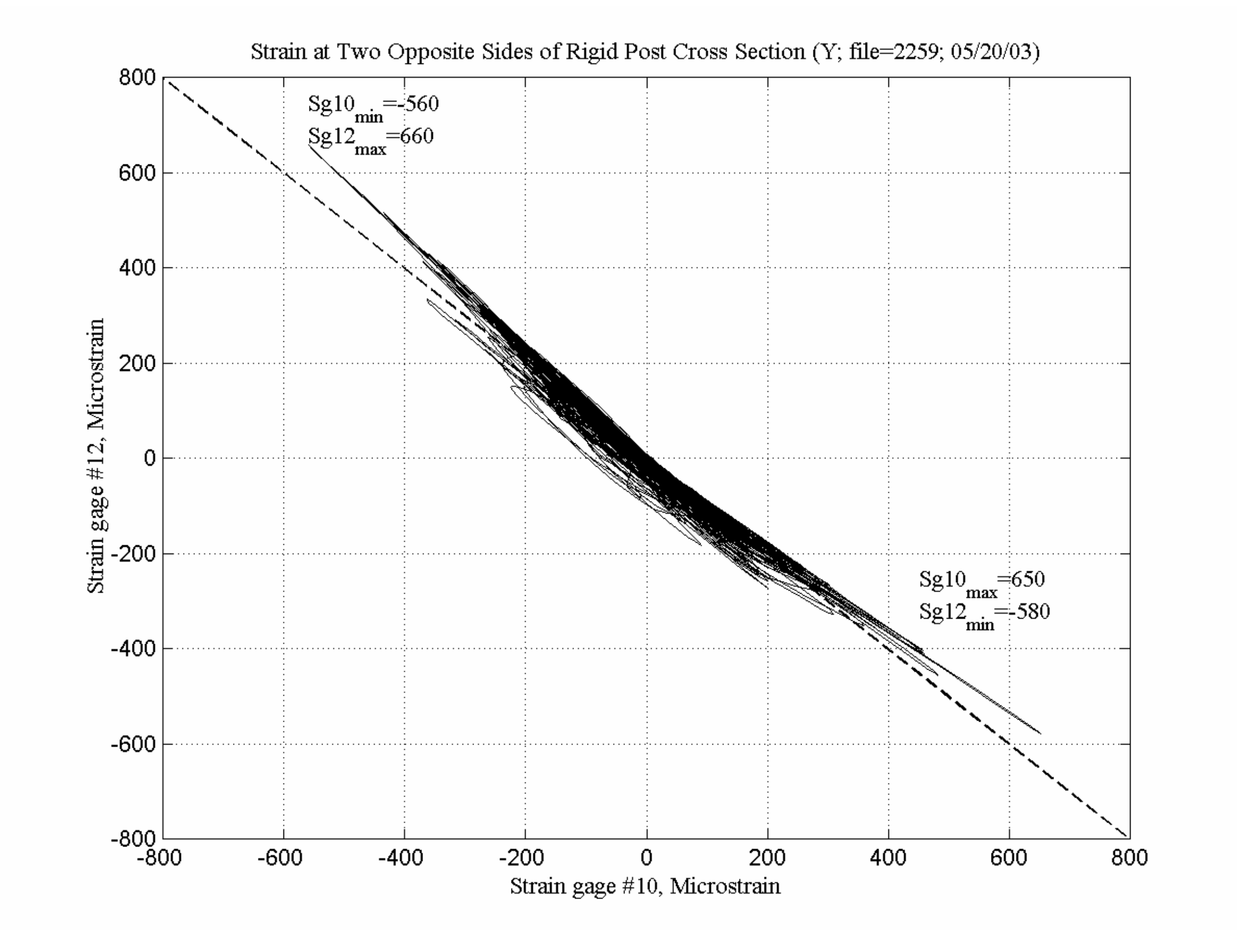

Fig. 3.5 Strain at two opposite sides of rigid post's cross section in Y direction during dynamic testing (dashed line shows a case when tension strain would be equal to compression strain with opposite sign)

Table 3.4 Summary of static cantilever strength tests for insulator posts

No.	File/Direction	Post	Section	Slope T, lbs/ms	Slope C, lbs/ms	Load, kips	Stiffness, kips/in.
1	030528131501/X	Rigid	Bottom	3.84	3.21	4.14	0.82
			Middle	4.16	3.41		
			Top	3.67	3.28		
3	030527152716/X	Rotating	Bottom	3.74	3.09	3.96	0.83
5	030528152311/X	Jaw	Bottom	3.93	3.37	4.31	0.85
			Middle	4.19	3.57		

Rigid post. Figure 6 shows the horizontal load versus deflection for the rigid post. The calibration and cantilever strength slopes are quite close to each other, although the peak-to-peak stiffness in the strength tests is about 10% less than that during the calibration test. The load-strain plots are also close to each other at low levels of loading, as shown in Figure 3.7

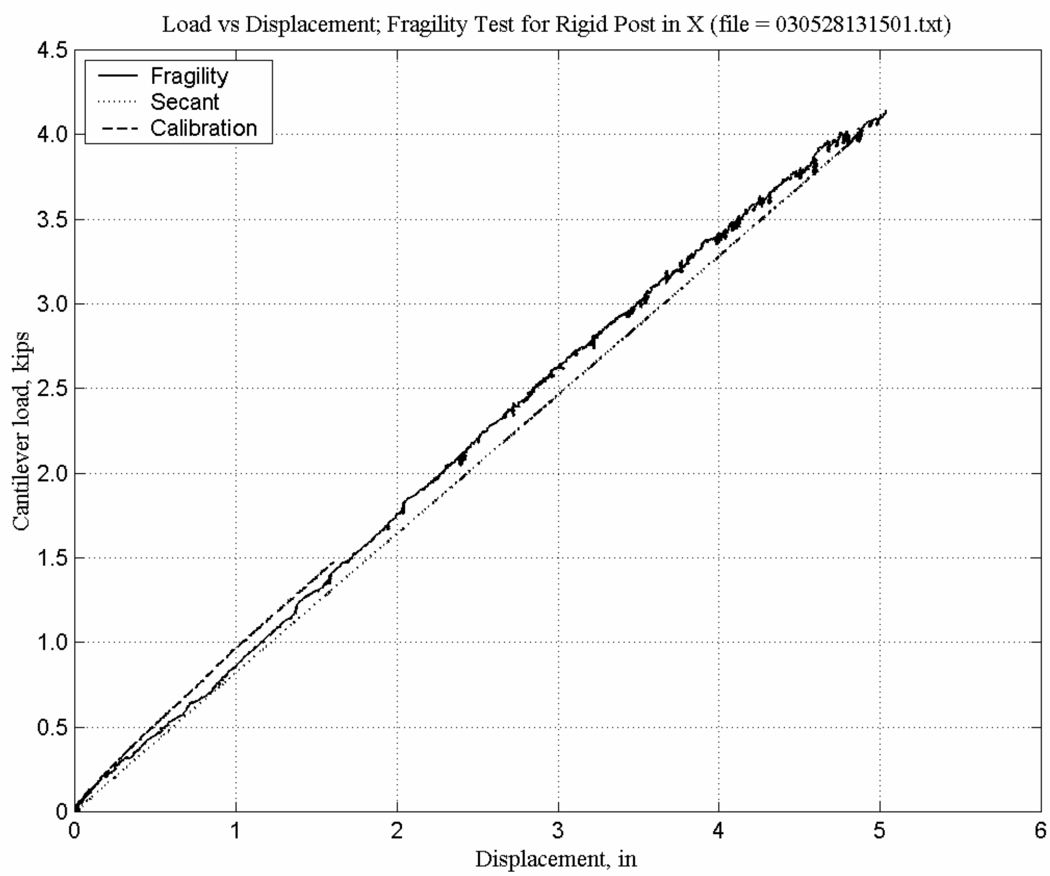

Fig. 3.6 Load-deflection diagram for static cantilever strength test (rigid post in X)

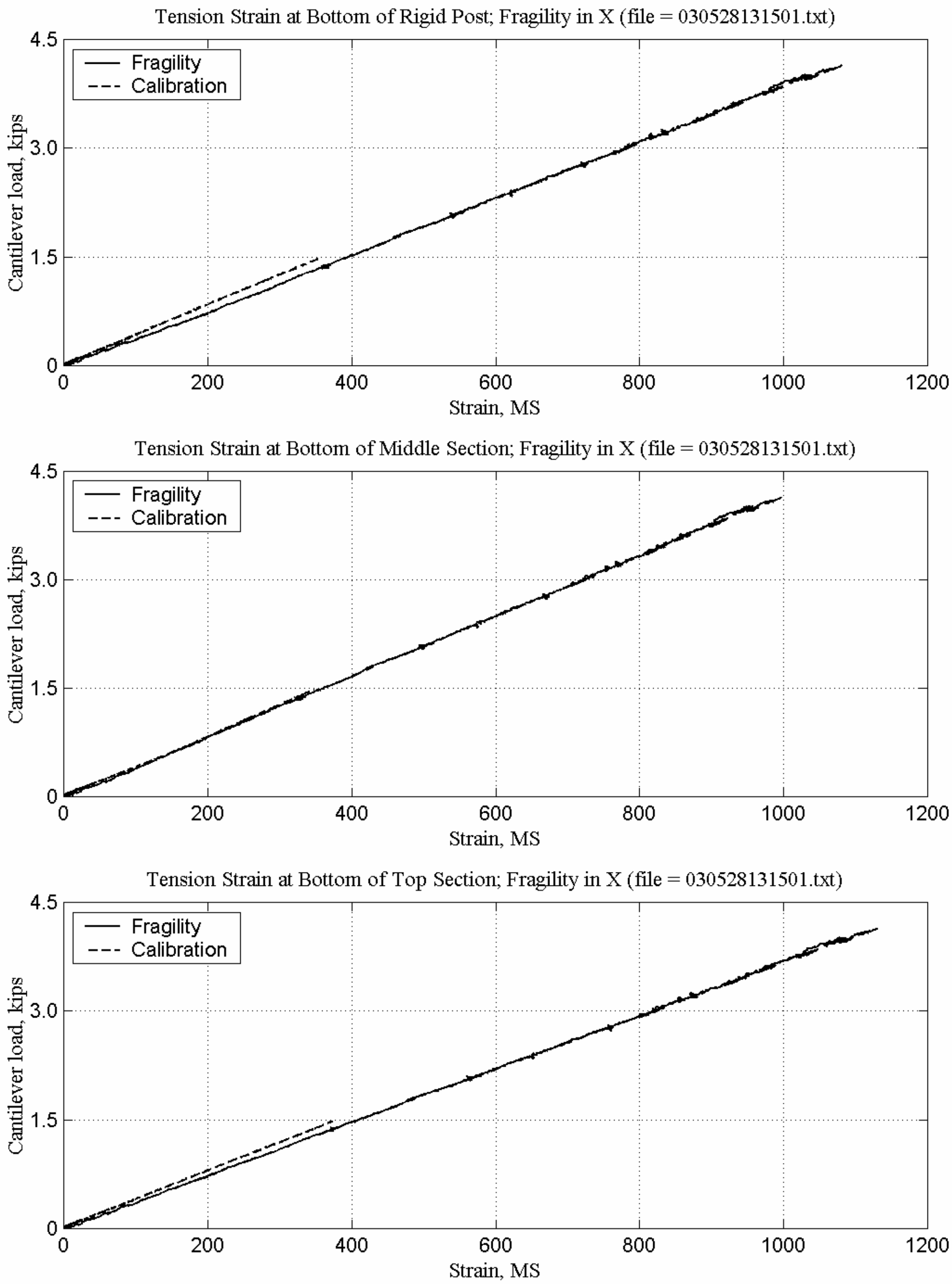

Fig. 3.7 Load-tension strain diagram for static cantilever strength test (rigid post in X direction

An insignificant change (within 10%) in the load-strain slope is observed. This small difference may be the result of slight damage, loosening of bolted or grouted joints, or measurement errors. The small changes in the stiffness and the load-strain slope lead to the following conclusions: (1) the material properties of the insulator post are close to linear up to its failure and (2) the large-amplitude dynamic tests did not significantly affect the material properties of the insulators. The rigid post failed at 4,140 lbs of cantilever load.

Rotating post. Figure 3.8 shows horizontal load versus tip deflection for the rotating post. The test results are similar to those for a rigid post, with close correlation between the calibration and fragility diagrams as for the load-deflection and load-strain diagrams (Fig. 3.9). The rotating post failed at 3,960 lbs of cantilever load.

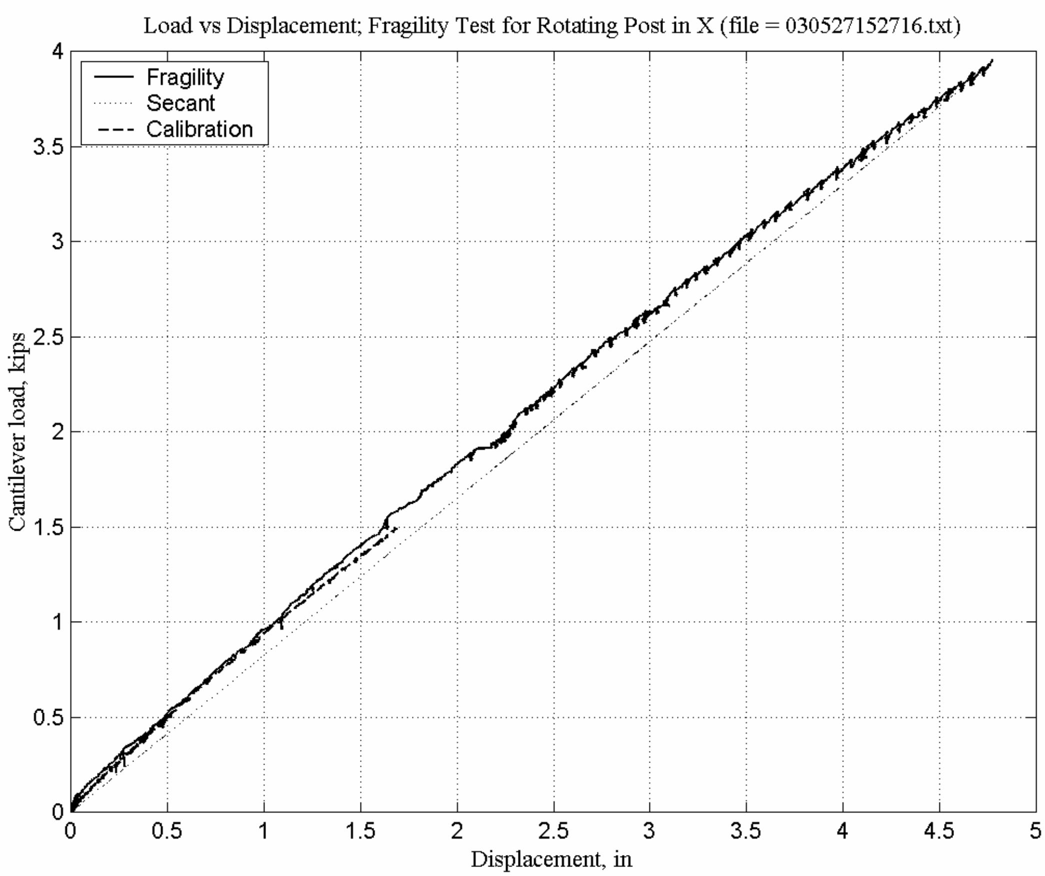

Fig. 3.8 Load-deflection diagram for static cantilever strength test (rotating post in X)

Jaw post. Similar results are obtained for testing of the jaw post, as shown in Figures 3.10–3.11. The stiffness is slightly less, by about 13%, than in the cantilever strength testing.. A remarkably close correlation can be seen between the load-strain diagram at the low level and the cantilever strength tests obtained for the jaw post (Fig. 3.11). Failure of the jaw post occurs at 4,310 lbs of cantilever load. The process of porcelain failure in the jaw post is presented in Figure 3.12 from several frames of a digital video recording. The failure starts at the base of the top section, propagates down, and destroys the middle section completely. A similar process was observed for the rigid post.

The mean ultimate cantilever load delivered from the cantilever strength tests for three insulator posts is about 4,140 lbs with a standard deviation of 176 lbs.

3.2.3 Data Provided by Insulator Manufacturer (Courtesy of NGK-Locke Insulators, Ltd.)

The cantilever strength data obtained from NGK-Locke Insulators, Ltd. (Japan) show that the mean breaking strength in bending for the insulator posts (NGK-Locke Cat. No. 8A-69446A) used in the experimental program is 3800 lbs based on four tests, with a standard deviation of 178 lbs. When combined with the three breaking strength tests conducted in this experimental program, the mean breaking strength is 3944 lbs with a standard deviation of 242 lbs. Low-level cantilever tests conducted by NGK-Locke reveal a linear relationship between the horizontal load and the tip deflection, and a stiffness of about 1.08 kips/in. up to about 1,200 lbs. This stiffness is close to the average stiffness found in this experimental program 0.93 kips/in. The cantilever rating of 8A-69446A is set by the manufacturer at 2900 lbs.

In addition to the data on 8A-69446A insulator posts, the manufacturer has also provided breaking strength data on a similar model (PX0603). PX0603 consists of three sections, each having the same core diameters as the model used in the experimental program, but different end fittings. The mean breaking strength of 19 specimens of PX0603 is 3941 lbs with a standard deviation of 287 lbs. The cantilever rating for PX0603 is set by the manufacturer at 2500 lbs.

The breaking strength from these two models of insulators demonstrates a typical practice of insulator manufacturers, which is to set cantilever ratings substantially below the mean breaking strength. In essence, these rated strengths represent guaranteed minimum breaking strengths.

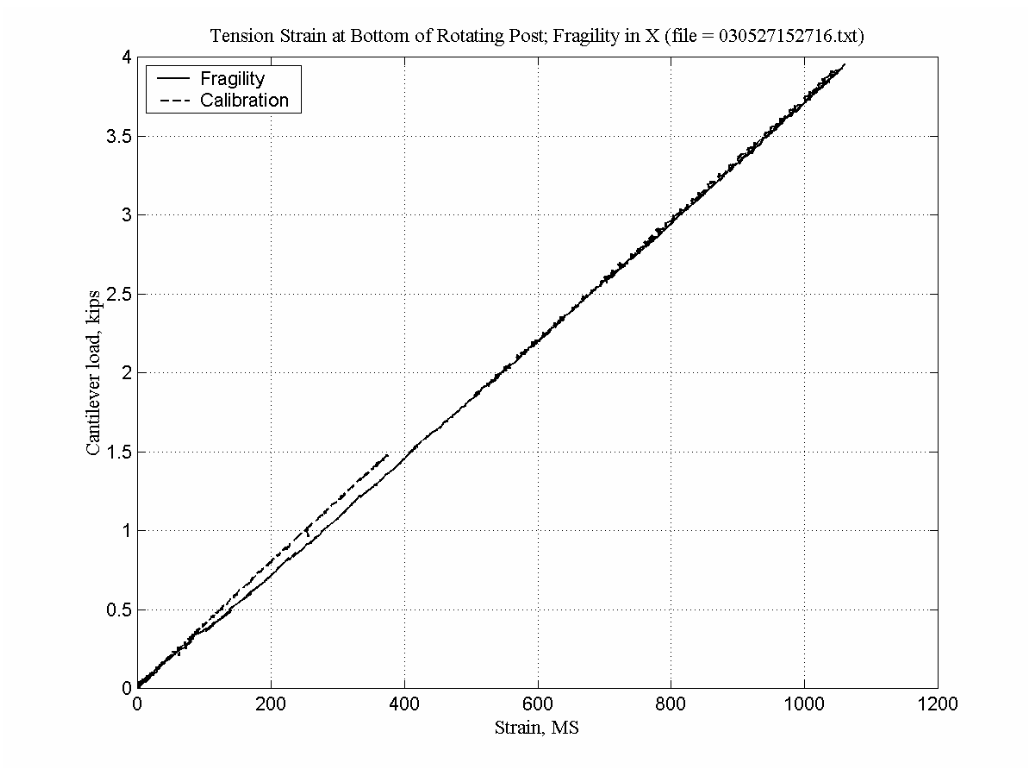

Fig. 3.9 Load vs. tension strain for static cantilever strength test (rotating post in X axis)

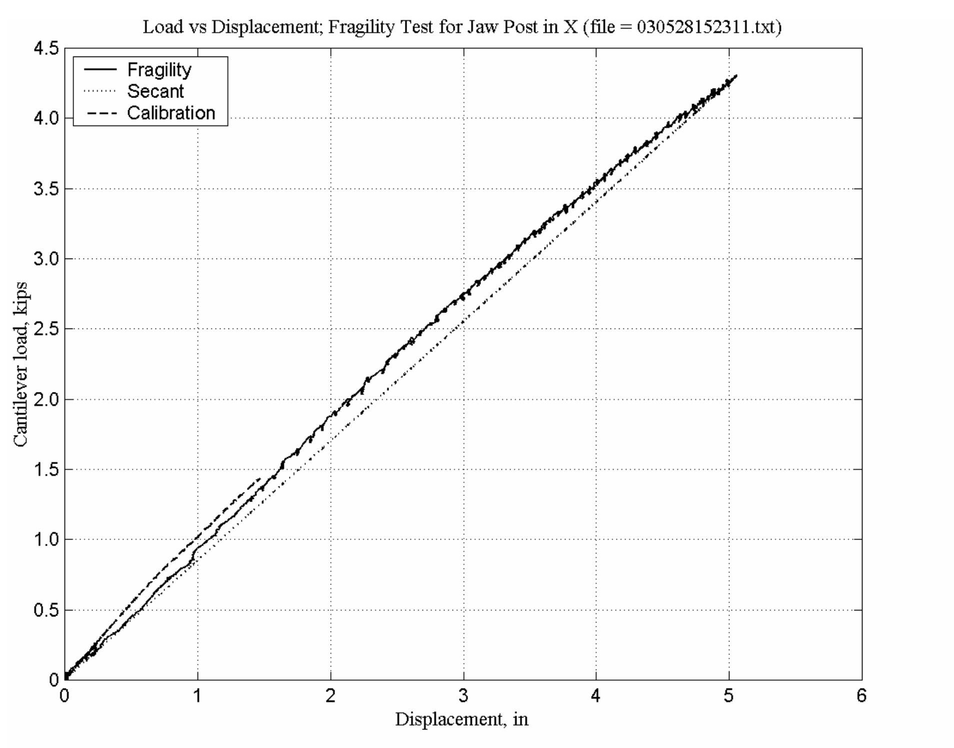

Fig. 3.10 Load-deflection diagram for static cantilever strength test (jaw post in X axis)

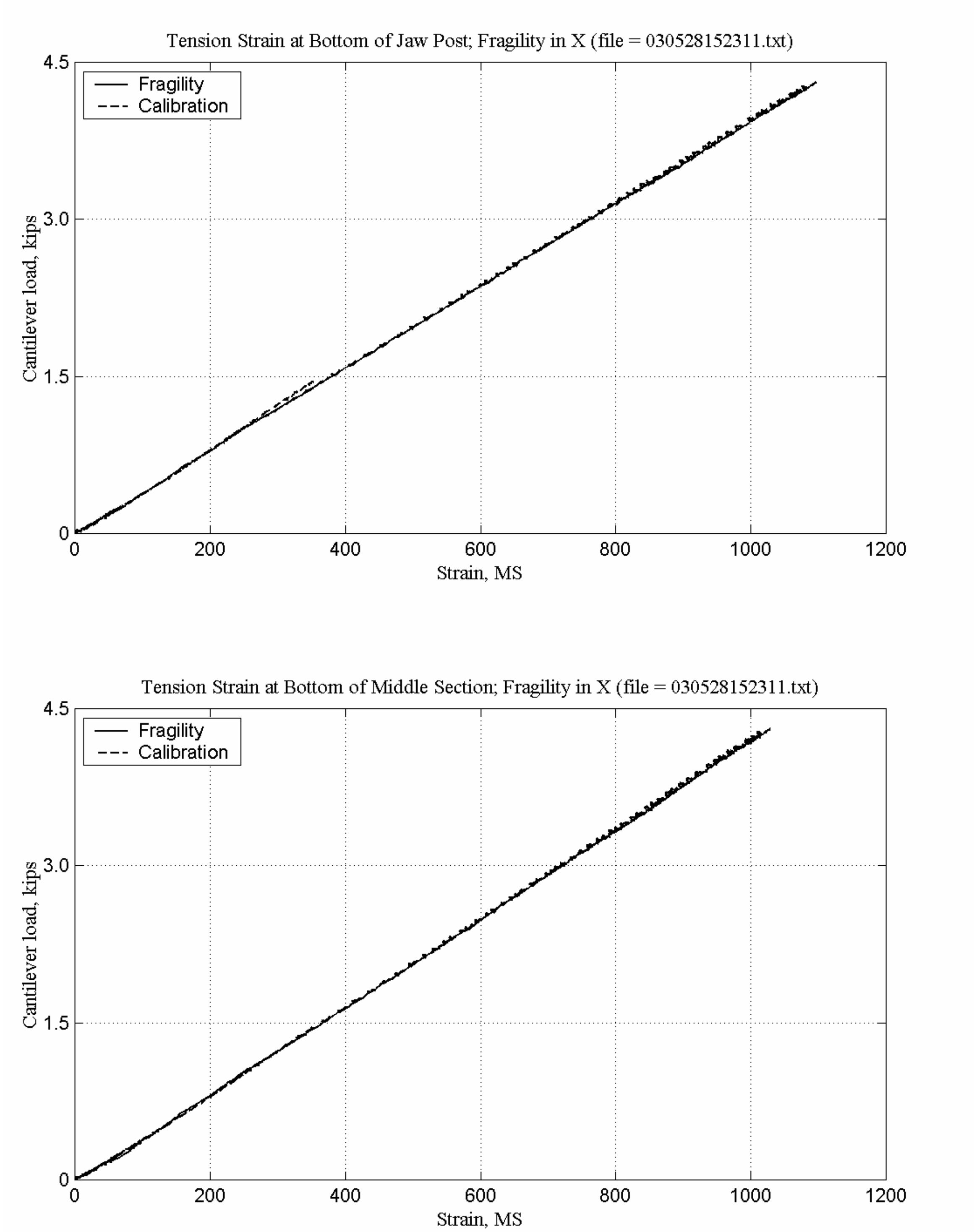

Fig. 3.11 Load-tension strain diagram for static cantilever strength test (jaw post in X direction)

Frame 1

Frame 2

Frame 3

Frame 4

Fig. 3.12 Step-by-step process of porcelain failure in jaw post

3.2.4 Design Properties of Ceramics

Ceramics have excellent mechanical properties in compression, but when tensile loads are applied, they typically fail in a brittle manner at much lower load (Callister, 2003). The summary of the strain gage data during cantilever strength tests confirms the difference between the behavior of ceramics in compression and tension (Table 3.5). For the same cantilever load the compression strain is greater for all sections of the posts than is the tension strain recorded on opposite sides of a cross section, as discussed in Section 3.2.1.

Tensile fracture of a ceramic is caused by the presence of pre-existing cracks and flaws in the material. When the material is placed in tension these cracks act as stress amplifiers, which in turn lead to a single dominant crack, starting at the tip of a flaw. The dominant crack quickly propagates through the material. In compression, however, the cracks close, and do not behave like stress amplifiers. As a result the ceramic can handle compressive stresses very well. The presence of cracks and defects in the ceramic materials is called "porosity." The porosity of a ceramic has a major effect on its modulus of elasticity and modulus of rupture.

Therefore, a tension strain may serve as a better indicator to predict porcelain failure. The ultimate tension strains recorded at the sections of the insulator posts during the cantilever strength tests are presented in Table 3.5, which also shows the section where the failure first started. The location of initial failure is consistent for all tests and is at the bottom of the top section. Unfortunately, the strain gages on the top section are installed only in the case of a rigid post, so there is only one data point for tension strain at this location. The fact that the strain maxima are consistent for all cantilever strength tests suggests that even this one data point correctly represents the critical value for the tension strain. The critical tension strain is close to 1100 ms, or 0.11%, presented in bold in Table 3.5.

The strain at the top sections of the two other insulator posts (Table 3.5) is estimated from Table 3.6, which calculates bending stress at all levels of the post normalized to that at the bottom section. Assuming all porcelain is the same in the posts, the top section is the most critical and expected to fail first, as shown in Table 3.6.

Load calculation procedure used throughout the study. Because the porcelain has lower strength in tension, only negative strains representing tension in the material are used for equivalent load calculation. Negative strain is multiplied by the corresponding tension load factor and an absolute value of equivalent load is calculated for gage readings in the X and Y directions. The modulus of these two loads in two orthogonal directions is produced by computing the square root of sums of squared loads for a particular time step. The same procedure is repeated for another set of gages 90-degrees apart from this one. At the final stage the maximum value of these two moduli is obtained, which in the study is called the "modulus of the equivalent cantilever load."

Table 3.5 Summary of strains in cantilever strength tests

Post	Section	Tension strain, ms	Compression strain, ms	Failure started at	File
Rigid	Bottom	1080	1290		030528131501
	Middle	1000	1220		
	Top	**1130**	1270	Bottom of top section	
Rotating	Bottom	1060	1290		030527152716
	Middle				
	Top	1103*		Bottom of top section	
Jaw	Bottom	1100	1280		030528152311
	Middle	1030	1210		
	Top	1145*		Bottom of top section	

*Calculated for cantilever loading of the tapered multi-sectional insulator post (Table 3.6).

Table 3.6 Stress estimation of cantilever loading of multi-sectional insulator post

Section	S_x, in.^{3}	Moment's arm, in	Stress normalized to that at bottom section
Top	11.7	47.88	1.04
Middle	26.71	97.88	0.93
Bottom	37.93	148.88	1.00

Strength vs. calibration load factors. A set of tests to estimate the cantilever strength of the insulators was conducted after completion of the switch testing. The switch was disassembled and the three posts were tested in a static pull-back test to failure, as discussed above. The strength test setup was similar to that for the calibration test. The load-vs.-strain plots show that the load factor did not change significantly; therefore (1) the dynamic testing did not significantly affect the elastic properties of the insulator and (2) the ceramic insulator performed elastically up to failure. Tables 3.3–3.4 present load factors before and after the switch's dynamic testing, which confirms that the tension load factor change is 10% for all insulator posts, near the accuracy of test measurements.

3.2.5 Conclusions

The slope of a load-strain diagram for the porcelain sections and the posts depends on the sign of the strain. The tension strain develops a steeper slope than that in compression by up to 20%. The difference in the slope may be related to the material properties of the ceramic and/or boundary condition effects. Since the strain gages were installed in close proximity to the joints between the sections, the bolted joints, a mortar between ceramic and a cap, a gap size between ceramic and the cap, and other factors may affect the strain reading. The small changes in overall stiffness and the load-strain slope for the insulator posts indicates that the material properties of the insulator post are close to linear up to failure and that the dynamic tests did not affect the insulators. The elastic stiffness of a post estimated during calibration tests is close to that provided by the manufacturer (NGK Insulators, Ltd.). The failure load is close to that repeated by the manufacturer for similar insulator posts.

4 Support-Mounted Switch with Original Design

This chapter presents the test results for a switch with an unreinforced base, called the “original switch.” The tests were conducted only at low levels up to 0.25g PGA. Since the equivalent cantilever loads in the insulator posts at 0.25g PGA appeared to be greater than the allowable loads, only a limited number of tests were conducted with the original switch. The base of the switch was reinforced before proceeding to more severe qualification testing. This chapter discusses the testing and performance of the original switch with an unreinforced base.

4.1 SWITCH RESPONSE AT LOW-LEVEL DYNAMIC TESTING

The manufacturer (Southern States, Inc., Georgia) provided two design modifications for the type “EV-1” 550 kV 4000 switch in this study. The first is called the “original switch,” the second the “modified switch.” The main difference between the two is in the details of the fixture at the base of the switch where the insulators are attached to the base. The design modifications were developed before the qualification test program and are based on extensive testing (Wyle Laboratories, 1993) and numerical analysis (Gundy and Associates, Inc, 2002).

The approach of the experimental study was to start from the most vulnerable type of switch design and proceed with testing of the modified switch until the seismic qualification requirements were satisfied in accordance with the IEEE 693 document (IEEE, 1998). The decision to modify the switch design was based on the equivalent cantilever load for the insulators, which was estimated from strain gage data during low-level dynamic tests (up to 0.25g PGA).

4.1.1 Experimental Program

The switch was assembled on the earthquake simulator platform to conduct static pull-back, free-vibration, resonance-search, and time history tests. The original switch was assembled and tested only on 14-ft-tall supports, with the main blade closed and the grounding blade open. A total weight of the switch was estimated as 4,130 lbs and a total weight of supports was about 1,620 lbs.

4.1.2 Summary on Static Pull-Back, Free-Vibration, and Resonance-Search Tests

The static pull-back test was conducted by pulling the top part of the switch horizontally with a load up to 480 lbs and by recording the deflection. The testing was conducted in two principal directions, and at least two tests in each direction were performed. The elastic stiffness of the switch in the X direction (out of plane) is estimated as 0.50 kips/in., whereas in the Y direction (in plane) it is estimated as 1.25 kips/in. Typical plots for the horizontal load vs. deflection relationship for the X and Y directions are presented in Figures 4.1–4.2.

Free-vibration tests are also performed in the two principal directions. The results for the free-vibration and resonance-search tests were consistent, showing a natural frequency in the X direction at 1.6 Hz, and 2.5 Hz in the Y direction. Critical damping was estimated as 1% for both directions.

4.1.3 Equivalent Cantilever Loads in Insulator Posts during Time History Tests

At the next stage of testing the switch was tested dynamically by means of the IEEE-compatible Landers strong motion (Landers5L) at two amplitudes: 0.125g and 0.25g PGA. Previous test experience with the 500 kV switches by both the project team and Southern States suggested that the porcelain insulators were identified as a likely critical element. Based on the value of the strain recorded at the bottom of the posts, the equivalent cantilever loads at the posts were estimated. The calculations showed that the porcelain insulators were overstressed (especially rigid post) even for these low levels of testing. Table 4.1 presents the maximum equivalent cantilever load for two principal directions and the maximum of load modulus (all associated with negative or tension strain). The equivalent load calculation was based on using equivalent load factors or load-strain slopes delivered from the calibration test for insulator posts (Table 3.3). The modulus of the equivalent load associated with negative strain was computed for each time data point and only the negative part of the strain record for each direction was used in the computation. The variation in the maximum equivalent cantilever load and the modulus of the equivalent cantilever load reveals close to a linear trend from 0.125g–0.25g levels.

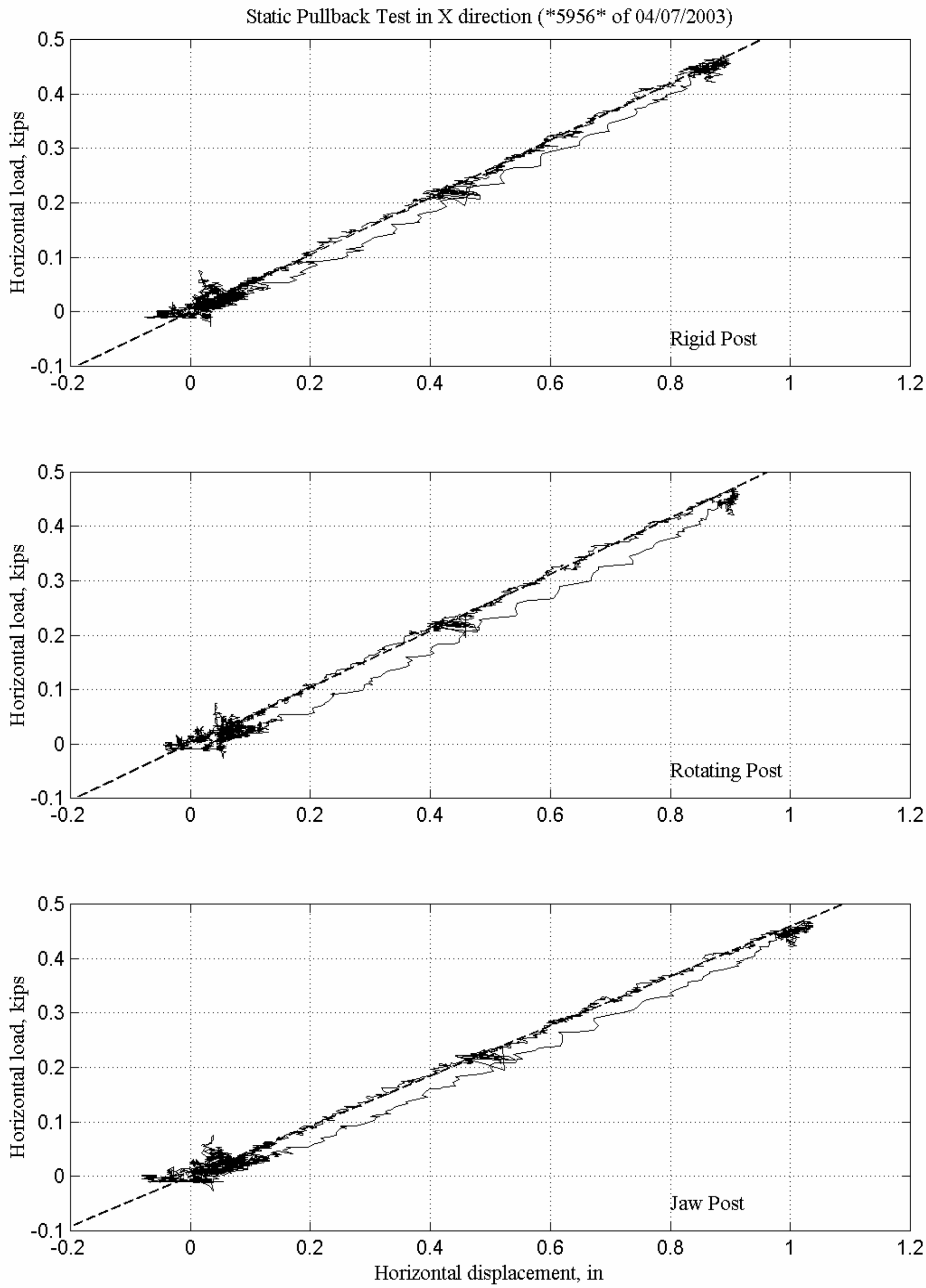

Fig. 4.1 Load versus deflection plots for out-of-plane static pull-back test (original switch)

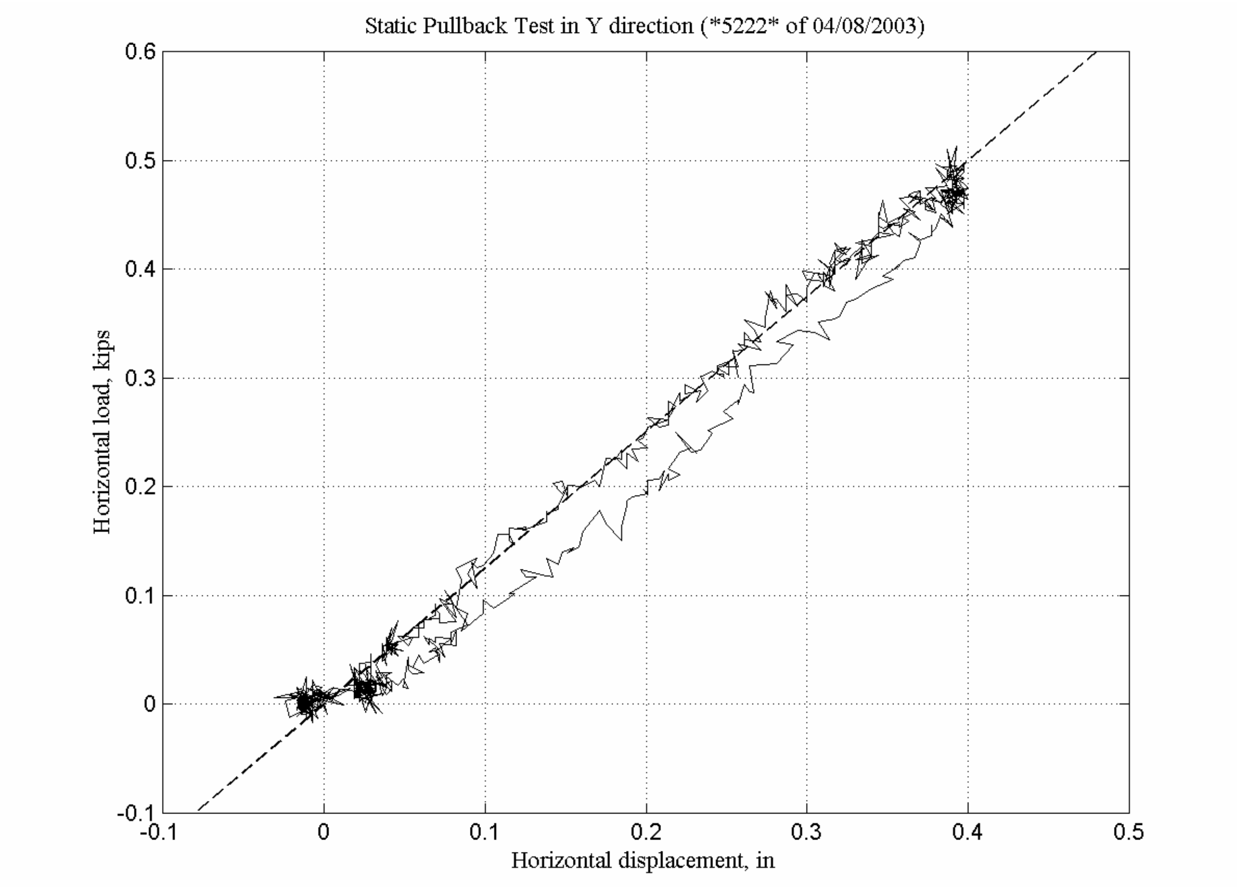

Fig. 4.2 Load versus deflection plots for in-plane static pull-back test (original switch)

Table 4.1 Equivalent cantilever load estimations for insulator posts in original switch

No.	Target PGA, g	Direction	Post	Equivalent cantilever load, lbs	Modulus of equivalent cantilever load, lbs
1	0.125	X	Rigid	727	871
		Y	Rigid	654	
		X	Rotating	181	195
		Y	Rotating	161	
		X	Jaw	452	690
		Y	Jaw	616	
2	0.25	X	Rigid	1536	1552
		Y	Rigid	1051	
		X	Rotating	332	334
		Y	Rotating	264	
		X	Jaw	923	1440
		Y	Jaw	1048	

Strains recorded at two sides (90 degrees apart) at the bottom cross section of each post at the 0.25g level are presented in Figures 4.3–4.4. In the X direction, the maximum strain in the rigid post is about 50% greater than that in the jaw post, whereas the strain in the rotating post is about four times lower than that for the rigid. This conclusion is consistent with equivalent load estimations presented in Table 4.1. It is obvious that the fixture at the base of the rotating post is more flexible than that at the base of the rigid post, which causes the rigid post to carry a portion of the inertial load of the rotating post as well, resulting in overstressing. Based on these load estimates, testing of the original switch was terminated and the modified switch was examined next.

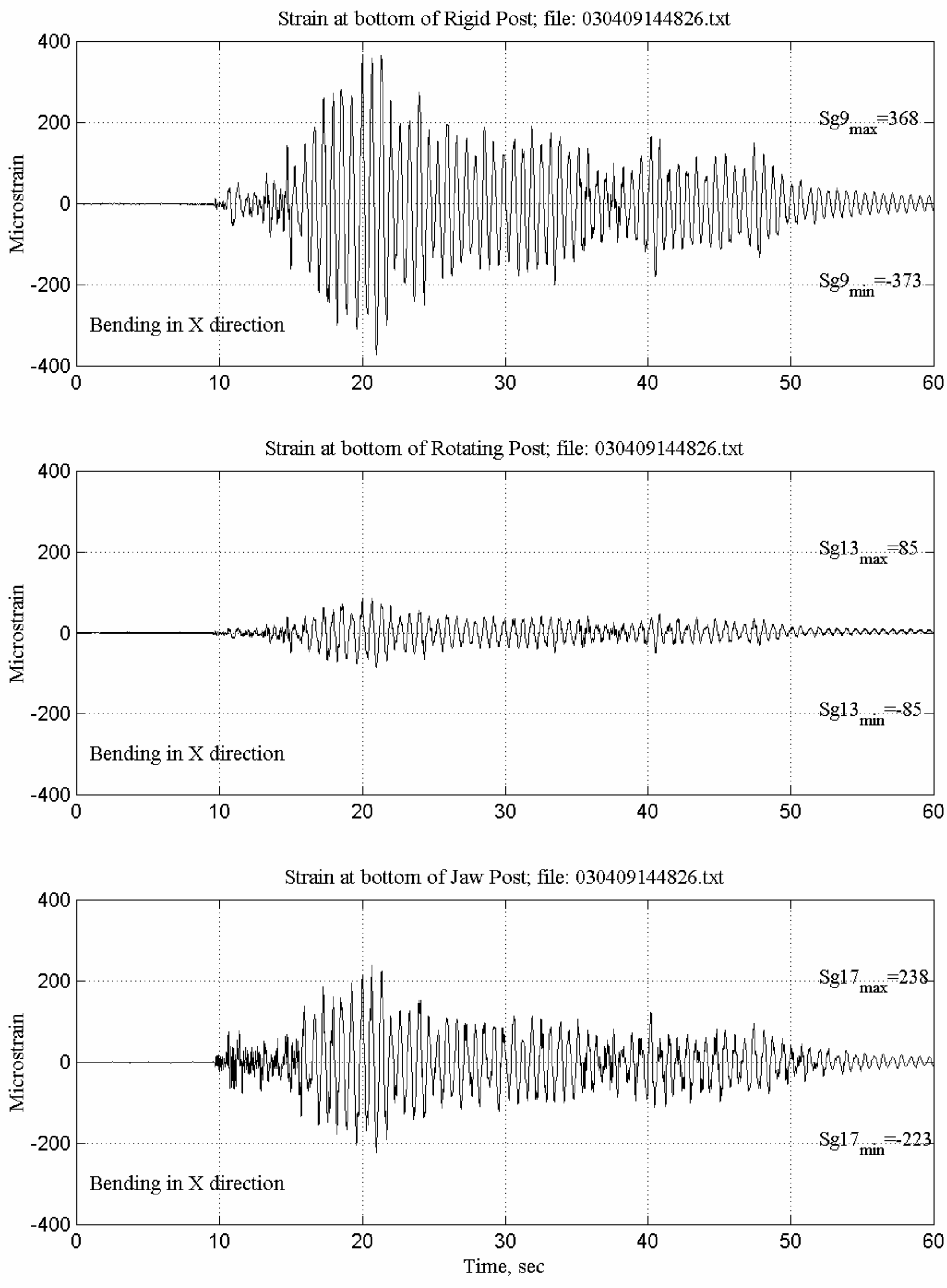

Fig. 4.3 Original switch: strain at bottom of posts associated with bending in X direction

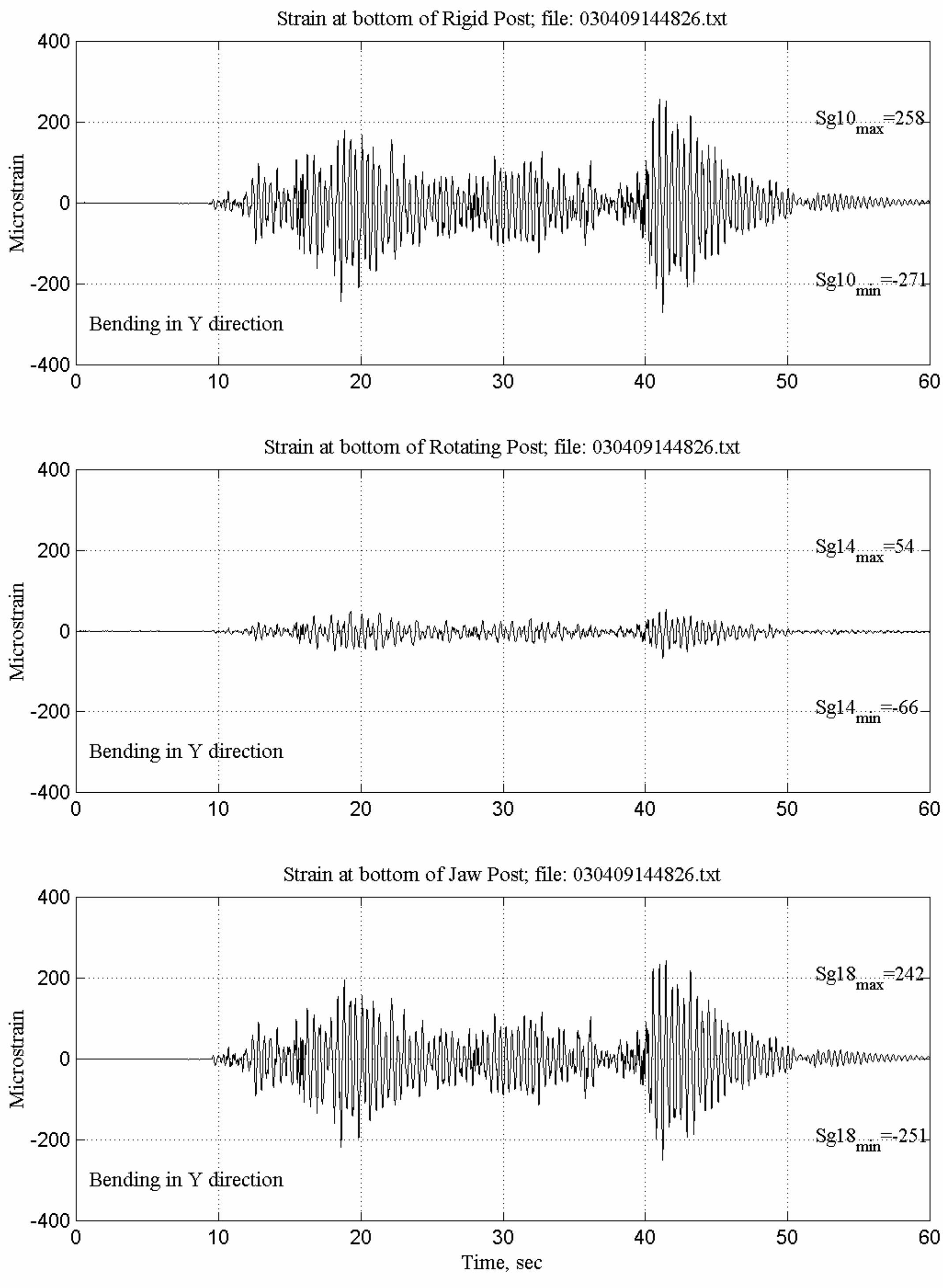

Fig. 4.4 Original switch: strain at bottom of posts associated with bending in Y direction

5 Qualification Tests for Modified Switch on Supports

In this chapter, the IEEE 693 (IEEE, 1998) qualification testing of the modified switch mounted on supports is presented. In a companion PEER report (Takhirov et al., 2004), an IEEE-compatible time history called "TestQke4IEEE" is developed for the IEEE seismic qualification testing, as summarized in Appendix A. This experimental study extensively uses two earlier versions of TestQke4IEEE, filtered to accommodate the capacity limits of the earthquake simulator at UC Berkeley's Richmond Field Station: Landers5L is for testing up to high RRS level and Landers5H for the high PL.

5.1 DETAILS OF DESIGN IMPOVEMENTS IN MODIFIED SWITCH

The main strategy in design improvement was to reinforce the fixture of all posts to the base, especially for the rotating post. In the modified switch the base plates were replaced by thicker plates, and the leveling bolts are replaced by larger bolts at the locations of the rigid and jaw posts. The rotating post fixture was reinforced by adding gussets to the base, replacing a shaft with ball bearings by a shaft with a conical bearing, and by increasing the prestress load in the fixture. Figure 5.1 presents the differences in fixture design for the rigid and rotating post locations. A photo of these two base designs supplied by the manufacturer is presented in Figure 5.2. The left side of the photo shows the base of the original switch, the right shows the base of the modified switch (both switches show views of the rigid post end).

All following tests were conducted on the modified switch, and Figure 5.3 shows the fully assembled switch at one of the test stages.

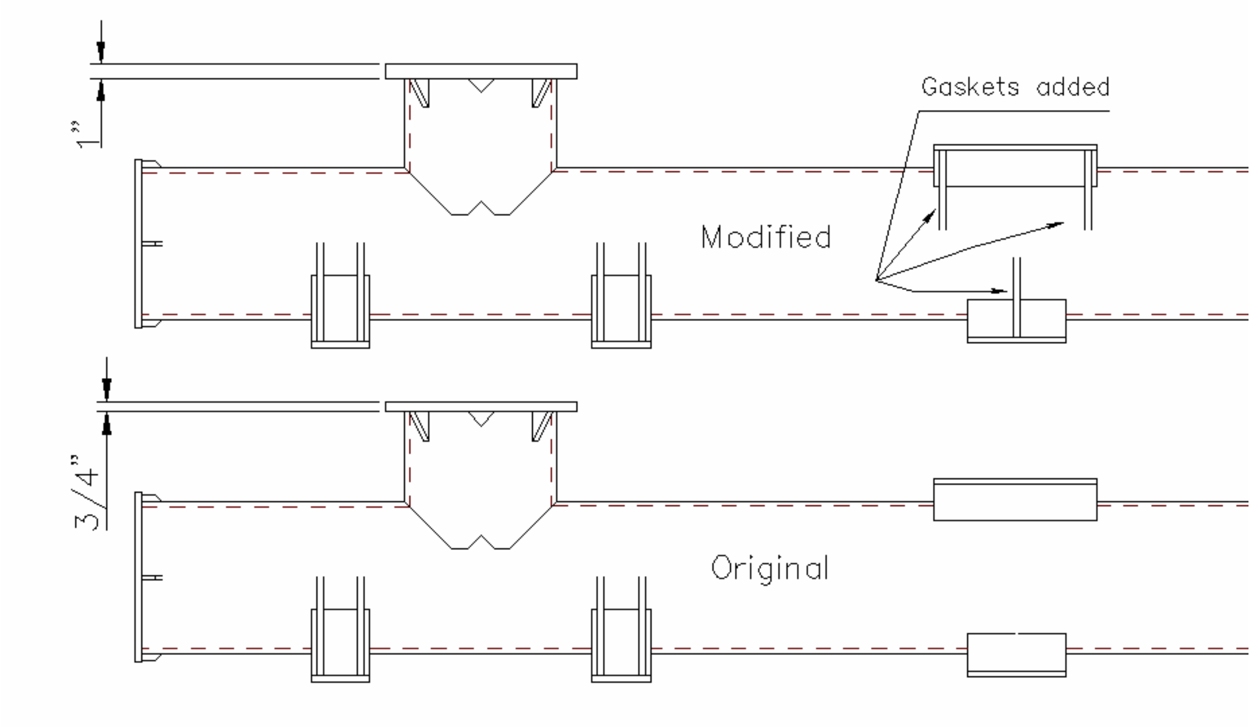

Fig. 5.1 Reinforcement details at base of switch

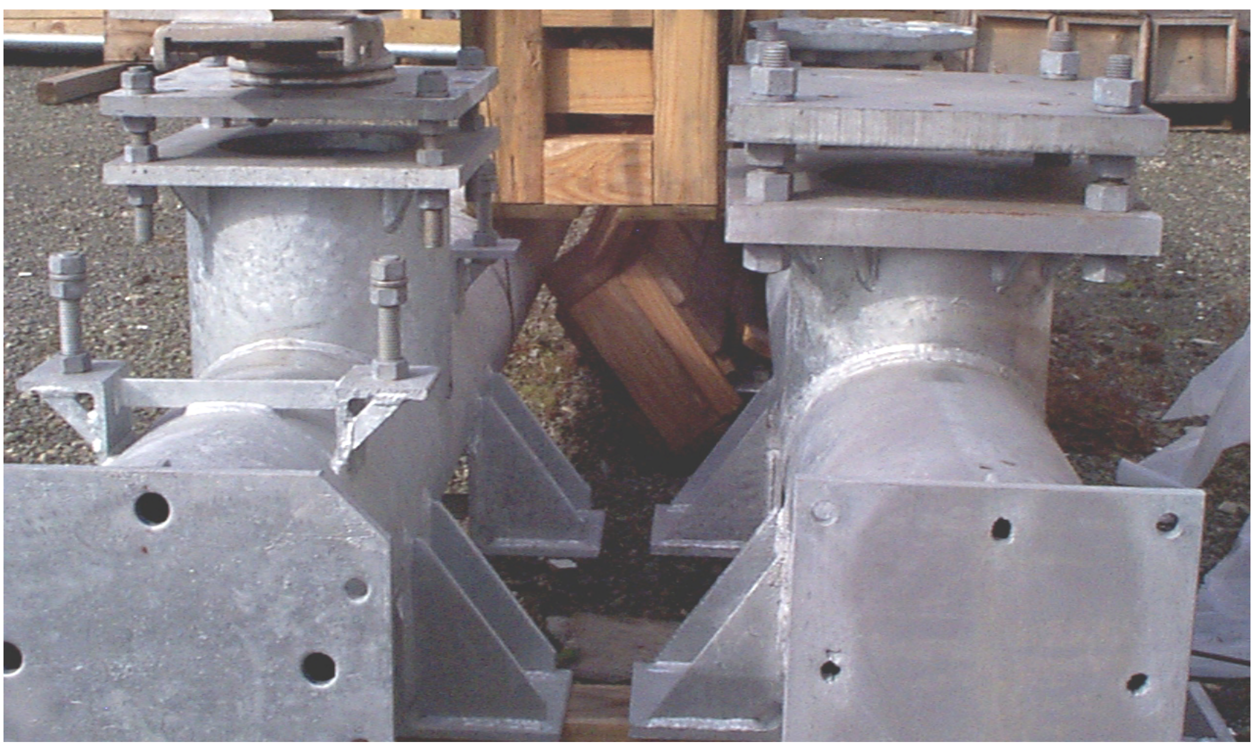

Fig. 5.2 Difference in base design for original (left) and modified (right) switches

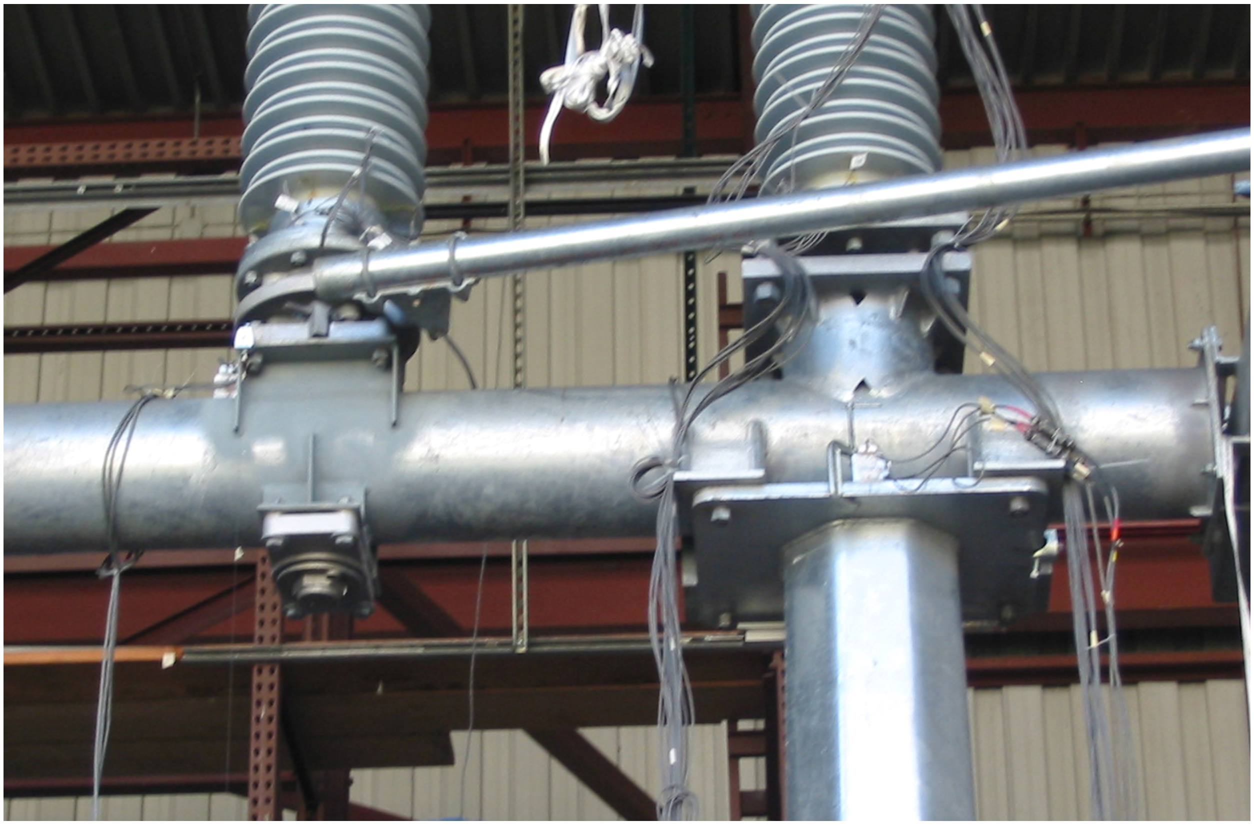

Fig. 5.3 Modified switch assembled on reinforced base

5.2 STIFFNESS, RESONANT FREQUENCY, AND DAMPING

The elastic stiffness of the modified switch was estimated from a static pull-back test conducted in two horizontal directions. The elastic stiffness of the switch in the X direction (out of plane) is estimated as 0.60 kips/in., whereas in the Y direction (in plane) it is estimated as 1.66 kips/in., which is greater than that for the original switch.

Free-vibration tests were also performed in two horizontal directions, showing a resonant frequency of the switch in the X direction and 1.7 Hz and 2.6 Hz in the Y. Critical damping is estimated as 1% for both horizontal directions. The resonant frequency and damping in two horizontal directions were confirmed by random time history and sweep signal testing at low levels of PGA. A summary on the elastic stiffness, the resonant frequency, and the damping is presented in Table 5.1. The plots for resonance-search tests are shown in Appendix C (Figs. C.2–C.4).

Table 5.1 Elastic stiffness, resonant frequency, and damping of modified switch mounted on supports

Direction	Elastic stiffness, kips/in.	Resonant frequency, Hz	Damping, %
X	0.6	1.7	1.0
Y	1.66	2.6	1.0

5.3 TIME HISTORY TESTING

5.3.1 Test Response Spectra at Various Severity Levels of Testing

In the next stage of testing the switch was tested dynamically by means of the IEEE-compatible Landers time history at several severity levels in incremental order from 0.125g–1.0g target PGA. Test response spectra (TRS) were computed at 2% damping and are based on acceleration data recorded at the rigid foundations, and for each level the TRS are plotted at 1/12 octave frequency resolution and compared with the IEEE required response spectrum, as shown in Figures 5.1–5.5. Spectral tolerance limits of –10%/+40% about the target spectra, as discussed in Appendix A, are shown in the plots. These tolerance limits are part of the new recommended requirements, and are not part of IEEE 693-1997.

Because of performance limitations of the earthquake simulator, a number of the spectral ordinates of the TRS are below the required spectrum. The valleys below the IEEE spectrum are sometimes deeper than –10% in the frequency range of the IEEE spectral plateau. The peaks and valleys of TRS are expressed in percents of the spectral accelerations of the RRS at 0.75g and the high PL spectrum at 1.0g, as shown in Figures 5.6–5.7. The vertical dashed line marks the resonant frequency of the modified switch in the direction specified. These plots are similar to the plots in Figures 5.4–5.5 presenting tolerance between the TRS and the required response spectra for the frequency range from 0.3 Hz–33 Hz, but the plots focus only on the spectral accelerations below and above the IEEE spectra that represent possible undertesting and overtesting of the switch in the frequency range from 1 Hz–20 Hz.

The spectral accelerations of the TRS at the resonant frequencies in both horizontal directions, presented in Figure 5.8, demonstrate an almost linear performance of the table. The earthquake simulator slightly underperforms at the high levels of testing in the horizontal directions, and has significant underperformance in the vertical direction.

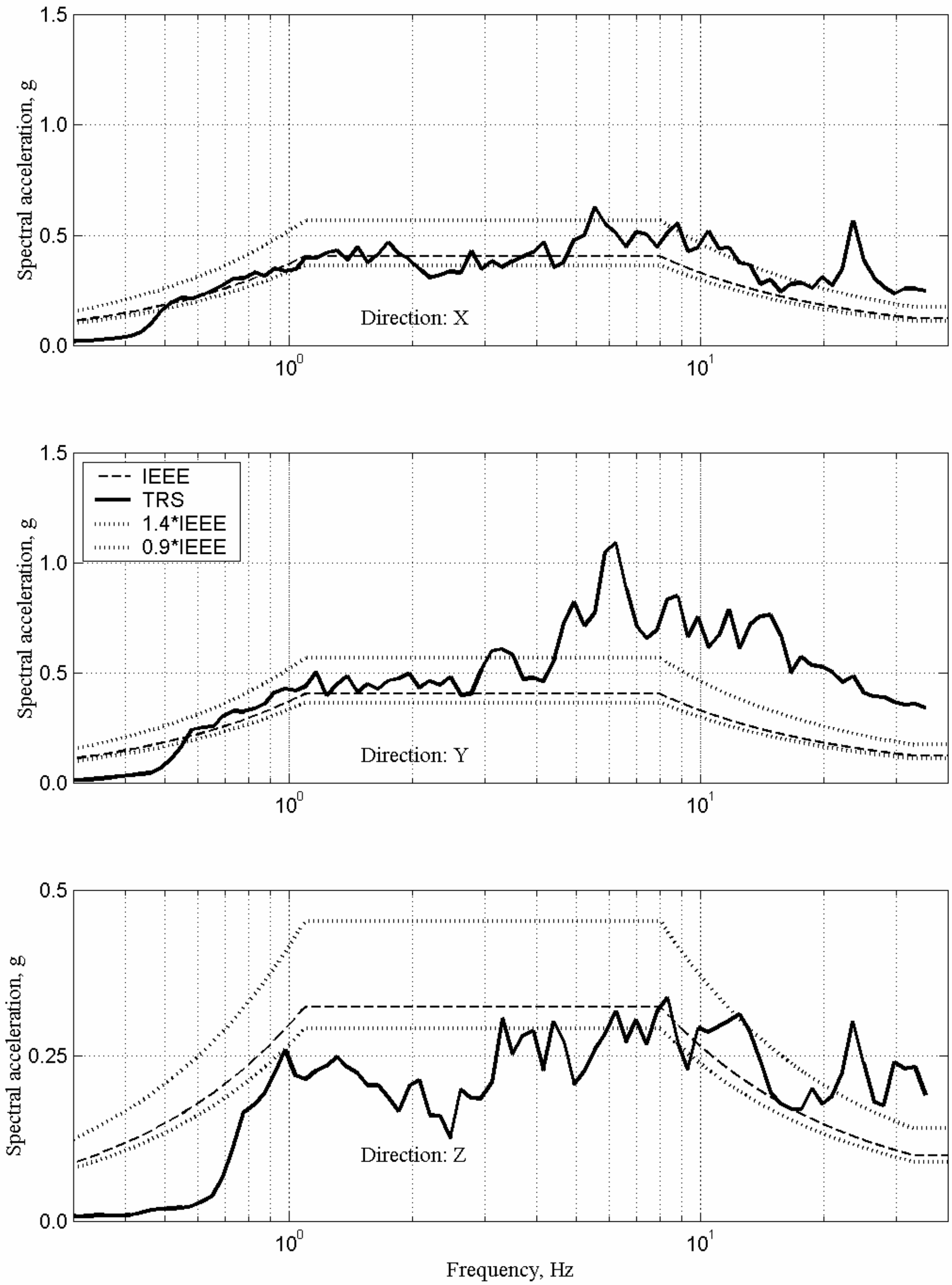

Fig. 5.4 Test response spectra of the modified switch testing at 0.125g for Landers5L

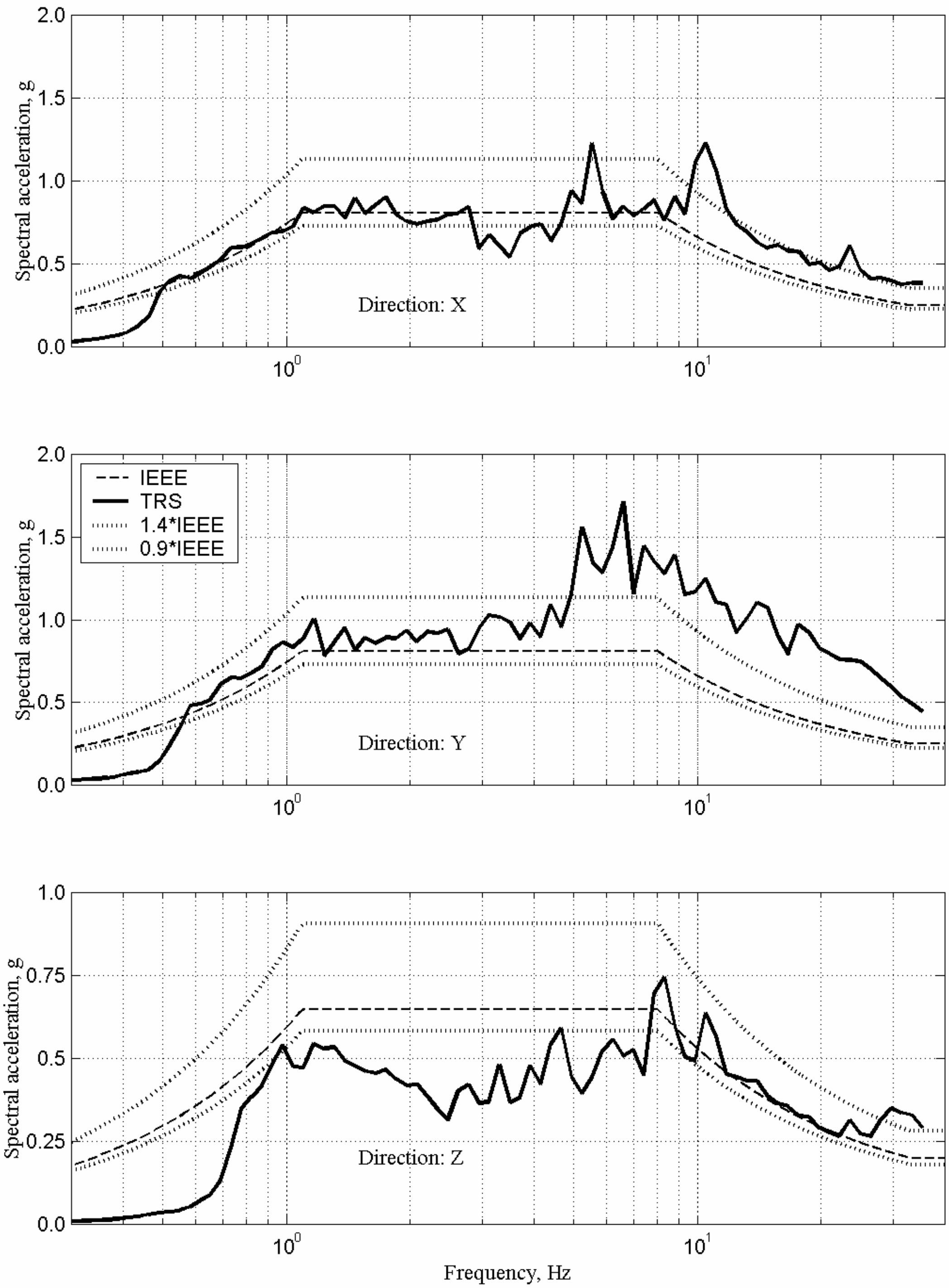

Fig. 5.5 Test response spectra of the modified switch testing at 0.25g for Landers5L

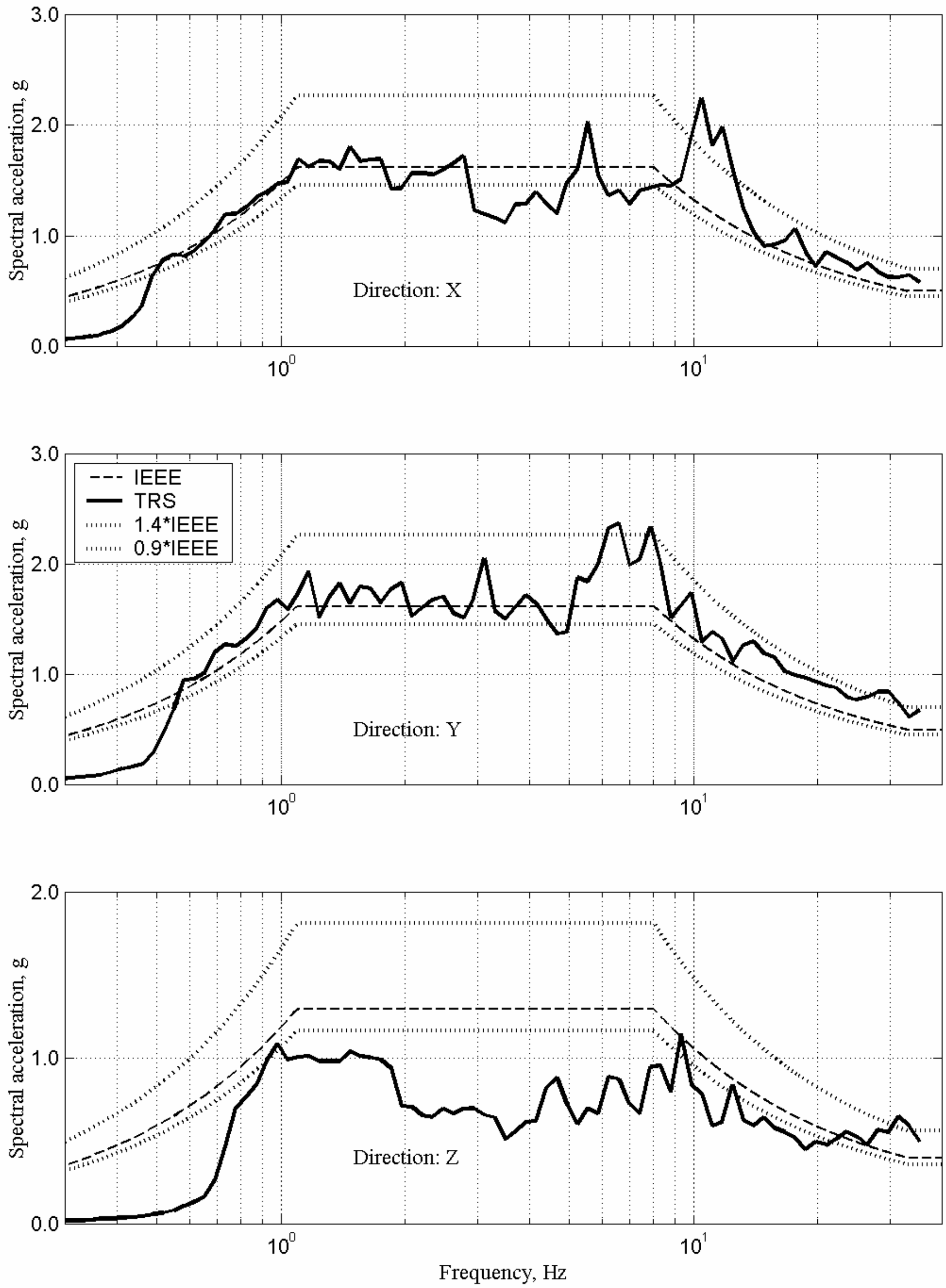

Fig. 5.6 Test response spectra of the modified switch testing at 0. 5g for Landers5L

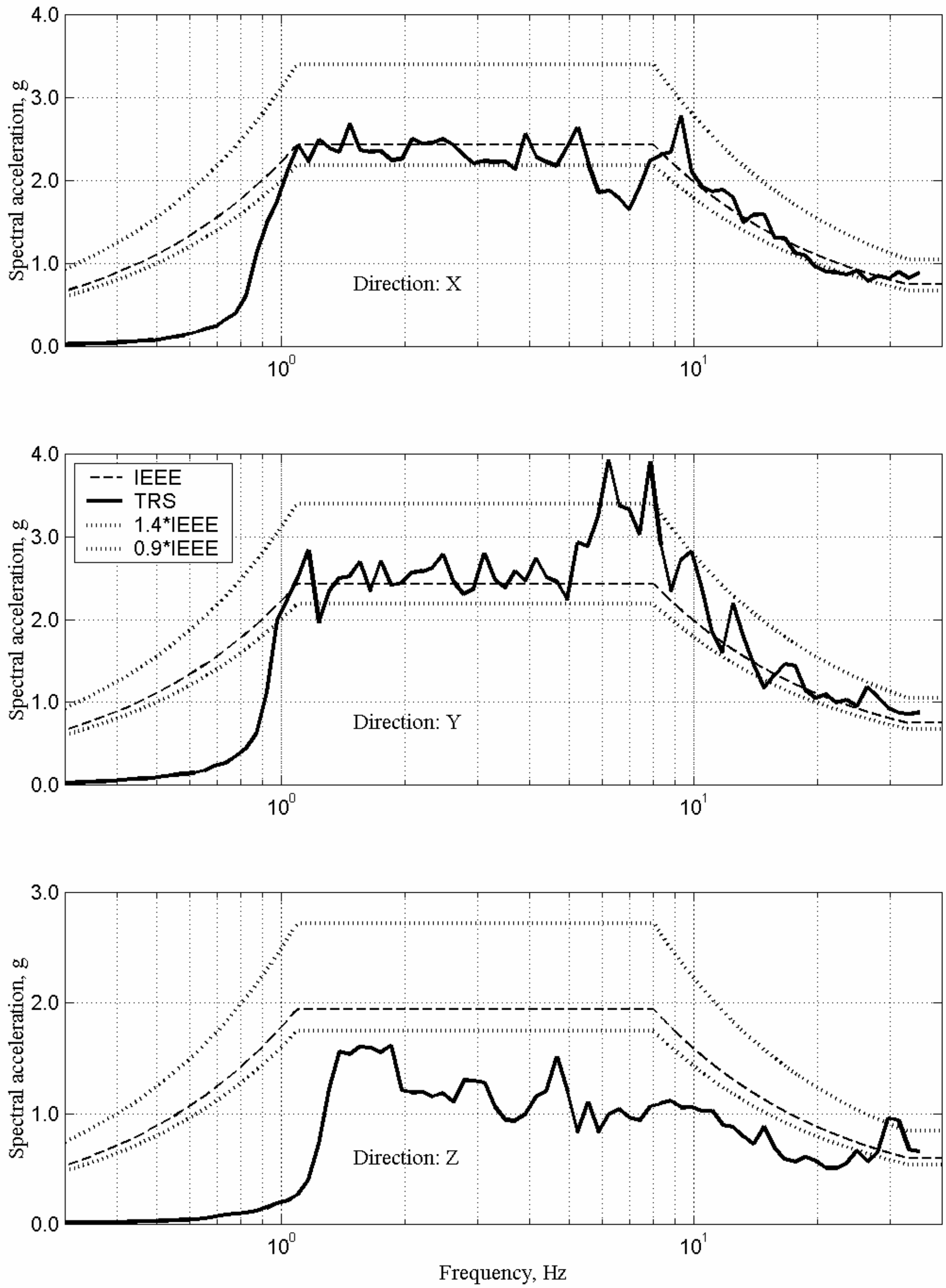

Fig. 5.7 Test response spectra of the modified switch testing at 0.75g for Landers5H

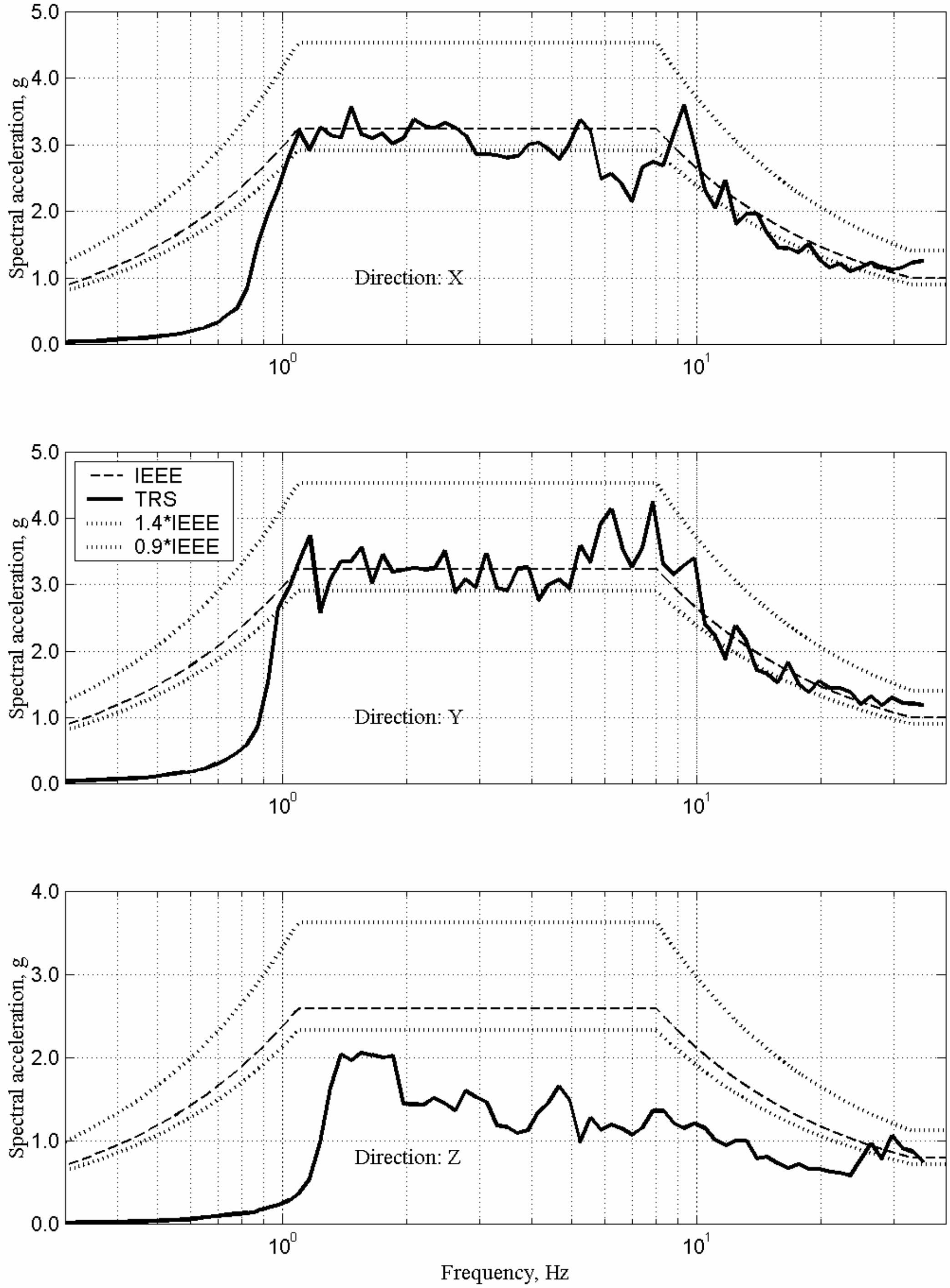

Fig. 5.8 Test response spectra of the modified switch testing at 1.0g for Landers5H

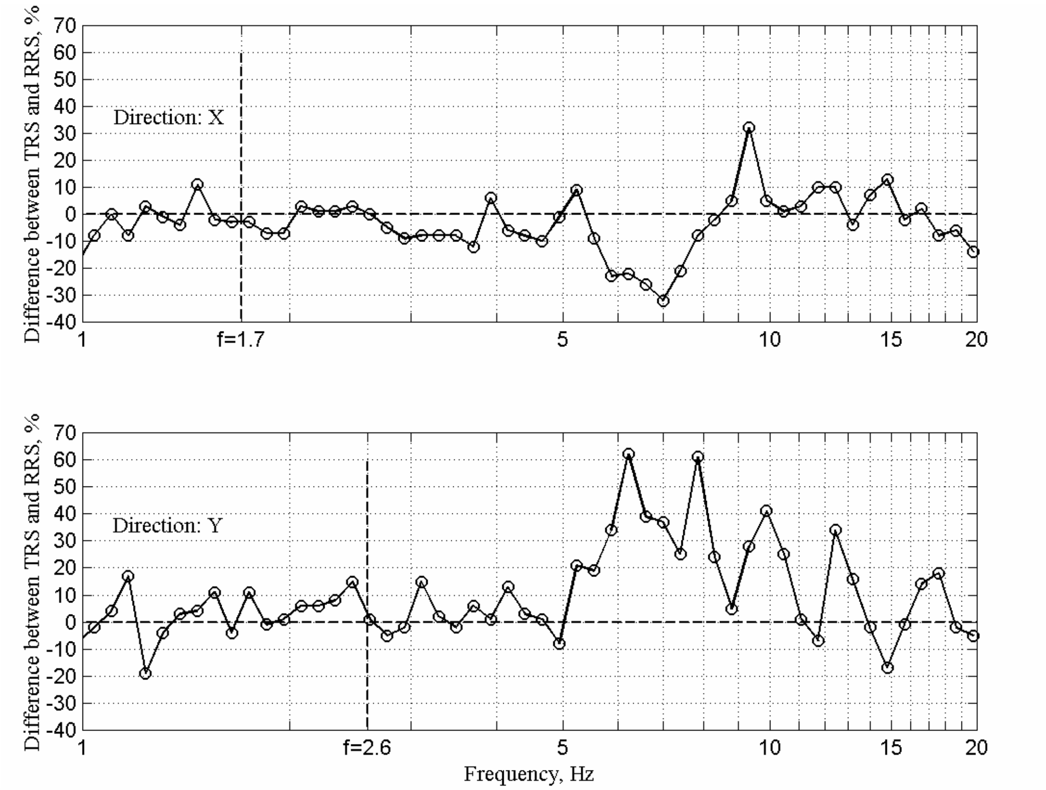

Fig. 5.9 Difference between TRS and high RRS for modified switch testing at 0.75g (Landers5H)

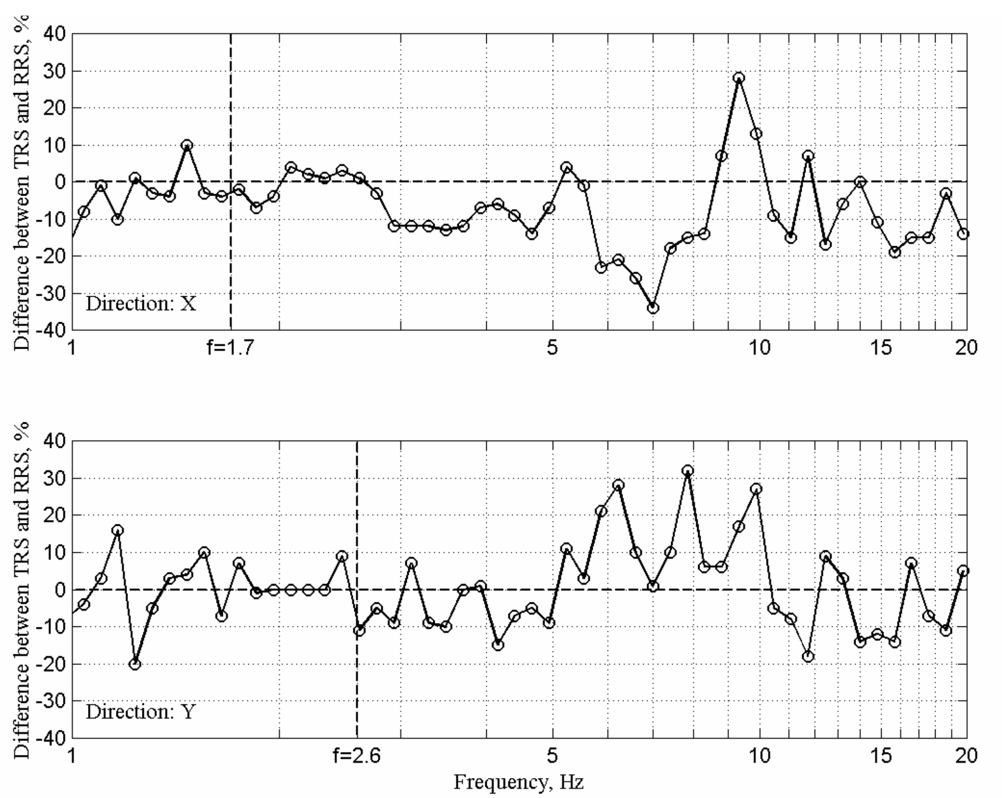

Fig. 5.10 Difference between TRS and high PL for modified switch testing at 1.0g (Landers5H)

Since the switch has no resonant frequency below 12 Hz in the vertical direction, the underperformance in this direction is considered acceptable.

5.3.2 Equivalent Cantilever Load in Insulator Posts

Table 5.2 presents the maximum of the equivalent cantilever load for the two horizontal directions and the maximum modulus of the load, all associated with a negative (tension) strain. The variation in the maximum equivalent cantilever load is quite consistent and is close to linear up to 0.5g target PGA. The modulus of the equivalent cantilever load reveals a linear trend from 0.125g–0.5g target PGA for all three posts, although the trend became nonlinear after 0.5g target PGA for the rigid and jaw posts, as shown in Figure 5.9.

IEEE 693 (IEEE, 1998) provides two options for seismic qualification testing, namely, testing at the RRS level and testing at PL. For high seismic qualification, the RRS testing shall be conducted at 0.5g PGA, whereas the PL testing shall be conducted at 1.0g PGA. In the first case, the acceptance criteria are that the stresses in the most vulnerable parts of a testing article shall be below the allowable stresses, no structural damage shall occur, and the equipment shall be able to perform its electrical functions. This option requires monitoring strain during qualification testing. The PL testing option requires structural integrity of equipment only during and after the test, and the ability to perform its electrical functions. The porcelain posts are rated at 2900 lbs the equivalent cantilever load. At the RRS level of 0.5g target PGA, the porcelain is stressed more than the allowable 50% of the insulator rating at the rigid and jaw posts. This fact means that the modified switch did not pass high seismic qualification testing based on the RRS option because the rigid post was stressed to 92% and the jaw post to 58% of the insulator rating, as shown in Table 5.2.

5.3.3 Summary of Other Response

Displacements, accelerations, and strains were monitored at numerous critical locations on the disconnect switch and supporting structure, as required by IEEE 693. The maximum displacements at the top of the insulator posts are summarized in Table 5.3, and the maximum accelerations in Table 5.4. A summary of the maximum strains, stresses, and equivalent cantilever loads on the posts is provided in Table 5.5. The stresses at strain gage locations on the supports are less than, but close to. the nominal 50 ksi yield stress of the support material. Since the strain gages were installed at 20 in. above the base plate of the support, the stress in the support at the base plate is estimated as 50 ksi, approximately equal to the yield stress of the steel.

5.3.4 Electrical Continuity and Resistance Checks

Low voltage continuity of the main circuit was monitored during each time history testing, and no continuity interruptions were observed. The resistance of the main circuit was checked before and after tests with 0.75 and 1.0g target PGA, and proved to be within the allowable resistance of up to 20% as required by IEC 60694 (IEC, 1996). For the shake table tests, low-current capacity fuses were inserted into the motor operator circuit and are designed to break the circuit in the event that the motor operator is activated during shaking. The fuses of the motor operator were also checked for continuity to make sure that they were not blown during dynamic testing, and switch functionality and assembly alignment were also checked after 0.75g and 1.0g tests (Table 5.6).

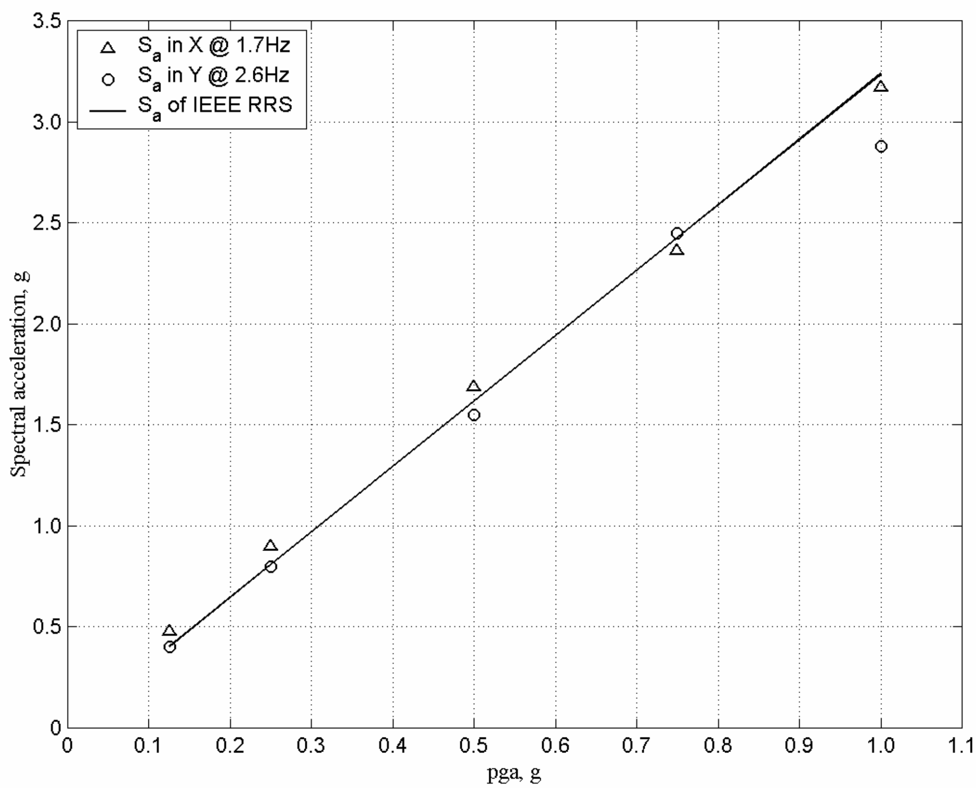

Fig. 5.11 Spectral accelerations of TRS at resonant frequencies for all levels of earthquake testing

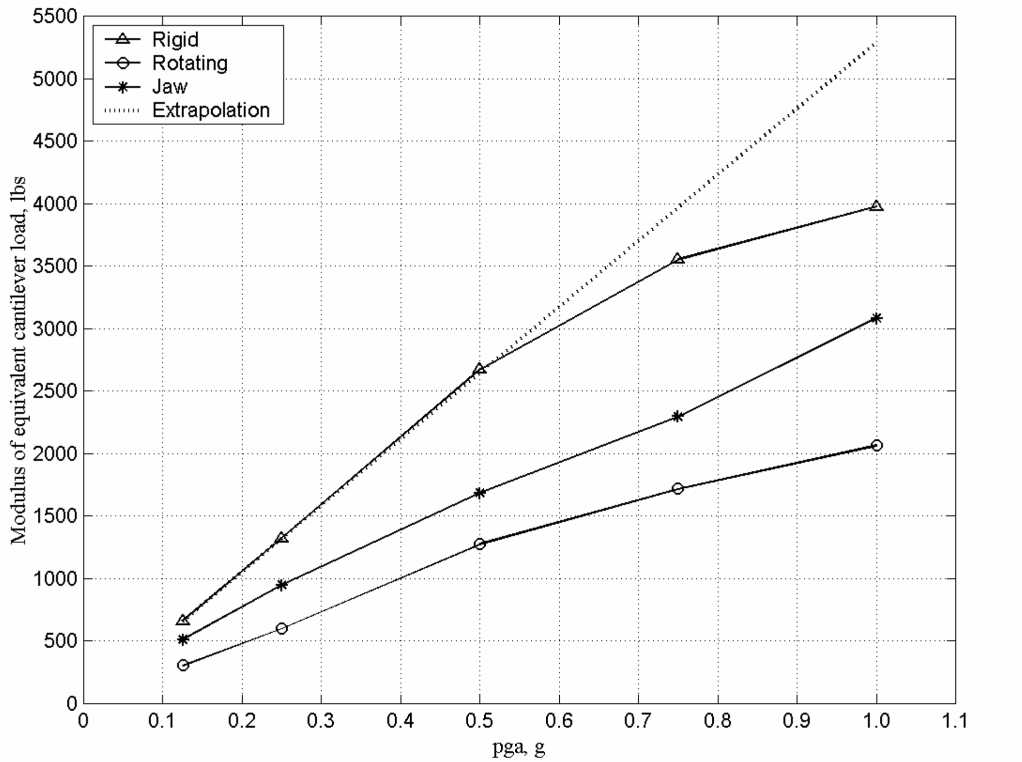

Fig. 5.12 Moduli of equivalent cantilever load for insulator posts for target PGA

Table 5.2 Equivalent cantilever loads at insulator posts for all severity levels

		Demand load (equivalent cantilever), lbs			Demand load/ Rated Cantilever load, %		
Target PGA, g	**Direction**	**Rigid**	**Rotating**	**Jaw**	**Rigid**	**Rotating**	**Jaw**
0.125	X	635	306	451	22	11	16
	Y	554	222	488	19	8	17
	Modulus	661	306	511	23	11	18
0.25	X	1211	589	735	42	20	25
	Y	914	397	948	32	14	33
	Modulus	1322	601	948	46	21	33
0.50	X	2459	1235	1302	**85**	43	45
	Y	1640	767	1672	**57**	26	**58**
	Modulus	2673	1275	1686	**92**	44	**58**
0.75	X	3395	1704	1849	**117**	59	64
	Y	2558	1128	2241	88	39	77
	Modulus	3552	1717	2296	**122**	59	79
1.0	X	3826	2061	2546	**132**	71	88
	Y	3103	1301	2703	**107**	45	93
	Modulus	3977	2066	3081	**137**	71	**106**

Table 5.3 Maximum displacements (relative to table) at all elevations of modified switch

Target PGA, g	Direction	East support, in.	West support, in.	Rigid post, in.	Rotating post, in.	Jaw post, in.	From Rotating to Jaw posts, in.
0.125	X	0.34	0.48	1.57	2.75	1.57	
	Y	0.25	0.25	1.05	1.05	0.98	0.08
	Modulus	0.34	0.48	1.58	2.75	1.58	
0.25	X	0.68	1.03	3.28	5.84	3.45	
	Y	0.45	0.44	1.92	1.92	1.84	0.30
	Modulus	0.71	1.03	3.35	5.88	3.51	
0.50	X	1.34	2.17	6.87	12.43	7.21	
	Y	0.74	0.71	3.67	3.67	3.42	1.17
	Modulus	1.39	2.20	7.23	12.64	7.56	
0.75	X	1.86	2.88	10.20	17.75	10.20	
	Y	1.23	1.20	6.33	6.33	5.34	3.01
	Modulus	1.91	2.88	10.46	17.95	10.50	
1.0	X	2.39	3.40	NA	NA	NA	
	Y	1.48	1.41	NA	NA	NA	4.13
	Modulus	2.40	3.42	NA	NA	NA	

Note: Displacement transducers were disconnected for 1.0g tests.

Table 5.4 Maximum accelerations (relative to table) at all elevations of modified switch

Target PGA, g	Direction	Table, g	West support, g	East support, g	Rigid post, g	Rotating post, g	Jaw post, g	Blade, g
0.125	X	0.21	0.65	0.82	1.07	1.32	1.56	2.46
	Y	0.30	0.60	0.60	1.16	1.27	1.00	1.28
	Z	0.12	0.17	0.17	0.23	0.43	0.21	0.66
	Modulus		0.70	0.85	1.18	1.37	1.60	2.46
0.25	X	0.39	0.92	0.82	1.94	2.02	1.48	2.29
	Y	0.46	1.06	1.06	1.86	NA(1)	1.97	2.28
	Z	0.21	0.23	0.19	0.24	0.52	0.24	0.77
	Modulus		1.10	1.22	2.13	NA(1)	2.03	2.46
0.50	X	0.53	1.58	1.15	3.97	4.16	2.14	4.14
	Y	0.60	1.41	1.43	3.17	NA(1)	3.60	4.16
	Z	0.31	0.31	0.25	0.44	0.90	0.59	1.86
	Modulus		1.61	1.55	4.51	NA(1)	3.63	4.40
0.75	X	0.68	2.05	1.97	5.30	5.10	3.11	NA(2)
	Y	0.82	2.46	2.52	5.03	NA(1)	3.88	NA(2)
	Z	0.36	0.35	0.47	0.73	2.00	0.67	5.91
	Modulus		2.53	2.52	5.60	NA(1)	4.40	7.24
1.0	X	1.04	2.12	2.27	5.64	5.43	4.63	NA(2)
	Y	1.14	2.44	2.43	5.24	5.91	3.98	NA(2)
	Z	0.47	0.56	0.51	1.29	3.87	1.14	NA(2)
	Modulus		2.81	2.77	6.73	7.00	5.37	NA(2)

Notes: (1) Accelerometer in Y direction is malfunctioning. (2) Accelerometer is out of range (accelerations are greater than 5.0g). (3) See Figure 2.1 for coordinate system definition.

Table 5.5 Strain, stress, and equivalent cantilever loads at east (E) and west (W) supports

Target PGA, g	Direction	StrainE, ms	StrainW, ms	StressE, ksi	StressW, ksi	LoadE, kips	LoadW, kips
0.125	X	160	247	4.65	7.16	1.37	2.11
	Y	133	132	3.84	3.83	1.13	1.13
	Modulus	167	254	4.83	7.36	1.42	2.17
0.25	X	336	496	9.74	14.37	2.87	4.23
	Y	234	238	6.79	6.90	2.00	2.03
	Modulus	351	505	10.18	14.65	3.00	4.31
0.50	X	647	999	18.75	28.98	5.52	8.53
	Y	372	366	10.78	10.61	3.18	3.12
	Modulus	665	1018	19.29	29.51	5.68	8.69
0.75	X	893	1322	25.90	38.34	7.63	11.29
	Y	637	634	18.48	18.39	5.44	5.42
	Modulus	893	1324	25.90	38.38	7.63	11.30
1.0	X	1134	1543	32.89	44.76	9.68	13.18
	Y	723	723	20.96	20.96	6.17	6.17
	Modulus	1136	1553	32.95	45.04	9.70	13.26

5.3.5 Minor Anomalies after PL Test at 1.0g Target PGA

The switch sustained the PL level of testing at 1.0g target PGA without major structural damage, and the electrical continuity of the switch was not interrupted. The switch functioned as required, although anomalies were observed in the post-test inspection. The stationary arc horn was bent by an impact during the test (Fig. 5.9). In addition, the joint of the vertical pipe with the box of the motor mechanism was dislocated (Fig. 5.10). Both anomalies were repaired easily, and appear to be amenable to simple corrective actions by the manufacturer.

Table 5.6 Results of functionality inspection

1 **General information:**

(a)	Specimen	Modified Switch	Modified Switch
(b)	Mounting	Support	Support
(c)	Main blade	Closed	Closed
(d)	Ground blade	Open	Open
(e)	Level of testing, g	0.75	1.0
(f)	Time history	Landers5H	Landers5H
(g)	Date	5/15/2003	5/15/2003

2 **Visual inspection results:**

(a)	Overall assembly for alignment	OK	OK
(b)	Insulators at base for cracks	OK	OK
(c)	Jacking bolts for deformation	OK	OK
(d)	Live part casting: hinge and jaw	OK	OK
(e)	Blade ring for impact	OK	OK
(f)	Motor operator fuses for continuity	OK	OK

3 **Millivolt drop test** (1)

a)	Before testing, mΩ	71	71
b)	Before testing, mΩ	71	74
c)	Resistance change, %	0	4
d)	Allowed, %	20	20

4 **Mechanical operating test** (2)

a)	Alignment during operation	OK	OK
b)	Operating functionality	OK	OK

5 **Main circuit continuity** (3)

a)	Any loss of continuity	No	No

6 **Anomalies**

	(a) four 5/8 SST bolts in rear hinge loose — retightened	(a) stationary arc horn bent — restored
	(b) VM-1 (motor mechanism) key bounced out of place — installed a bolt in lock ring	(b) main switch vertical pipe popped out of place — fixed
	(c) adjustable arm popped out of toggle	

Notes:

(1) Estimate change in resistance of the main circuit

(2) Open the main blade of the closed switch to the extent possible and return to the closed position

(3) Checked only for switch in closed position

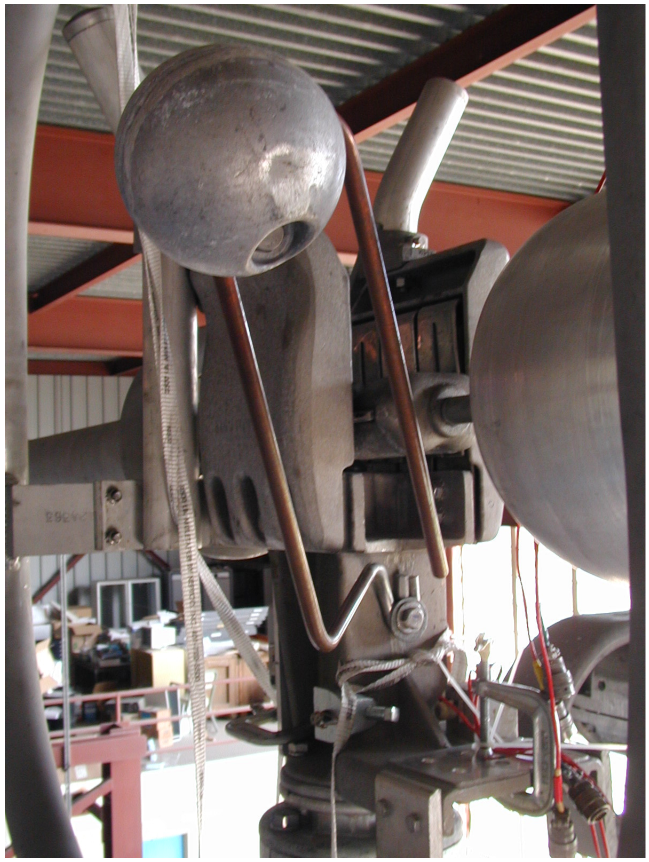

Fig. 5.13 Anomaly 1: stationary arc horn bent away from blade (formerly in contact with blade)

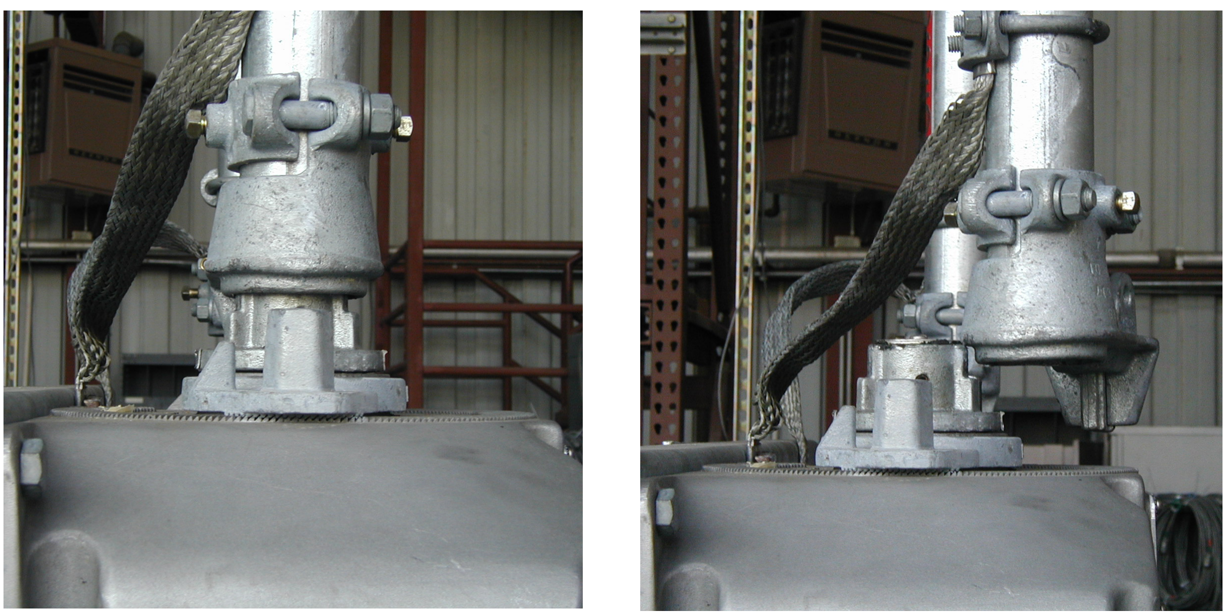

Before PL test **After PL test**

Fig. 5.14 Anomaly 2: vertical pipe of main switch out of joint

5.4 SUMMARY AND CONCLUSIONS

5.4.1 RRS Enveloping and Tolerance Zone Criteria

A comparison of the TRS with the target IEEE PL spectra anchored to 1.0g PGA is shown in Figure 5.11. These plots and the zoomed versions shown in (Fig. 5.12) show that the TRS fell below the target IEEE PL spectra in various frequency ranges in both the horizontal and vertical directions.

In general, deficiencies in the TRS for the vertical direction are not of interest when considering the seismic performance of the switch. The deficiencies in the TRS for the X and the Y horizontal directions vary up to about 30% within the plateau of the IEEE PL target spectra, but only about 3–10% in the region close to the important resonant frequencies of the switch. The new recommended specifications for development of input motions summarized in Appendix A permit a -10% deviation in the TRS compared to the required (RRS or PL) spectra.

It is of interest to note that the TRS falls only about 3% below the required PL spectrum for the X direction. The X direction (transverse to the switch base) loading dominates the total demand load on the rigid insulator post, which is the most highly stressed insulator (Table 5.2).

Strictly speaking, the TRS does not satisfy the requirements of the new recommended specification because of the deviations away from the RRS at the resonant frequencies of the equipment. However, because the switch behavior is dominated by the modes of vibration at 1.7 and 2.6 Hz in the X and Y directions, respectively, these deficiencies, had they been corrected, would not been expected to have a significant effect on switch performance.

5.4.2 Qualification Testing Acceptance Criteria Related to PL Testing

The disconnect switch preserved its major functions after the PL testing without any major damage. Some anomalies that occurred during the test were insignificant. The restoration work did not involve any installation of new parts. Parts impacted out from their original positions were simply repositioned back in place, and corrective actions required to prevent their recurrence appear to be relatively simple. Therefore, the disconnect switch complied with the functional requirements for PL testing.

Although the TRS came close to satisfying the new recommended input motion specifications for IEEE 693, the rigid insulator post in the PL test was loaded to a level 37%

beyond the rated cantilever strength of 2900 lbs assigned to this model of insulator by the manufacturer. Fracture of the porcelain insulator post did not occur during the PL test although the actual strength of the installed insulator exceeded the rated cantilever strength by more than 40%. This outcome highlights the conservatism associated with insulator cantilever strength ratings, which are essentially guaranteed minimum breaking strengths, as discussed previously.

One possible means of mitigating the high stresses experienced by the porcelain insulators is through the use of higher strength, lighter insulators. The insulators used in this project were extra-high-creep models, which are used by utilities in coastal or high air pollution areas. Insulators with extra-high-creep ratings have additional conical or more complex-shaped sheds, which generally add more mass to the insulator. At the time of this writing, the project utility participants were in the process of implementing new procurement specifications for improved insulators to be used with 500kV switches.

The acceptance criteria of IEEE 693-1997 for equipment qualified by PL testing permits the omission of strain gages during this very challenging test. The rationale for this provision is as follows: since the PL test subjects the equipment to a loading environment representative of the highest level of shaking that could be expected, maintaining its functions without severe structural damage, such as fracture, is sufficient to demonstrate qualification. The results of the PL test conducted in this project demonstrate that such a practice can lead to unconservative results when substantial overstrength or uncertainty in material strengths/ capacities are involved. This is particularly true for non-ductile components such as porcelain insulators. The shortcomings of the noted provisions of IEEE 693-1997 should be considered for revision.

Nevertheless, the overall performance of the switch mounted on a 14-ft-tall support structure tested in this project was very favorable. The tests were conducted to high levels of shaking with no failures and no significant anomalies. It should be noted that for 500kV disconnect switches, the closed position is of most interest to utilities, since switches of this voltage class are almost always in this position.

A detailed discussion of the qualification of the switch to IEEE 693-1997 will be presented in a separate report prepared by the equipment manufacturer.

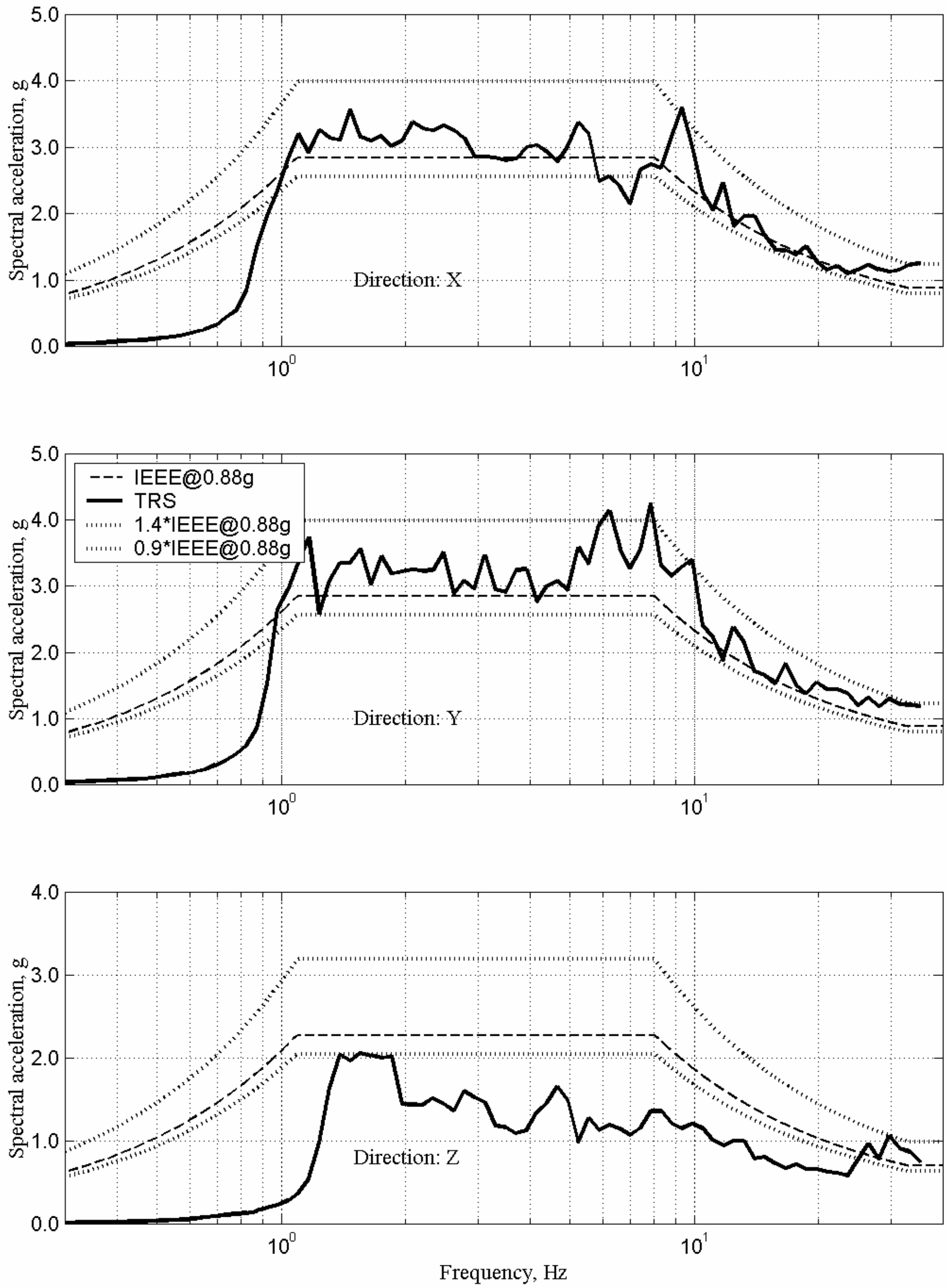

Fig. 5.15 Test response spectra plotted against high seismic PL response spectra at 0.88g

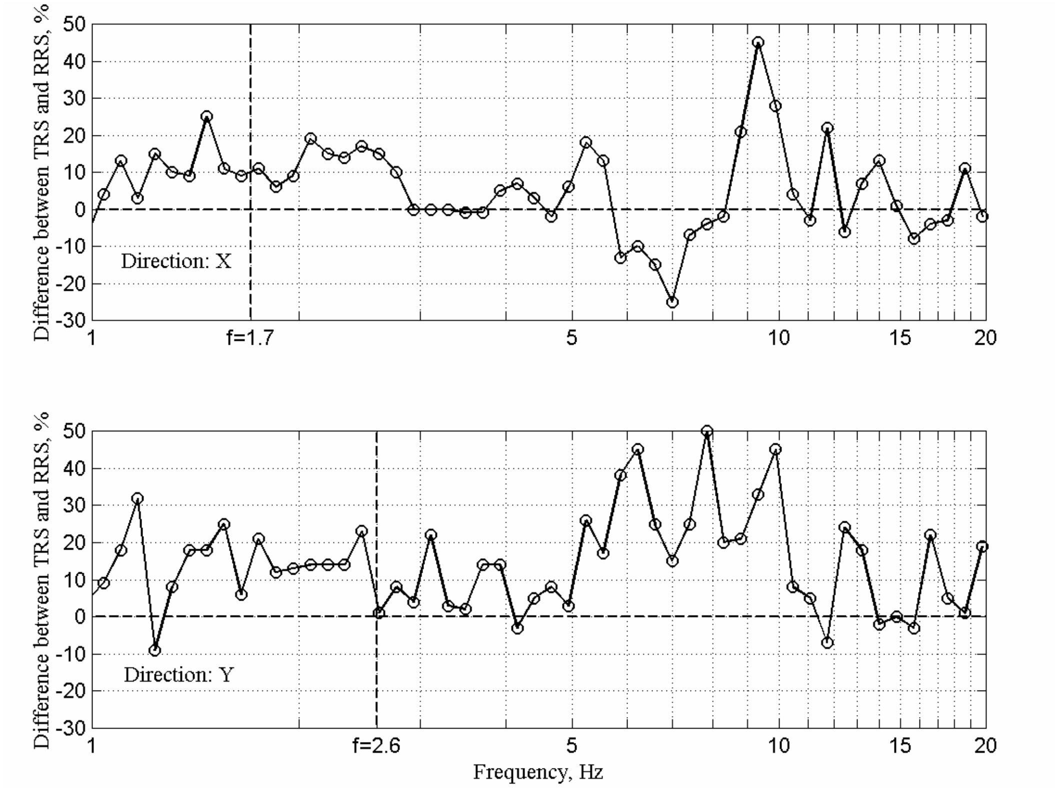

Fig. 5.16 Difference between TRS and high seismic PL spectra anchored at 0.88g

6 Qualification Tests for Modified Switch in Open Position without Supports

This chapter presents the experimental results and discussions related to the seismic qualification testing of the disconnect switch with the main contact open and without tall supports. The qualification testing of the switch mounted on the supporting structure was conducted only with the main blade in the closed position because of the limited vertical clearance above the earthquake simulator platform. To qualify the disconnect switch with the main contact open, it was tested without the supports, but the input motion was scaled to represent the dynamic amplification of the supports. A switch mounted on supports, on short spacers, and rigidly attached to the table (without the supports) was tested at 0.25g target PGA and the results were compared. Based on a ratio of response parameters at the critical locations of the switch observed in these three configurations, the amplification factor was established. Finally, at the stage of qualification testing of the switch in the open-blade position, the switch mounted on short spacers (without 14-ft-tall supports) was subjected to a time history scaled up by the amplification factor.

6.1 ESTIMATION OF AMPLIFICATION FACTOR

6.1.1 Configurations of Disconnect Switch with Main Blade Closed

The experimental study on the amplification factor was conducted for three configurations of the modified switch: mounted on 14-ft-tall supports, mounted on 4-in. spacers, and without the supports, as defined in Chapter 2. The spacer was used to replicate the local flexibility of a 1-in. plate on the top of the 14-ft-tall supports. To have comparable specimens, the switch in all three configurations was tested with the main blade closed, since the tallest configuration, the support-mounted switch, could not be tested with the main contact open.

6.1.2 Resonant Frequency and Damping

Table 6.1 summarizes the resonant frequency and damping of the switch in the three configurations, which were established from excitation-and-release (free-vibration) tests and random and sweep testing. As the stiffness of the system increases, the resonant frequencies in both horizontal directions steadily increase from the most flexible configuration (support mounted) to the least flexible one (switch rigidly mounted to the table). Since the resonant frequencies of all three configurations are within a frequency range covering the spectral plateau of the IEEE RRS, the data from time history testing in different configurations are assumed to be comparable.

Table 6.1 Resonant frequency and damping of modified switch with closed blade

Configuration	Direction	Resonant frequency, Hz	Damping, %
Support (with 14-ft-tall columns)	X	1.7	1.0
	Y	2.6	1.0
Spacer	X	2.5	2.0
	Y	3.4	2.0
Rigid	X	3.0	2.0
	Y	3.9	1.0

6.1.3 Amplification Factor Based on Critical Loads Ratio

The estimate of the amplification factor due to the supports is based on negative (tension) strain data gathered during time history testing of the switch in three configurations conducted at the same target PGA of 0.25g. The amplification factor was calculated from modulus ratios of the equivalent cantilever load for two pairs of configurations: support versus rigid and support versus spacer. All comparisons for determining the amplification factor are made with the main contact closed. The configuration pairs used in the cross comparisons are shown in Figure 6.1. The ratio is determined for each post, as summarized in Table 6.2. The ratios are quite consistent for these two comparisons: up to 1.7 for the jaw post, 1.83 for the rotating post, and up to 1.57 for the rigid post. The rigid post, which is the most overstressed post, has the smallest amplification factor, whereas the least overstressed post, the rotating post, has the largest amplification factor.

The differences in the amplification factor computed for the three insulator posts and the distribution of forces between the three insulator posts suggest that there are differences in behavior of the switch when mounted on the 14-ft-tall supports as opposed to spacer or rigid-support mounting. While the reasons for these differences cannot be known with certainty, they may be related to differences in the dynamic response caused by the support structures, differences in behavior related to play in the rotating bearing (at the base of the rotating insulator post), or other causes.

An alternative to the amplification factors may be to use a more gross measure of response such as the sum of equivalent cantilever loads in the rotating and rigid insulator posts. The rationale for this approach is that it provides a measure of total inertial loading on the two hinge-end insulators, whereas the distribution of forces on individual insulators may vary with the intensity of shaking. This approach would result in amplification factors of about 1.5 and 1.66 for the spacer and rigid-mounted conditions, respectively.

For simplicity, the most conservative amplification factor of 1.83 is selected as an amplification factor for qualification testing of the switch in the open position. The advantage of selecting the highest amplification factor for testing is that downward adjustments to the amplification factor can be made at a later date, after completion of testing.

Table 6.2 Amplification factor calculation at 0.25g target PGA testing based on use of negative strain

Configuration	Post	Modulus of equivalent cantilever load, lbs	Amplification factor
Support	Jaw	1089	
	Rotating	590	
	Rigid	1426	
Spacer	Jaw	672	1.62
	Rotating	322	**1.83**
	Rigid	1076	1.33
Rigid	Jaw	641	1.70
	Rotating	322	**1.83**
	Rigid	906	1.57

(a) Configuration without supports (rigid or spacer) (b) Support-mounted configuration

Fig. 6.1 Two cross-compared pairs of configurations used in amplification factor estimation

6.2 SEISMIC QUALIFICATION TESTING OF DISCONNECT SWITCH IN OPEN POSITION (GROUND BLADE CLOSED)

6.2.1 Resonant Frequency and Damping of Spacer-Mounted Switch in Open Position

The resonant frequencies and damping ratios of the spacer-mounted switch are presented in Table 6.3. The plots representing the results of the resonance search are shown in Appendix C (Figs. C.5–C.7).

Table 6.3 Resonant frequency and damping of spacer-mounted modified switch: main blade open and ground blade closed

Switch component	Direction	Resonant frequency, Hz	Damping, %
Jaw Post	X	3.6	2
	Y	4.0	2
Blade	X	1.3	4
	Y	1.0[1]	18
Rigid&Rotating Post	X	2.7	3
	Y	3.3	3

Note: [1]Since the blade is attached to a damper (counter balance assembly) in the Y direction, the resonant frequency of the blade in this direction is difficult to estimate precisely; the value presented in the table is a rough estimation.

6.2.2 Time History Testing of Spacer-Mounted Switch in Open Position

Severity level definitions for qualification purposes. The time history testing was conducted at various levels that are classified by target PGA of the strong motion. Because of some underperformance of the shake table, the TRS at a particular target PGA did not satisfy the IEEE 693 requirements and new recommendations (Takhirov et al., 2004) on enveloping the IEEE spectrum anchored at the same PGA. Therefore, a new term of "IEEE equivalent PGA" (or "equivalent qualification PGA") is introduced in this report, for the support-mounted and spacer-mounted configurations of the disconnect switch. These equivalent PGAs differ by the amplification factor, taken to be 1.83. The equivalent PGA (or equivalent qualification PGA) of a particular time-history testing is the anchoring PGA of the IEEE spectrum that is enveloped by the TRS in accordance with the IEEE 693 requirements and new recommendations (Takhirov et al., 2004). The following sections use three classifications of the intensity for qualification testing: target PGA, equivalent qualification PGA for a spacer-mounted switch, and equivalent qualification PGA for a support-mounted switch. Table 6.4 shows the relationships between the target PGA and the estimated equivalent qualification PGA in the configurations with and without supports. These terms are further discussed in the next section.

Table 6.4 Target and equivalent qualification PGA for tests conducted on spacer-mounted switch, assuming amplification factor = 1.83

No.	Target PGA, g	Equivalent qualification PGA, g	
		Spacer-mounted	Support-mounted[1]
1	0.5	0.41	0.22
2	0.85	0.69	0.38
3	1.0	0.85	0.46
4	1.17	0.92	0.50

Note: [1]Equivalent qualification PGA for support-mounted switch is a ratio of that for spacer-mounted switch to the amplification factor.

TRS at various target PGA. The switch was tested with the IEEE-compatible Landers time history, Landers5H, target PGA from 0.5g–1.17g PGA. The test response spectra (TRS) were computed at 2% damping and based on the acceleration data record at the rigid foundations for the switch. For each level of testing, the TRS is plotted at 1/12 octave frequency resolution and compared with the IEEE spectrum in Figures 6.2–6.5.

Due to limitations of the earthquake simulator, a number of spectral accelerations of the TRS are less than the required spectrum by as much as 10%. Therefore, the last test at 1.17g target PGA is compared with the IEEE spectrum anchored at 0.92g, as shown in Figure 6.6, to satisfy the enveloping criteria of IEEE 693. The TRS peaks and valleys obtained during 1.17g target PGA testing are expressed as a percentage of the plateau spectral acceleration for IEEE spectrum anchored at 1.17g and 0.92g (Figs. 6.7–6.8). The vertical dashed lines represent the resonant frequencies of the modified switch. These plots are similar to the plots in Figures 6.4 and 6.6 presenting tolerance between the TRS and the required response spectra for the frequency range from 0.3 Hz–33 Hz, but are focused only on the spectral accelerations below and above the IEEE spectra that represent possible undertesting and overtesting of the switch in frequency range from 1Hz–20 Hz).

Since the TRS at 1.17g PGA envelops the IEEE spectrum anchored at 0.92g, the equivalent qualification PGA for the spacer-mounted switch is 0.92g. Since the amplification factor is taken to be 1.83, the level is assumed to represent 0.5g equivalent qualification PGA for the support-mounted switch.

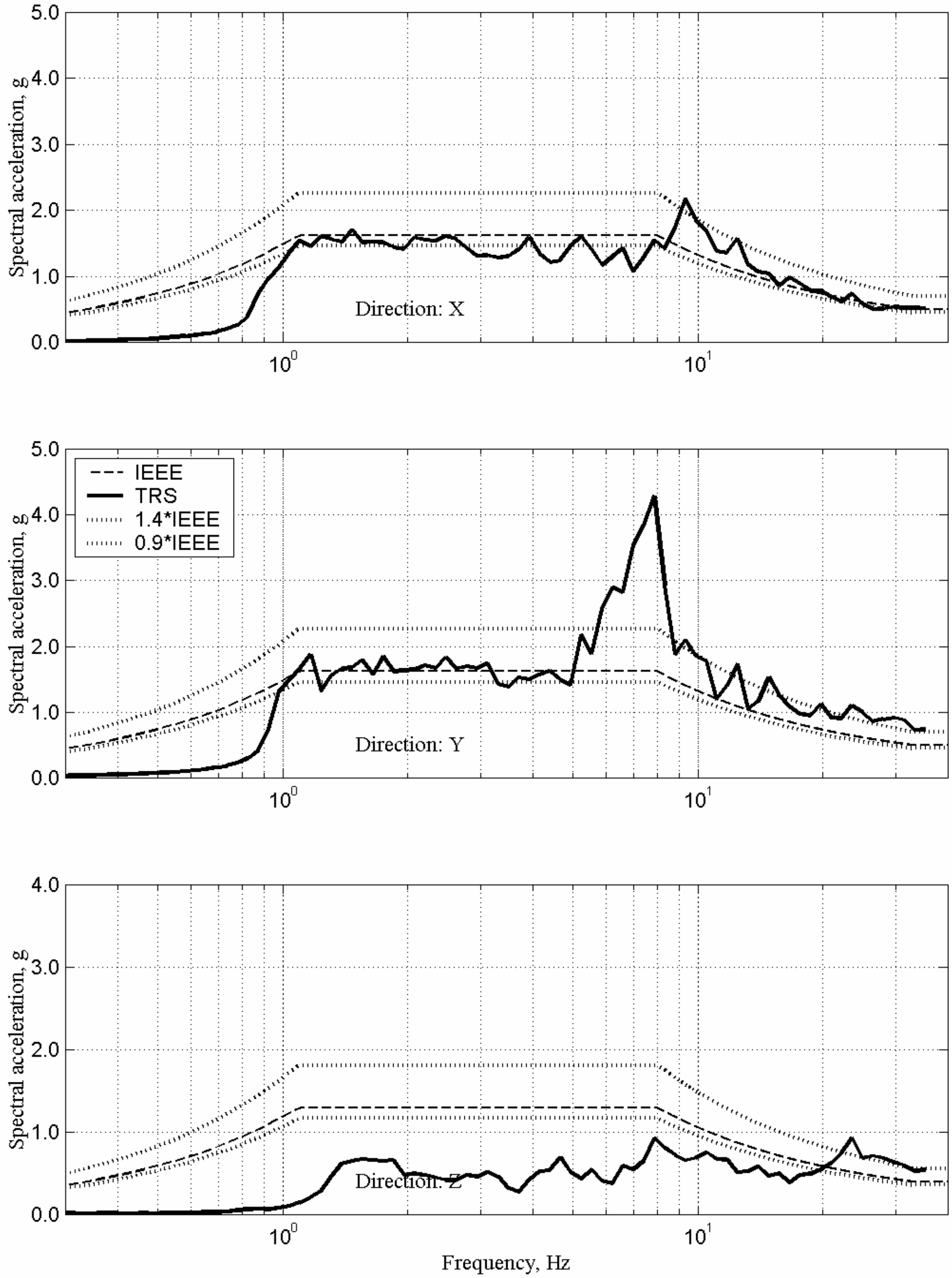

Fig. 6.2 Test response spectra of modified switch mounted on spacer (Landers5H at 0.5g)

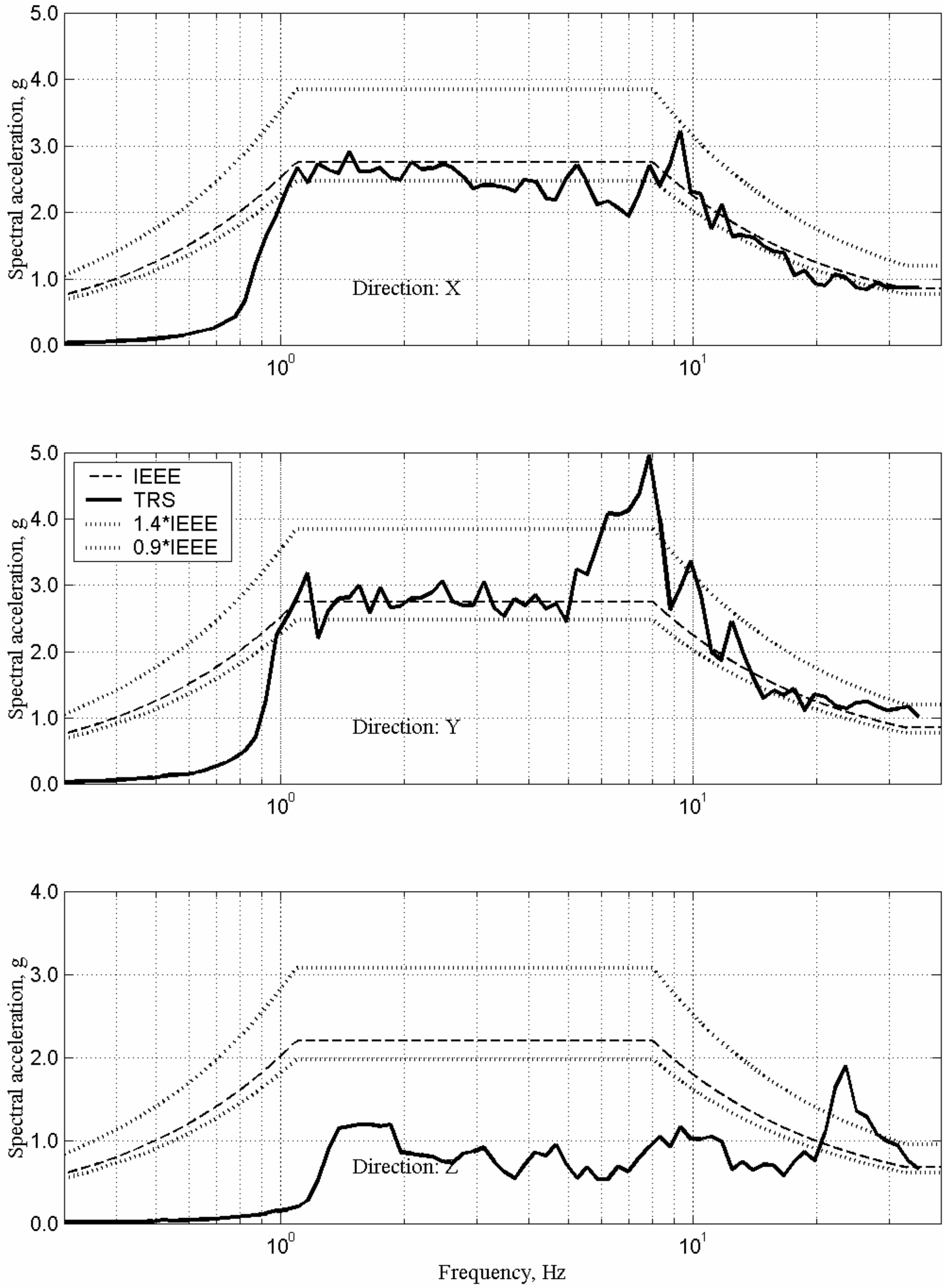

Fig. 6.3 Test response spectra of modified switch mounted on spacer (Landers5H at 0.85g)

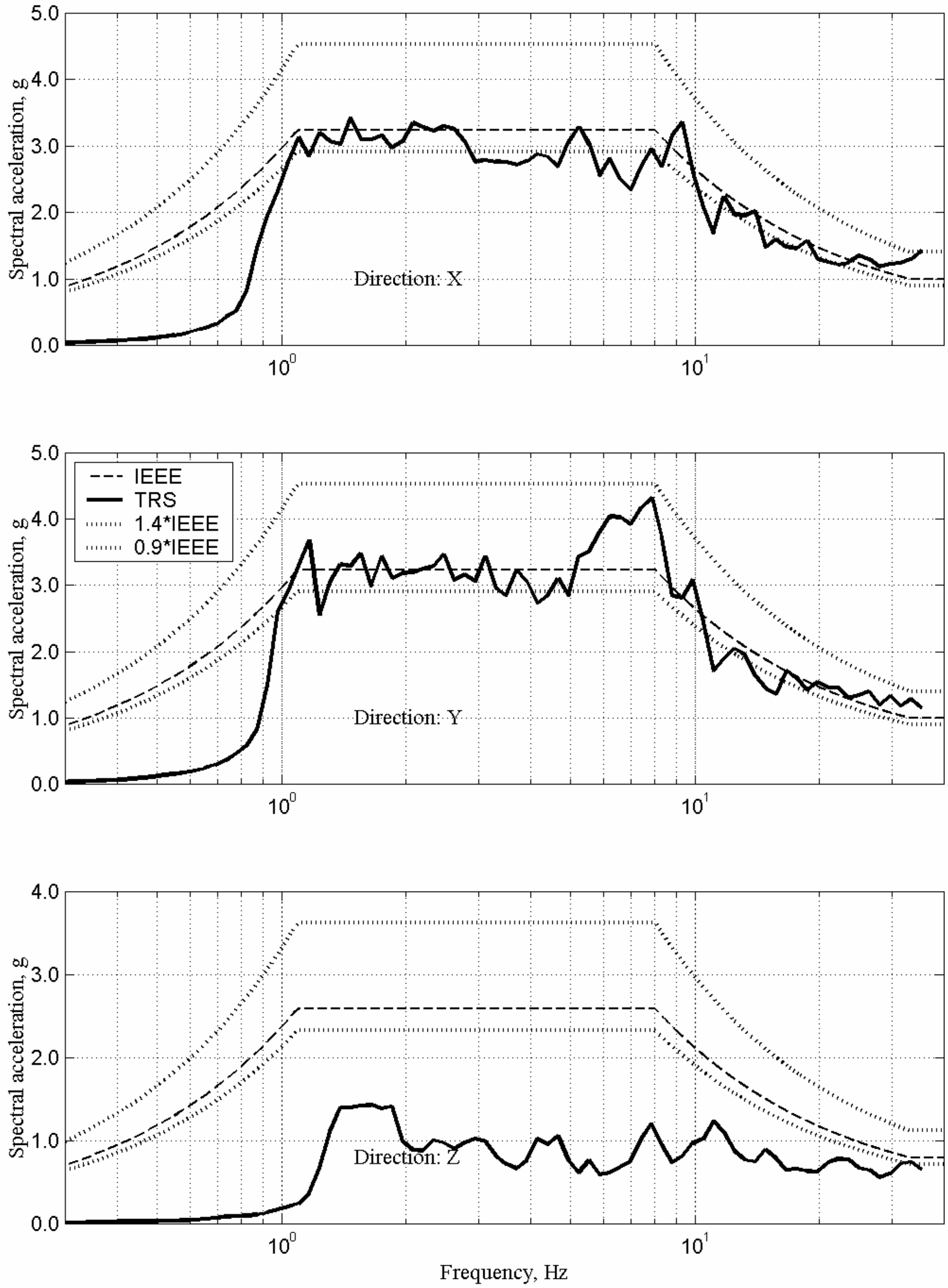

Fig. 6.4 Test response spectra of modified switch mounted on spacer (Landers5H at 1.0g)

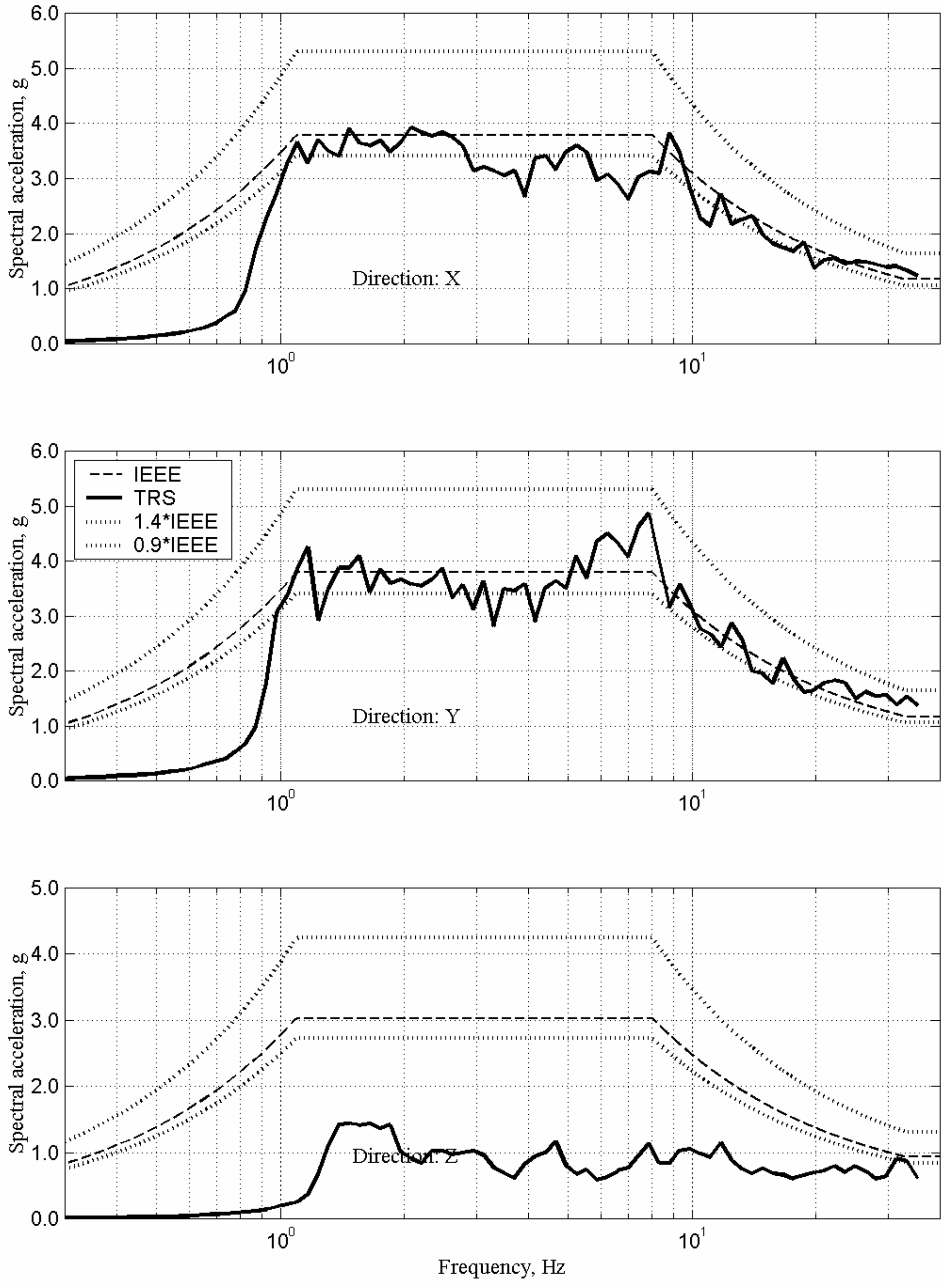

Fig. 6.5 Test response spectra of modified switch mounted on spacer (Landers5H at 1.17g)

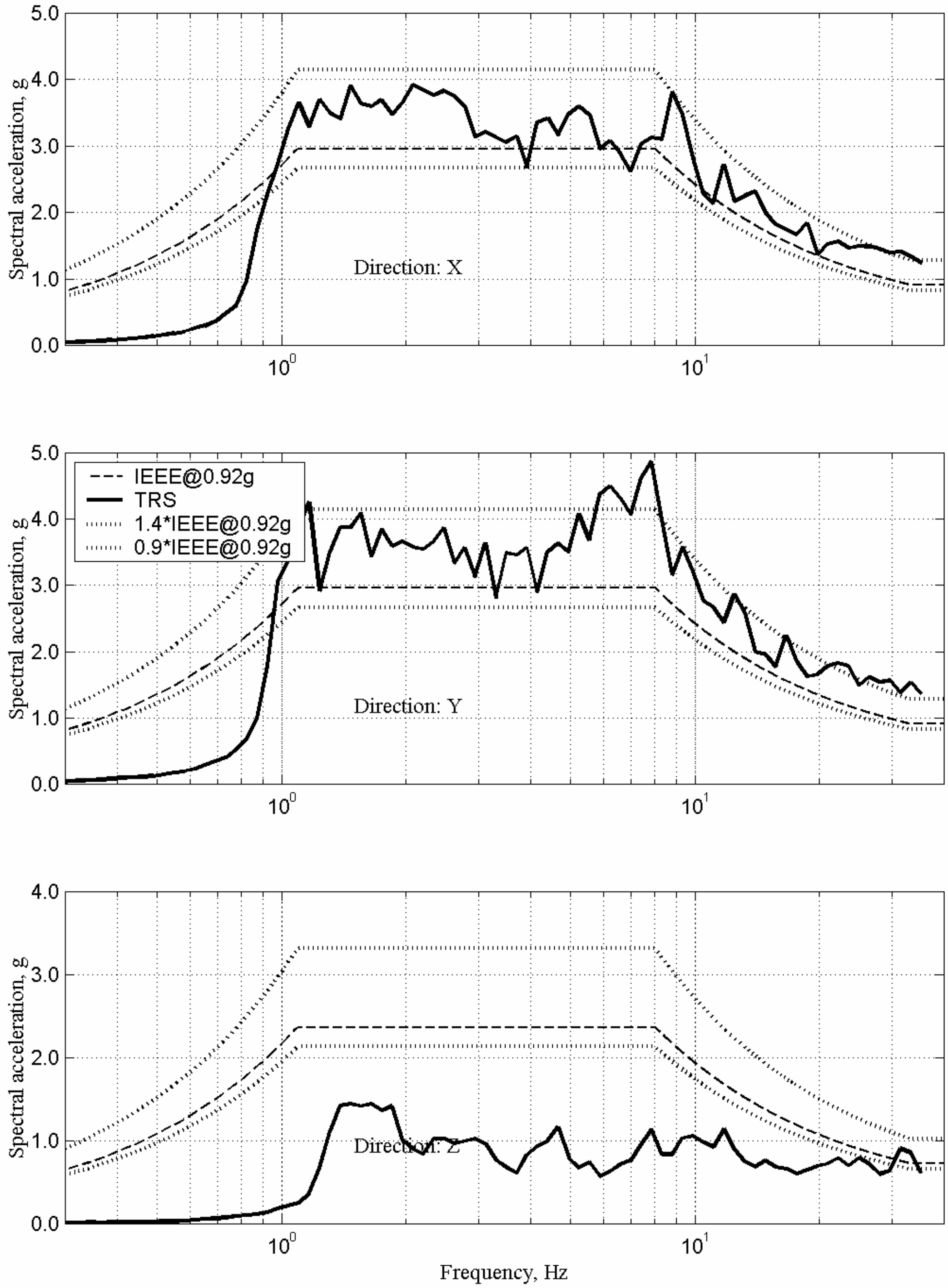

Fig. 6.6 TRS at 1.17g PGA plotted against IEEE spectrum anchored at 0.92g

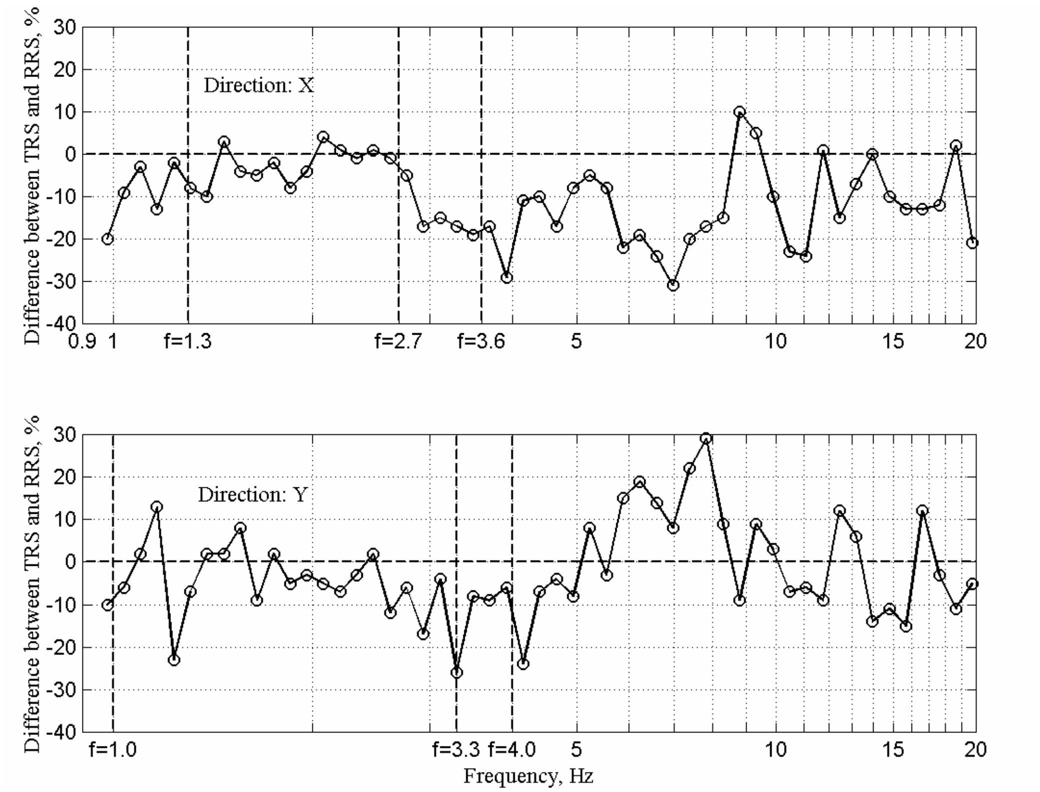

Fig. 6.7 Difference between TRS and IEEE spectra at 1.17g for modified switch testing at 1.17g

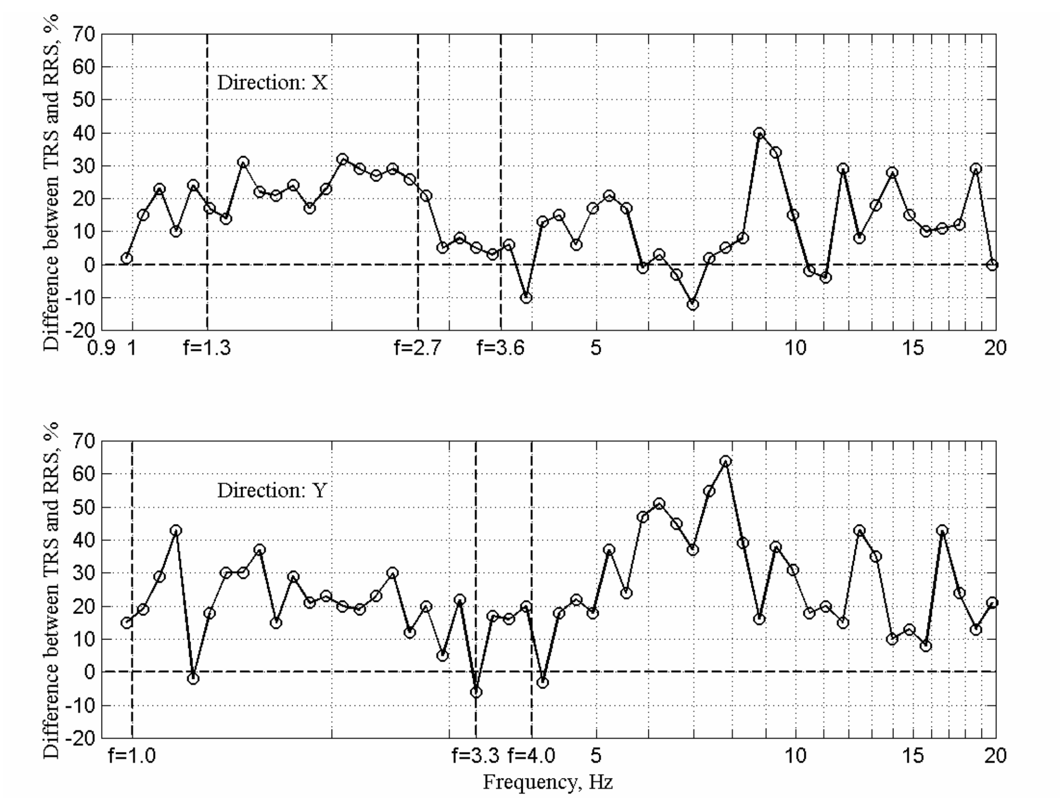

Fig. 6.8 Difference between TRS and IEEE spectra at 0.92g for modified switch testing at 1.17g

Equivalent cantilever load in insulator posts. Table 6.5 presents the maximum of the equivalent cantilever loads and the maximum modulus of the loads. The variation in the maximum equivalent cantilever load from level to level is consistent and is close to linear up to 0.5g target PGA. The modulus of the equivalent cantilever load has a linear trend from 0.5g–1.0g target PGA testing for all three posts, although it becomes nonlinear after 1.0g target PGA for the rigid post.

Table 6.5 Equivalent cantilever loads at insulator posts for all target PGA

		Demand load (equivalent cantilever), lbs			Demand load/ Rated Cantilever load), %		
Target PGA, g	**Direction**	**Rigid**	**Rotating**	**Jaw**	**Rigid**	**Rotating**	**Jaw**
0.50	X	921	420	774	32	14	27
	Y	1308	328	855	45	11	29
	Modulus	1308	420	855	45	14	29
0.85	X	1450	727	1235	50	25	43
	Y	2032	609	1541	70	21	53
	Modulus	2032	756	1541	70	26	53
1.0	X	1821	859	1428	63	30	49
	Y	2241	705	1804	77	24	62
	Modulus	2327	1012	1804	80	35	62
1.17	X	1896	980	1645	65	34	57
	Y	2294	831	1925	79	29	66
	Modulus	2352	1186	2024	81	41	70

Assuming an amplification factor of 1.83, the rigid and jaw posts are overstressed at all severity levels of qualification testing except for 0.5g target PGA based on the 2900 lbs equivalent cantilever load rating. Nevertheless, the switch preserved its structural integrity up to 1.17g target PGA, which is downgraded to 0.92g equivalent qualification PGA (spacer-mounted configuration) to comply with requirements of the new recommended input motion specification for the IEEE 693 document. Since the amplification factor is assumed to be 1.83, this equivalent PGA for the spacer-mounted switch corresponds to 0.92g/1.83=0.50g equivalent qualification PGA for the switch mounted on the supports. The performance of the switch for different values of amplification factor can be evaluated by scaling. A more detailed discussion of qualification of the switch to IEEE 693-1997 will be provided in a separate report prepared by the equipment manufacturer.

6.2.3 Summary of Other Monitored Data

The maximum displacements at the top of all insulators posts are summarized in Table 6.6 and the accelerations are summarized in Table 6.7. A summary of the maximum strains, stresses, and equivalent cantilever loads at the main blade is shown in Table 6.8.

Table 6.6 Maximum displacements (relative to table) of modified switch

Target PGA, g	Direction	Rigid Post, in.	Rotating Post, in.	Jaw Post, in.	From Rotating to Jaw Posts, in.
0.5	X	2.08	2.33	1.43	
	Y	2.20	2.20	1.33	2.22
	Modulus	2.47	2.51	1.46	
0.85	X	3.44	3.83	2.32	
	Y	3.46	3.46	2.37	3.58
	Modulus	3.97	3.94	2.61	
1.0	X	4.29	5.39	2.69	
	Y	3.92	3.92	2.80	4.08
	Modulus	4.90	5.70	3.09	
1.17	X	4.47	6.39	3.08	
	Y	4.07	4.07	3.35	5.03
	Modulus	5.06	6.56	3.51	

Table 6.7 Maximum accelerations (relative to table) at all elevations of modified switch

Target PGA, g	Direction	Table, g	West support, g	East support, g	Rigid Post, g	Rotating Post, g	Jaw Post, g	Blade, g
0.5	X	0.21	1.00	0.94	1.93	2.05	2.04	NA[2]
	Y	0.30	1.45	1.45	2.41	NA[1]	1.85	3.52
	Z	0.12	0.27	0.28	0.38	0.85	0.42	3.86
	Modulus		1.48	1.45	2.42	NA[1]	2.04	NA[2]
0.85	X	0.39	1.72	1.57	3.30	3.59	3.06	NA[2]
	Y	0.46	1.87	1.88	3.84	NA[1]	3.41	NA[2]
	Z	0.21	0.30	0.41	0.42	1.36	0.49	NA[2]
	Modulus		1.91	1.92	3.85	NA[1]	3.57	NA[2]
1.0	X	0.53	2.18	1.83	4.09	4.35	3.70	NA[2]
	Y	0.60	2.27	2.28	4.59	NA[1]	3.70	NA[2]
	Z	0.31	0.34	0.31	0.54	1.97	0.46	NA[2]
	Modulus		2.36	2.42	4.67	NA[1]	4.12	NA[2]
1.17	X	0.68	2.498	2.243	4.629	5.028	4.226	NA[2]
	Y	0.82	2.747	2.731	4.919	NA[1]	4.13	NA[2]
	Z	0.36	0.446	0.48	0.582	2.399	0.633	NA[2]
	Modulus		2.841	2.932	5.25	NA[1]	4.826	NA[2]

Notes:
[1]Accelerometer in Y direction is malfunctioning.
[2]Accelerometer is out of range (accelerations are greater than 5.0g).

Table 6.8 Strains, loads, and accelerations of blade estimated based on strain data

Target PGA, g	Direction	Blade strain, ms	Equivalent cantilever load[1], lbs	Equivalent cantilever acceleration[1], g	Tip acceleration[2], g
0.5	X	254	881	5.9	6.6
	Y	134	467	3.1	3.5
0.85	X	348	1208	8.1	9.0
	Y	225	783	5.2	5.9
1.0	X	434	1509	10.1	11.3
	Y	254	881	5.9	6.6
1.17	X	486	1688	11.3	12.6
	Y	283	984	6.6	7.4

Notes:
[1]Estimation of equivalent cantilever load and acceleration is based on mass less blade model with mass of the blade concentrated at center of gravity.
[2]Estimation of tip acceleration is based on comparison of strains with tip accelerations at low levels of testing.

6.2.4 Electrical Continuity and Resistance Checks

The low voltage continuity of the main circuit was monitored during the time history testing, and no interruptions were observed. The resistance of the main circuit was checked before and after tests at 0.85g, 1.0g, and 1.17g target PGA. The resistance change was within that allowable of up to 20% as required by IEC 60694 (IEC, 1996). The fuses of the motor operator were also checked for continuity to make sure that they were not blown during dynamic testing. The switch's main functionality and assembly alignment were also inspected, and the results of the inspection after tests at 0.85g, 1.0g, and 1.17g target PGA are documented. The last two are summarized in Table 6.9.

The switch sustained all levels of testing without major structural damage, and the electrical continuity of the switch was not interrupted. The major functionality of the switch was preserved and only one minor anomaly was observed in the after-test inspection. The stationary arc horn was bent by an impact during the test, in a manner observed for the support-mounted switch (Fig. 5.13).

Table 6.9 Results of functionality inspection

1	**General information:**		
(a)	Specimen	Modified switch	Modified switch
(b)	Mounting	4-in. spacer	4-in. spacer
(c)	Main blade	Open	Open
(d)	Ground blade	Closed	Closed
(e)	Level of testing, g	1.0	1.17
(f)	Time history	Landers5H	Landers5H
(g)	Date	5/20/2003	5/20/2003
2	**Visual inspection results:**		
(a)	Overall assembly for alignment	OK	OK
(b)	Insulators at base for cracks	OK	OK
(c)	Jacking bolts for deformation	OK	OK
(d)	Live part casting: hinge and jaw	OK	OK
3	**Millivolt drop test (main circuit)**[1]		
(a)	Before testing, mΩ	76	89
(b)	After testing, mΩ	89	83
(c)	Resistance change, %	17	-7
(d)	Allowed, %	20	20
4	**Millivolt drop test (grounding circuit)**[4]		
(a)	Before testing, mΩ	185	185
(b)	After testing, mΩ	185	175
(c)	Resistance change, %	0	-5
(d)	Allowed, %	20	20
5	**Mechanical operating test** [2]		
(a)	Alignment during operation	OK	OK
(b)	Operating functionality	OK	OK
6	**Grounding circuit continuity** [3]		
(a)	Any loss of continuity	No	No
7	**Anomalies**		
		(a) stationary arc horn bent	(a) stationary arc horn bent

Notes:

[1]Estimate change in resistance of the main circuit.

[2]Open the main blade of the closed switch to the extent possible and return to the closed position.

[3]Checked only for grounding switch in closed position.

[4]Estimate change in resistance of the grounding circuit.

6.3 SUMMARY AND CONCLUSIONS

6.3.1 RRS Enveloping and Tolerance Zone Criteria

Since TRS of the table output at 1.17g target PGA enveloped the IEEE PL spectrum anchored at 0.92g, as shown in Figure 6.6, the equivalent seismic qualification level for the spacer-mounted switch is estimated as 0.92g. The test response spectra (Takhirov et al., 2004) envelop the IEEE PL spectrum anchored at 0.92g up to 7 Hz. As presented in Figure 6.8, the valleys below the IEEE spectral plateau are not deeper than –10%, as recommended by the companion theoretical study (Takhirov et al., 2004) provided that at least two adjacent points are equal to or higher than the required spectrum. Resonant frequencies of the disconnect switch with the main blade open varied from 1 Hz–4 Hz; therefore, the out-of-range value at 7 Hz in the TRS of the X direction is assumed acceptable.

6.3.2 Qualification Testing Acceptance Criterion Related to PL Testing

The disconnect switch mounted on a 4-in. spacer with the main blade open and the grounding blade closed preserved its major functions after the 1.17g target PGA testing without major damage. Therefore, the disconnect switch complies with IEEE 693 functional criterion for seismic qualification at PL testing. The fact that the TRS adequately enveloped the IEEE PL spectrum at 0.92g and that the amplification factor is assumed to be 1.83 leads to the conclusion that the modified disconnect switch with the main blade open mounted on the supporting structure is seismically qualified at the moderate PL with the IEEE spectrum anchored at 0.5g PGA.

In order to qualify the switch to the high seismic qualification level, allowable stresses in critical elements are reviewed. Demand-to-capacity ratios for porcelain insulators reported in Table 6.5 show that at the highest level of testing, insulators are stressed to about 80% of their cantilever strength rates. Assuming a 1.83 amplification factor, these insulator demands exceed the allowable rates by about 60%.

The issues associated with insulator overstress, rated cantilever capacities, and possible methods for mitigating these overstresses have been previously discussed in Chapter 5. In addition, alternative interpretations of the most appropriate amplification factor are possible.

Testing of the switch on rigid and spacer-type supports conducted in this project highlight some of the difficulties related to the elimination of the actual support structure. Differences in the behavior of the equipment when mounted on actual supports as opposed to modified or rigid supports, the nonlinear behavior of mechanical components, and difficulties in the selection of parameters to be used as the basis for setting amplification factors are among the challenges for qualification. The high levels of shake table output required for such tests also present an obstacle to equipment qualification testing without supports.

A detailed discussion of the qualification of the switch to IEEE 693-1997 will be presented in a separate report prepared by the equipment manufacturer.

7 Feasibility Study on Blade Replacement by Equivalent Mass or Shortened Blade

This chapter presents results and discussions related to the feasibility study of testing the disconnect switch with an equivalent mass or a shortened blade. The issue is important for the development of a seismic qualification procedure for tall electrical equipment such as the vertical break disconnect switch tested, which becomes even taller after opening of the main blade. The switch with an equivalent mass replacing the main blade was tested in the support-mounted configuration, and the spacer-mounted configuration was used for a switch with a shortened blade. The former configuration was tested at low levels of time history testing up to 0.5g target PGA and in resonance-search testing, whereas the latter configuration was subjected to resonant search tests only. The tests were conducted on the modified switch with the grounding blade in the closed and open positions.

7.1 TESTS WITH EQUIVALENT MASS REPLACING BLADE

7.1.1 Equivalent Mass Selection

The total mass of the blade was estimated as 150 lbs with the center of gravity located at 114 in. from the root fixture of the blade attaching it to the switch. In order to replicate the total weight of the blade, a massive steel plate with an additional mass was directly attached to the root fixture. Therefore, after this modification, the total weight of the switch mounted on the tall supports was preserved. The blade replacement by the concentrated mass had several disadvantages: first, it changed the resonant frequencies of the whole system and second, it failed to replicate the moment at the root fixture of the blade due to the elevated location of the center of gravity.

7.1.2 Summary of Low-Level Testing of Switch with Mass Replacing Blade

Overall elastic stiffness. A summary of the overall elastic stiffness of the support-mounted switch with the dummy mass is presented in Table 7.1. Since the rotating post adds some stiffness to the rigid and rotating post assembly, the overall stiffness of the respective assembly is slightly greater than that of the jaw post in both directions. The rigid and rotating post assembly is much stiffer in the Y direction than in the X direction. The same trend is observed for the stiffness of the jaw post, although the difference of the stiffnesses in two directions is less dramatic.

Table 7.1 Overall stiffness of support-mounted modified switch (concentrated mass)

Post	Stiffness (X), kips/in.	Stiffness, kips/in.
Rigid&Rotating	0.37	0.85
Jaw	0.33	0.55

Resonant frequency. A summary on the resonant frequency of the switch with the main blade replaced by the equivalent concentrated mass is presented in Table 7.2. The resonant frequencies of the switch elements appear to be within the plateau of the IEEE spectra, and vary from 1.6 Hz (for the rigid and the rotating posts in the X direction) to 3.4 Hz (the jaw post in the Y direction).

Table 7.2 Resonant frequencies of support-mounted modified switch with concentrated mass instead of main blade

Grounding blade	Post	Frequency (X), Hz	Frequency (Y), Hz
Open	Rigid&Rotating	1.60	2.6
	Jaw	2.5	3.5
Closed	Rigid&Rotating	1.60	2.6
	Jaw	2.5	3.4

Time history tests. Time history testing was conducted by means of Landers5L (from 0.125g–0.5g target PGA) and the results are summarized in Table 7.3. The results of the time history tests at various levels of severity for the switch with the blade closed and the blade replaced by a dummy mass (switch was on 14-ft-tall supports in both cases) are presented in Figure 7.1. The modulus of the equivalent cantilever load in the rigid post is shown in the top plot of Figure 7.1, whereas the loads in the jaw and rotating posts are presented in the middle and bottom plots, respectively. The most overstressed insulator post was again the rigid post, with loads much greater for the blade-closed position (difference for the rigid post is about 30%). The same phenomenon is seen for the jaw post (bottom plot Fig. 7.1), although there is a small difference between the loads for these two switch configurations. A different conclusion is made for the rotating post: the loads in the post with the blade mass concentrated on top are greater than the load for the closed switch. Therefore the modulus of the equivalent cantilever load becomes greater than the allowable load of 1450 lbs at 0.5g target PGA.

The fact that the rigid post, generally the most overstressed post, is stressed less is considered as one more indicator that the posts in the switch-closed configuration experience greater loads compared to a similar configuration with a dummy blade or with the blade open.

Table 7.3 Modulus of equivalent cantilever load for support-mounted modified switch with blade removed (grounding blade closed) during time history tests by means of Landers5L

No.	Target PGA, g	Post	Modulus of equivalent cantilever load, lbs
1	0.125	Jaw	463
		Rotating	483
		Rigid	489
2	0.25	Jaw	755
		Rotating	839
		Rigid	858
3	0.5	Jaw	**1553**
		Rotating	**1511**
		Rigid	**1890**

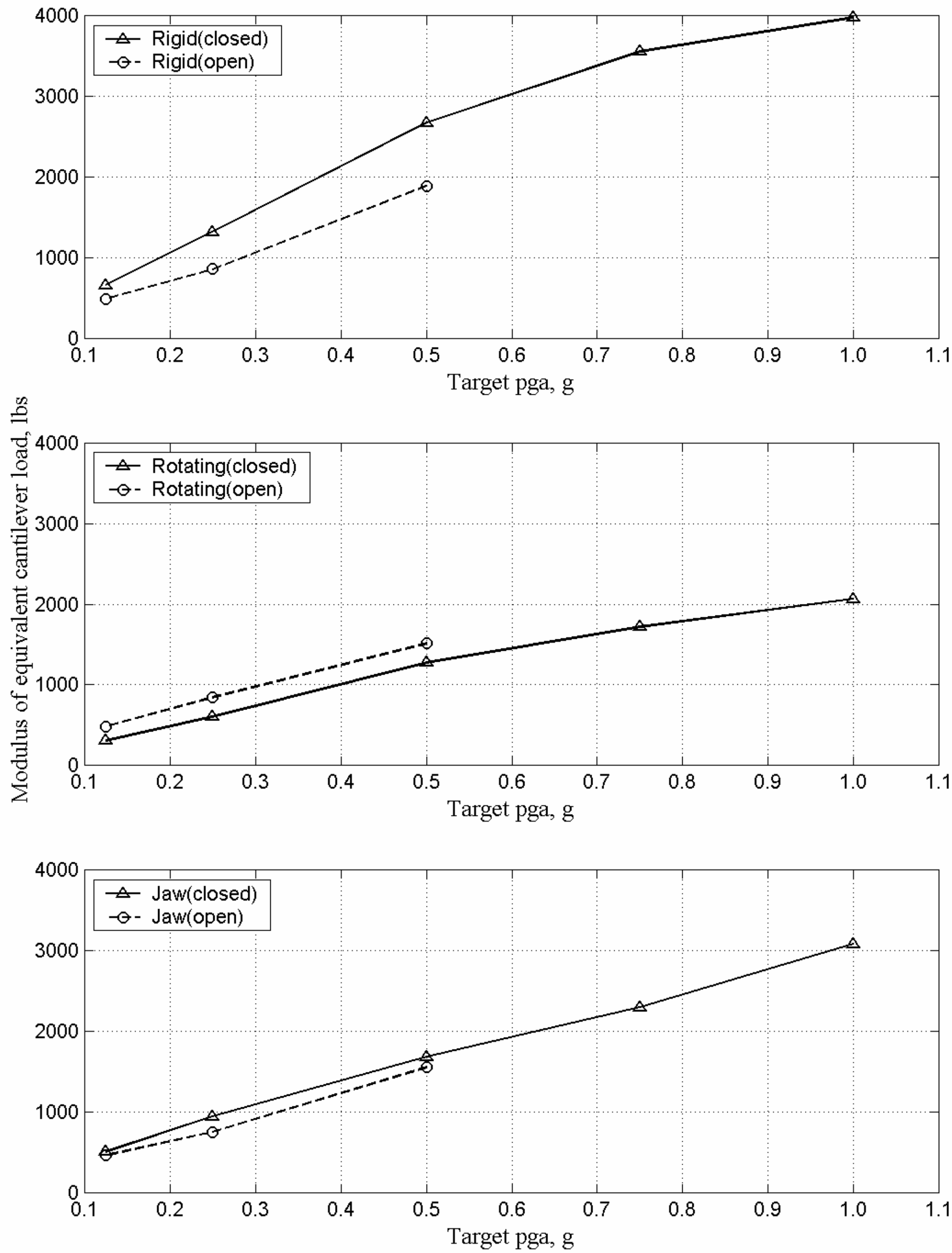

Fig. 7.1 Variation of modulus of equivalent cantilever load in blade closed and blade removed configurations

7.2 TESTS WITH EQUIVALENT SHORTENED BLADE

7.2.1 Design of Shortened Blade

The design of the shortened blade was based on the assumption that the blade can be presented as a weightless rod with the lumped mass of the blade concentrated at the center of gravity (CG). The shortened blade was required to have the same resonant frequency as the full-size blade based on the previous assumption. Therefore, the shortened blade had almost the same ratio of total weight to a CG distance as that for the full-size blade. Figure 7.2 is a schematic representation of the full-size blade and the shortened blade. The shortened blade consists of a shortened part of the blade pipe and added masses to preserve the resonant frequency of the blade. A photo of the shortened blade installed in the switch is shown in Figure 7.3.

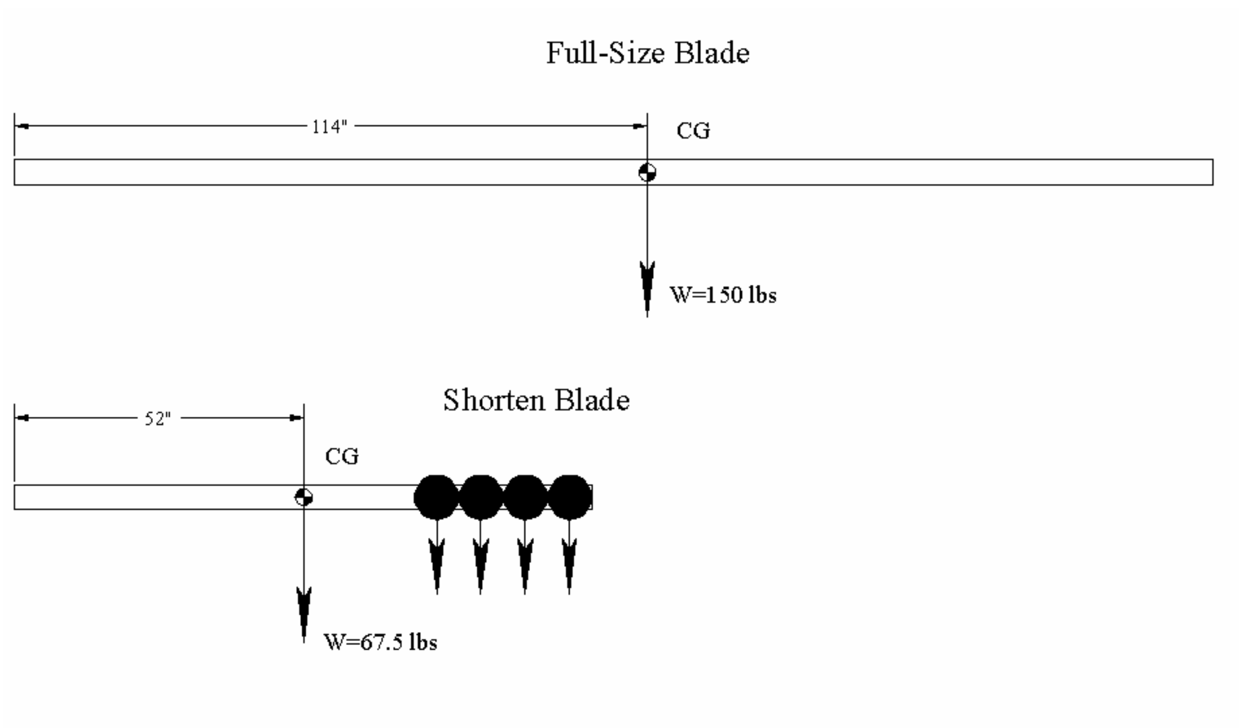

Fig. 7.2 Schematic comparison of full-size blade with shortened blade

7.2.2 Resonant Frequency

Resonant frequencies of the spacer-mounted switch with a shortened blade in the vertical position are compared with that of the switch with full-size blade opened. A summary of the results is presented in Table 7.4. As expected, the frequency of a stand-alone jaw post remains the same, whereas the frequencies of the rigid and rotating posts' assemblies and the blade increase in both directions, with one exception for the blade in the Y direction. The increase in the resonant frequency is connected with a reduction in length of the blade; the increase in the frequency of the shortened blade affects the whole assembly of rigid and rotating posts, since the blade is attached to the respective post.

Only random, sweep, and free-vibration tests are conducted for the spacer-mounted switch with a shortened blade.

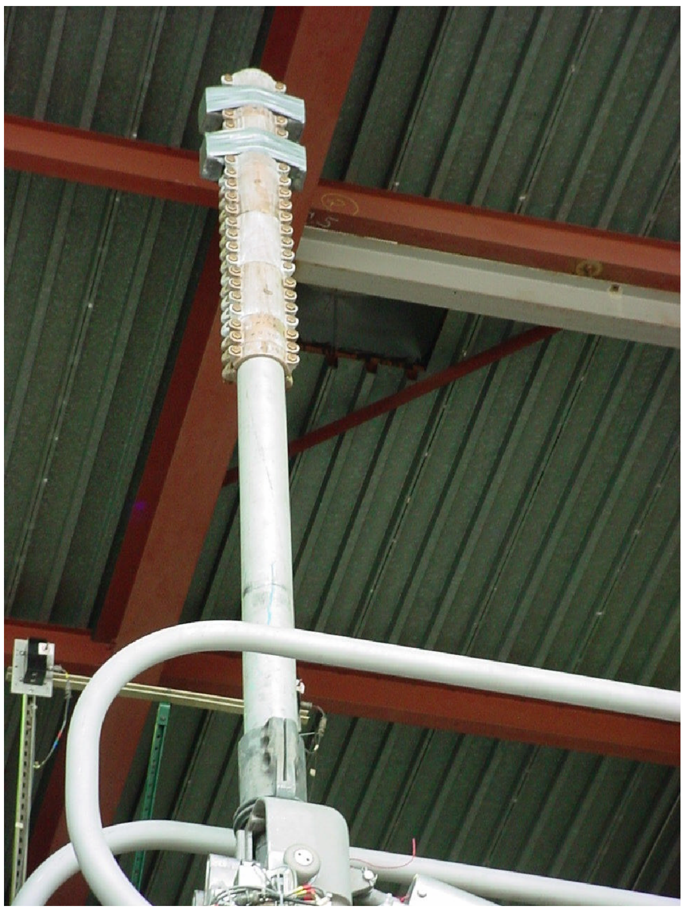

Fig. 7.3 Shortened blade installed in the switch

Table 7.4 Resonant frequencies of spacer-mounted modified switch with shortened blade and full-size blade in open position

Main blade	Post	Frequency (X), Hz	Frequency (Y), Hz
Open (full-size)	Rigid&Rotating	2.7	3.3
	Jaw	3.6	4.0
	Blade	1.3	1.0[1]
Open (shortened)	Rigid&Rotating	3.3	3.6
	Jaw	3.6	4.0
	Blade	1.6	1.0[(1)]

Note:
[1]Since the blade is attached to a damper in the Y direction, the resonant frequency of the blade in this direction is difficult to estimate precisely; the value presented in the table is a rough estimation.

7.3 SUMMARY AND CONCLUSIONS

The blade replacement by an equivalent one has at least one of two disadvantages: it changes the resonant frequencies of the whole system and/or it fails to replicate the moment at the root fixture of the blade due to the elevated location of the center of gravity. Therefore, the experimental seismic qualification procedure has to be supported by a detailed numerical analysis for electrical equipment that would require an extensive component testing to supply the analysis with reliable data on the component properties. Furthermore, the approach requires a number of equipment-specific efforts in order to achieve results that ultimately cannot be verified by the experiments. Due to the complexity and equipment dependency of the approach, a simplified and universal component-replacement procedure should be the objective of a separate theoretical study supported by experimental research.

8 Summary and Conclusions

This chapter provides a summary of the key findings and conclusions drawn from the research project.

8.1 COMPONENT TESTING

The slope in a load-strain diagram for the porcelain sections and the posts appears to depend on the sign of the strain: the tension strain develops a steeper slope than that in compression. The difference in the slope value was found to be as much as 20%. The difference in the slope may be related to the material properties of the ceramic, boundary condition effects (the strain gages were installed between the sections in close proximity to the joints), the flexibility of bolted joints, the mortar between the ceramic and a cap, or a gap between the ceramic and the cap.

Small changes in the overall stiffness and load-strain slope for the insulator posts were observed in tests before and after shake table tests. From these tests, it is concluded that (1) the material properties of the insulator post are close to linear up to failure and (2) the violent dynamic tests did not significantly affect the material properties of the insulators.

The elastic stiffness of insulator posts estimated during the calibration tests is close to that provided by the manufacturer (NGK Insulators, Ltd.). The linear relationship between a horizontal load and a tip deflection estimated in the manufacturer's tests is confirmed in this study. The failure load is close to that observed in the tests conducted by the manufacturer for similar insulator posts.

Since the strength rating of an insulator is significantly less than the mean ultimate cantilever load, the use of PL alternative failure criteria seems to be more appropriate for switches utilizing porcelain insulators. The results of the PL testing would be more predictable if insulator manufacturers would provide statistical data (such as mean and dispersion) on breaking strengths in addition to strength rating. Strain gage data monitoring and comparison with its ultimate value would provide valuable data for design improvements during and after qualification tests

8.2 SWITCH WITH ORIGINAL DESIGN

The 550-kV disconnect switch with the original design needs reinforcement at the base of the insulator posts in order to improve its seismic performance. The modifications introduced in the so-called modified switch significantly improved its performance and allowed it to withstand the high levels of shaking imposed in this test program.

8.3 QUALIFICATION TESTING OF SUPPORT-MOUNTED SWITCH (BLADE CLOSED)

The disconnect switch preserved its major functions up to the highest of PL testing conducted in this project, without any major damage. Some anomalies that occurred during the test were insignificant and minor. The restoration work did not involve any installation of new parts: the parts impacted out from their original positions were simply repositioned back in place. Therefore, the disconnect switch complied with seismic qualification criteria for PL testing, up to the level conducted in the project. Although the TRS achieved in the test program technically does not satisfy the new recommended specification for IEEE 693 for qualification to the high seismic PL, the deficiencies in the TRS are limited to frequency ranges not close to the important modal frequencies of the equipment.

Although the TRS came close to satisfying the new recommended input motion specifications for IEEE 693, the rigid insulator post in the PL test was loaded to a level 37% beyond the rated cantilever strength of 2900 lbs assigned to this model of insulator by the manufacturer. Fracture of the porcelain insulator post did not occur during the PL test because the actual strength of the installed insulator exceeded the rated cantilever strength by over 40%. This outcome highlights the conservatism associated with insulator cantilever strength ratings.

High stresses in the insulators may be mitigated through the use of higher strength, lighter insulators. At the time of this writing, project utility participants were in the process of implementing new procurement specifications for improved insulators to be used with 500-kV switches.

The acceptance criteria of IEEE 693-1997 for equipment qualified by PL testing permits the omission of strain gages during the PL test; however, the results of this project demonstrate that such a practice can lead to unconservative results when substantial overstrength or uncertainty in material strengths/capacities are involved. This is particularly true for non-ductile components such as porcelain insulators. The shortcomings of the noted provisions of IEEE 693-1997 should be considered for revision.

Nevertheless, the overall performance of the switch mounted on a 14-ft-tall support structure tested in this project was very favorable. Tests were conducted to high levels of shaking, with no failures and no significant anomalies. It should be noted that for 500kV disconnect switches, the closed position is of most interest to utilities, since switches of this voltage class are almost always in this position.

A detailed discussion of the qualification of the switch to IEEE 693-1997 will be presented in a separate report prepared by the equipment manufacturer.

8.4 QUALIFICATION TESTING OF SPACER-MOUNTED SWITCH (MAIN CONTACT OPEN)

The disconnect switch mounted on a 4-in. spacer with the main blade in the open position and the grounding blade closed preserved its major functions after the 1.17g target PGA testing without major damage. Therefore, the disconnect switch complies with IEEE 693 criteria for qualification at the moderate seismic PL, using the new recommended input motion specifications for IEEE 693.

In order to qualify the switch to the high seismic PL, allowable stresses in critical elements are reviewed. Demand-to-capacity ratios for porcelain insulators were found to exceed allowable values by about 60%, assuming that a 1.83 amplification factor is used.

Similar to the case of the switch mounted on 14-ft-tall supports, the high stresses in the insulators may be mitigated through the use of higher strength, lighter insulators. At the time of this writing, project utility participants were in the process of implementing new procurement specifications for improved insulators to be used with 500kV switches. In addition, alternative interpretations of the most appropriate amplification factor are possible.

Testing of the switch on rigid and spacer-type supports conducted in this project highlight some of the difficulties related to elimination of the actual support structure. Differences in the behavior of the equipment when mounted on actual supports as opposed to modified or rigid supports, the nonlinear behavior of mechanical components, and difficulties in the selection of parameters to be used as the basis for setting amplification factors are among the challenges for qualification. The high levels of shake table output required for such tests also present an obstacle to equipment qualification testing without supports.

A detailed discussion of the qualification of the switch to IEEE 693-1997 will be presented in a separate report prepared by the equipment manufacturer.

8.5 FEASIBILITY OF BLADE REPLACEMENT WITH EQUIVALENT MASS OR SHORTENED BLADE

The blade replacement by an equivalent one has at least one of two disadvantages: it changes the resonant frequencies of the whole system and/or it fails to replicate the moment at the root fixture of the blade due to the elevated location of the center of gravity. Therefore, the experimental seismic qualification procedure has to be supported by a detailed numerical analysis for electrical equipment that would require extensive component testing to supply the analysis with reliable data on component properties. Therefore the approach requires a number of equipment-specific efforts in order to achieve results that ultimately cannot be verified by the experiments. Due to the complexity and equipment dependency of the approach, a simplified and universal component-replacement procedure needs to be developed. This should be an objective of a separate experimental study combined with theoretical research.

8.6 SUGGESTIONS FOR FUTURE WORK

Both numerical and experimental studies should be conducted to develop a reliable procedure for estimation of the amplification factor. Such procedures or guidelines are needed in order to streamline the qualification procedure, particularly for large equipment that cannot be practically tested on their supports and also for equipment that may be supported on several different types of support structures. In addition, the consideration of alternative methods of testing, possibly using substitute support structures that are intended to provide the same equipment response as a full-scale structure, would be valuable.

Further material studies on porcelain insulator acceptance criteria are needed. IEEE 693 acceptance criteria for qualification require a safety factor of 2.0 and 1.0 for the RRS and PL, respectively, against the “ultimate strength” of the insulator. The current practice of most utilities, manufacturers, or consulting engineers is to use the rated cantilever strength as the ultimate strength of the insulator. As highlighted in the tests conducted in this project, the rated cantilever strengths of insulators are frequently set at levels representing a guaranteed minimum breaking strength. Alternative definitions of ultimate strength should be explored for use when designing for extreme events such as a large earthquake.

The differences between the stiffness of porcelain insulators in tension and compression should be investigated further. Investigations should include further tests on multiple-section insulators, porcelain material studies and tests, and collaboration with insulator manufacturers. The differences observed in this project may be significant enough to influence the outcome of qualification tests.

References

ASTM, 1986. ASTM E1049 - 85. (Reapproved 1997) *Standard Practices for Cycle Counting in Fatigue Analysis.* American Society for Testing and Materials, Annual Book of ASTM Standards, Section 3: Metals Test Methods and Analytical Procedures, Vol. 03.01-Metals-Mechanical Testing; Elevated and Low-Temperature Tests, ASTM, Philadelphia, 1986, pp. 836-848.

Callister, William D. 2003. *Materials Science and Engineering: An Introduction.* New York, NY : John Wiley & Sons.

Chopra A.K. *Dynamics of Structures: Theory and Applications to Earthquake Engineering*. Prentice Hall: Englewood Cliffs, New Jersey.

Downing, S.D., and Socie D.F., *Simplified Rainflow Counting Algorithms*, Int. J. Fatigue, Vol. 4, No. 1, 1982, pp. 31-40.

Gilani A.S.J., Chavez J.W, Fenves G.L. and Whittaker A.S. 1998. *Seismic Evaluation of 196-Porcelain Transformer Bushings*. Pacific Earthquake Engineering Research Center report 1998/14. PEER, University of California at Berkeley.

Gilani A.S.J., Whittaker A.S., and Fenves G.L. 1999. *Seismic Evaluation and Retrofit of 230-kV Porcelain Transformer Bushings*. Pacific Earthquake Engineering Research Center report 1999/14. PEER, University of California at Berkeley.

Gilani A.S.J., Whittaker A.S., Fenves G.L., Chen C-H., Ho H. and Fujisaki E. 2000. *Seismic Evaluation and Analysis of 230-kV Disconnect Switches*. Pacific Earthquake Engineering Research Center, Report 2000/06. PEER, University of California at Berkeley.

Gundy W.E. & Associates. 2002. *Design and Analysis of a Disconnect Switch Support Structure.* Report 1195-17 for Southern States, Inc. W.E.Gundy and Associates, Inc.: Hailey, ID.

IEEE, 1998. IEEE Standard 693-1997. 1997. *Recommended Practices for Seismic Design of Substations*. Piscataway, N.J.: IEEE Standards Department.

IEC, 1996. IEC 60694. *Common Specifications for High-Voltage Switchgear and Controlgear Standards.* International Electrotechnical Commission, Geneva, Switzerland.

IEC, 2001. IEC 60168. *Tests on Indoor and Outdoor Post Insulators of Ceramic Material or Glass for Systems with Nominal Voltages Greater Than 1000V.* International Electrotechnical Commission, Geneva, Switzerland.

Kennedy, R.P. 2004. Personal communication with Anshel Schiff regarding development of input motion requirements for the Nuclear Regulatory Commission, RPK Structural Mechanics Consulting.

Thornberry, L. R. and Hardy, R. 1997. *Seismic simulation test program on type CGCB-G 230kV disconnect switch.* Report No. 45998-1 Huntsville, Ala.: Wyle Laboratories.

Wyle Laboratories, 1993. *Wyle Laboratories' Seismic Test Report No. 47072-2 (Revision 2).* Huntsville, Alabama: Wyle Laboratories Scientific Services and Systems Group.

Takhirov, S., Fenves, G., Fujisaki, E. and Clyde, D. *Ground Motions for Earthquake Simulator Qualification of Electrical Substation Equipment.* Pacific Earthquake Engineering Research Center, Report 2004/xx. PEER, University of California at Berkeley (to be published).

Schiff, A. (editor), 1999. *Manual No. 96, Guide to Improved Earthquake Performance of Electric Power Systems*, American Society of Civil Engineers, Electric Power and Communications Committee, Technical Council on Lifeline Earthquake Engineering.

Appendix A IEEE 693 Specifications and New Recommendations for Seismic Qualification Testing

The equipment and supporting structure shall be subjected to at least one time history test. The input motion time history shall satisfy the requirements given below. The Recommended Practice (IEEE, 1998) principally uses response spectra to establish the characteristics of the time histories used to seismically qualify substation equipment. When taken alone, it is an imprecise method of specifying excitation motions. A time history may be such that its response spectrum envelops the RRS, but the energy content in certain frequency ranges will be low, so that equipment having important resonant frequencies in that range may not be adequately excited. This can be the result of the design of the time history or due to the interaction of the equipment and the shake table. There is a need to balance the concern that the equipment be adequately excited with the desire to avoid overtesting equipment during its qualification. While imposing a power spectral density requirement on the input time history can assure an acceptable distribution of energy over the frequency range of interest, this has proved problematic in attempting to address this issue (Kennedy, 2004). If the response spectrum of a time history is reasonably smooth, a reasonable distribution of the energy in the record is also assured (Kennedy, 2004). To avoid overtesting, the TRS is permitted to dip slightly below the RRS, with appropriate limitations. All of the table motions cited below refer to accelerations or signals that ultimately will be evaluated as accelerations

Spectral matching. The theoretical response spectrum developed for testing shall envelop the RRS according to the requirements of this section. When the high seismic level is specified, the RRS shown in Figure A.1 from Appendix A of IEEE 693 (IEEE, 1998) shall be used. When the moderate seismic level is specified, the RRS shown in Figure A.2 from Appendix A of IEEE 693 (IEEE, 1998) shall be used.

The theoretical response spectrum for testing shall be computed at 2% damping, at the resolution stated, and shall include the lower corner point frequency of the RRS (1.1 Hz), for comparison to the RRS.

Duration. The input motion shall have a duration of at least 20 sec of strong motion. Ring-down time or acceleration ramp-up time shall not be included in the 20 sec of strong motion. The duration of strong motion shall be defined as the time interval between when the plot of the time history reaches 25% of the maximum value to the time when it falls for the last time to 25% of the maximum value.

Theoretical input motion. The spectrum matching procedure shall be conducted at 1/24 octave resolution or higher, and result in a theoretical response spectrum that is within ± 10% of the RRS at 2% damping.

Filtering limits. The theoretical input motion record used for testing may be high-pass filtered at frequencies less than or equal to 70% of the lowest frequency of the test article, but not higher than 2 Hz. The lowest frequency of the test article shall be established by testing.

Filtered theoretical input motion to table. The response spectrum of the filtered table input motion shall envelop the RRS within a –5%/ +30% tolerance band at 1/12 octave resolution or higher. A –5% deviation is allowed at a given point, provided that the spectrum of the filtered table input motion at 2 or more adjacent points meets or exceeds the RRS, and not more than a total of 5 points fall below the RRS at the stated resolution. Exceedance of the +30% tolerance limit is acceptable with the concurrence of the equipment manufacturer. Exceedances of the stated upper tolerance limit at frequencies above 20 Hz are generally not of interest but should be accepted unless resonant frequencies are identified in that range.

The filtered input motion to the table shall include at least 2, and a maximum of about 25, high-amplitude cycles of a single-degree-of-freedom (SDOF) oscillator response at 2% damping. A “high-amplitude cycle” is a cycle defined by ASTM E1049 (ASTM, 1997; Downing, 1982) that consists of two positive or negative peaks of the same range with a peak of opposite sign between them, having an amplitude greater than or equal to 70% of the maximum response of the SDOF oscillator. SDOF oscillators in the frequency range from 0.78–11.78 Hz shall be included, and oscillator frequencies shall be selected with 1/12 octave band resolution. The minimum number of high-amplitude cycles is permitted to drop to 1 at no more than 5 frequency points in the specified frequency range. The number of high-amplitude cycles may exceed the stated maximum value with the concurrence of the equipment manufacturer. Procedures for computing the number of high-amplitude cycles are available at the IEEE web page. A detailed explanation of this requirement is given in the companion report (Takhirov et al., 2004).

The strong part ratio of the table input motion record shall be at least 30%. The "strong part ratio" of a given record is defined as the ratio of the time required to accumulate from 25%–75% of the total cumulative energy of the record to the time required to accumulate from 5%–95% of the total cumulative energy of the record.

Where:

$$\text{Cumulative Energy} = \int a(\tau)^2 \, d\tau$$

$a(\tau)$ = acceleration time history

Table output motion. The table output TRS shall envelop the RRS within a –10%/ +40% tolerance band at 1/12 octave resolution or higher. A –10% deviation is allowed at a given point, provided that the TRS at 2 or more adjacent points meet or exceed the RRS, and not more than a total of 5 points fall below the RRS at the stated resolution. Overtesting that exceeds the +40% limit is acceptable with the concurrence of the equipment manufacturer. Exceedances of the stated upper tolerance limit at frequencies above 20 Hz are generally not of interest but should be accepted unless resonant frequencies are identified in that range.

Appendix B Complete List of All Test Steps Performed

Table B.1 List of all tests performed from 03/25/2003–05/28/2003

Full-Length Supports' Calibration: 03/25/2003

	File Name	Signal name\Test	Strain gages	Gage Location
1	030325092908	Pull-back test in Y direction@300lbs	5–8	West 14' Support
2	030325111853	Pull-back test in X direction@300lbs	5–8	West 14' Support
3	030325140725	Pull-back test in Y direction@300lbs	1–4	East 14' Support
4	030325142832	Pull-back test in X direction@300lbs	1–4	East 14' Support

Insulator Posts' Calibration: 03/31/2003 and 04/01/2003

	File Name	Signal name\Test	Strain gages	Gage Location
5	030331105124	Stiffness and Gage Calibration in X	13–16	Rotating Post
6	030331120748	Stiffness and Gage Calibration in Y	13–16	Rotating Post
7	030331150436	Stiffness and Gage Calibration in X	25–28	Middle unit of Rigid Post
8	030331154004	Stiffness and Gage Calibration in Y	25–28	Middle unit of Rigid Post
9	030331165623	Stiffness and Gage Calibration in X	29–34	Top unit of Rigid Post
10	030331171107	Stiffness and Gage Calibration in Y	29–34	Top unit of Rigid Post
11	030401101557	Stiffness and Gage Calibration in X	9–12, 25–28, 29–34	Rigid Post
12	030401111157	Stiffness and Gage Calibration in Y	9–12, 25–28, 29–34	Rigid Post

Table B.1 *(continued)*

	File Name	Signal name\Test	Strain gages	Gage Location
13	030401135335	Stiffness and Gage Calibration in X	17–20, 21–24	Jaw Post
14	030401141308	Stiffness and Gage Calibration in Y	17–20, 21–24	Jaw Post

Static Pull-Back and Free Vibration Tests for Original Switch: 04/07/2003

	File Name	Signal name\Test	Switch Design	Mounting	Main Blade	Ground Switch
15	030407141830	Pull-back test in X direction@500lbs	Original	14' Support	Closed	Open
16	030408085222	Pull-back test in Y direction@500lbs	Original	14' Support	Closed	Open
17	030407143653	Manual excitation in X direction	Original	14' Support	Closed	Open
18	030407145351	Manual excitation in Y direction	Original	14' Support	Closed	Open

Dynamic Tests of Original Switch on 14' Supports; Blade closed: 04/09/2003

	File Name	Signal name\Test	Switch Design	Mounting	Main Blade	Ground Switch
19	030409132831	Random in X direction	Original	14' Support	Closed	Open
20	030409133836	Random in Y direction	Original	14' Support	Closed	Open
21	030409134232	Random in Z direction	Original	14' Support	Closed	Open
22	030409135109	Sweep24 in X direction	Original	14' Support	Closed	Open
23	030409140346	Sweep24 in Y direction	Original	14' Support	Closed	Open
24	030409140941	Sweep24 in Z direction	Original	14' Support	Closed	Open
25	030409142115	Landers5L@0.125g	Original	14' Support	Closed	Open
26	030409144826	Landers5L@0.25g	Original	14' Support	Closed	Open
27	030409155007	CERL@0.25g	Original	14' Support	Closed	Open

Free Vibration Tests for Modified Switch Rigidly Mounted; Blade closed: 04/15/2003

	File Name	Signal name\Test	Switch Design	Mounting	Main Blade	Ground Switch
28	030415150345	Manual excitation in X direction	Modified	Rigid	Closed	Open

Table B.1 ***(continued)***

	File Name	Signal name\Test	Strain gages	Gage Location		
29	030415152334	Manual excitation in Y direction	Modified	Rigid	Closed	Open

Free Vibration Tests for Modified Switch Rigidly Mounted; Blade open: 04/15/2003

	File Name	Signal name\Test	Switch Design	Mounting	Main Blade	Ground Switch
30	030415153805	Manual excitation in Y (Jaw)	Modified	Rigid	Open	Open
31	030415153938	Manual excitation in X (Jaw)	Modified	Rigid	Open	Open
32	030415155025	Manual excitation in X (Rigid&Rotating)	Modified	Rigid	Open	Open
33	030415155231	Manual excitation in Y (Rigid&Rotating)	Modified	Rigid	Open	Open

Dynamic Tests of Modified Switch Rigidly Mounted to Table; Blade closed: 04/16/2003

	File Name	Signal name\Test	Switch Design	Mounting	Main Blade	Ground Switch
34	030416124631	Random in X direction	Modified	Rigid	Closed	Open
35	030416123616	Random in Y direction	Modified	Rigid	Closed	Open
36	030416130719	Random in Z direction	Modified	Rigid	Closed	Open
37	030416131927	Sweep24 in X direction	Modified	Rigid	Closed	Open
38	030416133220	Sweep24 in Y direction	Modified	Rigid	Closed	Open
39	030416134339	Sweep24 in Z direction	Modified	Rigid	Closed	Open
40	03041613**5700**	Amplified Landers5L@0.25g; scale 1/4	Modified	Rigid	Closed	Open
41	03041614**4312**	Amplified Landers5L@0.25g; full scale	Modified	Rigid	Closed	Open
42	03041615**1618**	Amplified Landers5L@0.25g; scale 2	Modified	Rigid	Closed	Open

Dynamic Tests of Modified Switch Rigidly Mounted to Table; Blade open: 04/16/2003

	File Name	Signal name\Test	Switch Design	Mounting	Main Blade	Ground Switch
43	030416165053	Sweep24 in X direction	Modified	Rigid	Open	Open
44	030416164723	Sweep24 in Y direction	Modified	Rigid	Open	Open

Table B.1 ***(continued)***

	File Name	Signal name\Test	Strain gages	Gage Location		
45	030416165355	Sweep24 in Z direction	Modified	Rigid	Open	Open
46	03041617**1831**	Amplified Landers5L@0.25g; scale 1/4	Modified	Rigid	Open	Open

Tests of Modified Switch Rigidly Mounted to Table; Blade open: 04/18/2003

	File Name	Signal name\Test	Switch Design	Mounting	Main Blade	Ground Switch
47	030419134039	Manual excitation in X (Blade)	Modified	Rigid	Open	Open
48	030419134736	Manual excitation in Y (Blade)	Modified	Rigid	Open	Open
49	03041914**2759**	Landers5L@0.125g	Modified	Rigid	Open	Open

Dynamic Tests of Modified Rigidly Mounted to Table; Blade closed: 04/18/2003

	File Name	Signal name\Test	Switch Design	Mounting	Main Blade	Ground Switch
50	03041915**0732**	Landers5L@0.25g	Modified	Rigid	Closed	Open

Free Vibration Tests of Modified Switch Mounted on 4" Spacer; Blade closed: 04/24/2003

	File Name	Signal name\Test	Switch Design	Mounting	Shorten Blade	Ground Switch
51	030424141957	Manual excitation in X	Modified	4" spacer	Closed	Open
52	030424143341	Manual excitation in Y	Modified	4" spacer	Closed	Open

Dynamic Tests of Modified Switch Mounted on 4" Spacer; Blade closed: 04/24/2003

	File Name	Signal name\Test	Switch Design	Mounting	Main Blade	Ground Switch
53	030424154239	Random in X direction	Modified	4" spacer	Closed	Open
54	030424154411	Random in Y direction	Modified	4" spacer	Closed	Open
55	030424154521	Random in Z direction	Modified	4" spacer	Closed	Open
56	030424154951	Sweep24 in X direction	Modified	4" spacer	Closed	Open
57	030424155249	Sweep24 in Y direction	Modified	4" spacer	Closed	Open

Table B.1 ***(continued)***

	File Name	Signal name\Test	Strain gages	Gage Location		
58	030424155628	Sweep24 in Z direction	Modified	4" spacer	Closed	Open
59	030424160518	Amplified Landers5L@0.25g; full scale	Modified	4" spacer	Closed	Open
60	030424161120	Landers5L@0.25g	Modified	4" spacer	Closed	Open

Free Vibration Tests of Modified Switch Mounted on 4" Spacer; Blade open: 04/24/2003

	File Name	Signal name\Test	Switch Design	Mounting	Main Blade	Ground Switch
61	030424144012	Manual excitation in Y (Jaw)	Modified	4" spacer	Open	Open
62	030424144145	Manual excitation in X (Jaw)	Modified	4" spacer	Open	Open
63	030424144437	Manual excitation in X (Rigid&Rotating)	Modified	4" spacer	Open	Open
64	030424144604	Manual excitation in Y (Rigid&Rotating)	Modified	4" spacer	Open	Open
65	030424145339	Manual excitation in Y (Blade)	Modified	4" spacer	Open	Open
66	030424145459	Manual excitation in X (Blade)	Modified	4" spacer	Open	Open

Free Vibration Tests of Modified Switch Mounted on 4" Spacer; Shorten blade open: 04/25/2003

	File Name	Signal name\Test	Switch Design	Mounting	Shorten Blade	Ground Switch
67	030425151344	Manual excitation in Y (Rigid&Rotating)	Modified	4" spacer	Open	Open
68	030425152559	Manual excitation in X (Rigid&Rotating)	Modified	4" spacer	Open	Open
69	030425153216	Manual excitation in X (Jaw)	Modified	4" spacer	Open	Open
70	030425153347	Manual excitation in Y (Jaw)	Modified	4" spacer	Open	Open
71	030425155805	Manual excitation in X (Blade)	Modified	4" spacer	Open	Open
72	030425160003	Manual excitation in Y (Blade)	Modified	4" spacer	Open	Open

Static Pull-Back and Free Vibration Test for Modified Switch on Full-Length Supports: 05/06/2003

	File Name	Signal name\Test	Switch Design	Mounting	Main Blade	Ground Switch
73	030506085536	Pullback test in X direction@500lbs	Modified	14' Support	Closed	Open

Table B.1 ***(continued)***

	File Name	Signal name\Test	Strain gages	Gage Location		
74	030506103627	Pullback test in Y direction@500lbs	Modified	14' Support	Closed	Open
75	030506143402	Manual excitation in X direction	Modified	14' Support	Closed	Open
76	030506143934	Manual excitation in Y direction	Modified	14' Support	Closed	Open

Dynamic Tests of Modified Switch Mounted on 14' Supports; Blade closed: 05/07/2003

	File Name	Signal name\Test	Switch Design	Mounting	Main Blade	Ground Switch
77	030507100920	Random in X direction	Modified	14' Support	Closed	Open
78	030507104414	Random in Y direction	Modified	14' Support	Closed	Open
79	030507103710	Random in Z direction	Modified	14' Support	Closed	Open
80	030507134125	Sweep24 in X direction	Modified	14' Support	Closed	Open
81	030507140115	Sweep24 in Y direction	Modified	14' Support	Closed	Open
82	030507140924	Sweep24 in Z direction	Modified	14' Support	Closed	Open
83	03050714**2414**	Landers5L@0.125g	Modified	14' Support	Closed	Open
84	03050714**4116**	Landers5L@0.25g	Modified	14' Support	Closed	Open
85	03050715**2023**	CERL@0.25g	Modified	14' Support	Closed	Open

Dynamic Tests of Modified Switch Mounted on 14' Supports; Blade closed: 05/08/2003

	File Name	Signal name\Test	Switch Design	Mounting	Main Blade	Ground Switch
86	030508122001	Landers5L@0.125g	Modified	14' Support	Closed	Open
87	030508124144	Landers5L@0.5g	Modified	14' Support	Closed	Open

Pull-back tests of Modified Switch Mounted on 14' Supports; Blade replaced by dummy mass: 05/09/2003

	File Name	Signal name\Test	Switch Design	Mounting	Main Blade	Ground Switch
88	030509141030	Stiffness X (Rigid&Rotating)	Modified	14' Support	Removed	Open
89	030509155710	Stiffness Y (Rigid&Rotating)	Modified	14' Support	Removed	Open

Table B.1 ***(continued)***

	File Name	Signal name\Test	Strain gages	Gage Location		
90	030509145357	Stiffness X (Jaw)	Modified	14' Support	Removed	Open
91	030509160459	Stiffness Y (Jaw)	Modified	14' Support	Removed	Open

Dynamic Tests of Modified Switch Mounted on 14' Supports; Blade removed: 05/12/2003

	File Name	Signal name\Test	Switch Design	Mounting	Main Blade	Ground Switch
92	030512084123	Manual excitation in X (Rigid&Rotating)	Modified	14' Support	Removed	Open
93	030512085756	Manual excitation in Y (Rigid&Rotating)	Modified	14' Support	Removed	Open
94	030512090009	Manual excitation in X (Jaw)	Modified	14' Support	Removed	Open
95	030512090159	Manual excitation in Y (Jaw)	Modified	14' Support	Removed	Open
96	030512090521	Manual excitation in X (Jaw)	Modified	14' Support	Removed	Closed
97	030512090640	Manual excitation in Y (Jaw)	Modified	14' Support	Removed	Closed
98	030512100336	Random in X direction	Modified	14' Support	Removed	Open
99	030512101051	Random in Y direction	Modified	14' Support	Removed	Open
100	030512101205	Random in Z direction	Modified	14' Support	Removed	Open
101	030512110613	Sweep24 in X direction	Modified	14' Support	Removed	Open
102	030512111952	Sweep24 in Y direction	Modified	14' Support	Removed	Open
103	030512112301	Sweep24 in Z direction	Modified	14' Support	Removed	Open
104	030512113839	Random in X direction	Modified	14' Support	Removed	Closed
105	030512114023	Random in Y direction	Modified	14' Support	Removed	Closed
106	030512114145	Random in Z direction	Modified	14' Support	Removed	Closed
107	030512114614	Sweep24 in X direction	Modified	14' Support	Removed	Closed
108	030512114937	Sweep24 in Y direction	Modified	14' Support	Removed	Closed
109	030512115803	Sweep24 in Z direction	Modified	14' Support	Removed	Closed

Table B.1 ***(continued)***

Dynamic Tests of Modified Switch Mounted on 14' Supports; Blade removed (GSW open): 05/12/2003

	File Name	Signal name\Test	Switch Design	Mounting	Main Blade	Ground Switch
110	030512124245	Landers5L@0.125g	Modified	14' Support	Removed	Open
111	030512142536	Landers5L@0.25g	Modified	14' Support	Removed	Open
112	030512143921	Landers5L@0.5g	Modified	14' Support	Removed	Open

Dynamic Tests of Modified Switch Mounted on 14' Supports; Blade removed (GSW closed): 05/12/2003

	File Name	Signal name\Test	Switch Design	Mounting	Main Blade	Ground Switch
113	030512151835	Landers5L@0.125g	Modified	14' Support	Removed	Closed
114	030512152035	Landers5L@0.25g	Modified	14' Support	Removed	Closed
115	030512152232	Landers5L@0.5g	Modified	14' Support	Removed	Closed

Dynamic Tests of Modified Switch Mounted on 14' Supports; Blade removed (GSW closed: Retest): 05/13/2003

	File Name	Signal name\Test	Switch Design	Mounting	Main Blade	Ground Switch
116	030513114033	Landers5L@0.125g	Modified	14' Support	Removed	Closed
117	030513114305	Landers5L@0.25g	Modified	14' Support	Removed	Closed
118	030513114511	Landers5L@0.5g	Modified	14' Support	Removed	Closed

Dynamic Tests of Modified Switch Mounted on 14' Supports; Blade closed: 05/15/2003

	File Name	Signal name\Test	Switch Design	Mounting	Main Blade	Ground Switch
119	030515102324	Landers5L@0.125g	Modified	14' Support	Closed	Open
120	030515103702	Landers5L@0.25g	Modified	14' Support	Closed	Open
121	030515120814	Landers5L@0.5g	Modified	14' Support	Closed	Open
122	030515124835	Landers5H@0.75g	Modified	14' Support	Closed	Open
123	030515150039	Landers5H@1.0g (PL)	Modified	14' Support	Closed	Open

Table B.1 ***(continued)***

Dynamic and Free-Vibrations of Modified Switch Mounted on 4" Spacer; Blade closed: 05/19/2003

	File Name	Signal name\Test	Switch Design	Mounting	Main Blade	Ground Switch
124	030519100141	Random in X direction	Modified	4" spacer	Closed	Open
125	030519100254	Random in Y direction	Modified	4" spacer	Closed	Open
126	030519100353	Random in Z direction	Modified	4" spacer	Closed	Open
127	030519102013	Sweep24 in X direction	Modified	4" spacer	Closed	Open
128	030519102307	Sweep24 in Y direction	Modified	4" spacer	Closed	Open
129	030519102652	Sweep24 in Z direction	Modified	4" spacer	Closed	Open
130	030519111046	Landers5L@0.25g	Modified	4" spacer	Closed	Open
131	030519104714	Landers5L@0.5g	Modified	4" spacer	Closed	Open
132	0305191120651	Manual excitation in X	Modified	4" spacer	Closed	Open
133	030519120927	Manual excitation in Y	Modified	4" spacer	Closed	Open
134	030519121645	Manual excitation in X (Jaw)	Modified	4" spacer	Open	Open
135	030519121501	Manual excitation in Y (Jaw)	Modified	4" spacer	Open	Open
136	030519121928	Manual excitation in X (Jaw)	Modified	4" spacer	Open	Closed
137	0305191212018	Manual excitation in Y (Jaw)	Modified	4" spacer	Open	Closed
138	030519123020	Manual excitation in X (Blade)	Modified	4" spacer	Open	Closed
139	030519123228	Manual excitation in Y (Blade)	Modified	4" spacer	Open	Closed
140	030519123537	Manual excitation in X (Rigid&Rotating)	Modified	4" spacer	Open	Closed
141	030519123650	Manual excitation in Y (Rigid&Rotating)	Modified	4" spacer	Open	Closed
142	missing	Random in X direction	Modified	4" spacer	Open	Closed
143	030519134145	Random in Y direction	Modified	4" spacer	Open	Closed
144	030519134340	Random in Z direction	Modified	4" spacer	Open	Closed
145	030519134808	Sweep24 in X direction	Modified	4" spacer	Open	Closed
146	030519135102	Sweep24 in Y direction	Modified	4" spacer	Open	Closed
147	030519135359	Sweep24 in Z direction	Modified	4" spacer	Open	Closed
148	030519140246	Random in X direction	Modified	4" spacer	Open	Open

Table B.1 ***(continued)***

	File Name	Signal name\Test	Strain gages	Gage Location		
149	030519140356	Random in Y direction	Modified	4" spacer	Open	Open
150	030519140521	Random in Z direction	Modified	4" spacer	Open	Open
151	030519141003	Sweep24 in X direction	Modified	4" spacer	Open	Open
152	030519141250	Sweep24 in Y direction	Modified	4" spacer	Open	Open
153	030519141542	Sweep24 in Z direction	Modified	4" spacer	Open	Open
154	030519151233	Landers3@0.25g	Modified	4" spacer	Closed	Open
155	030519152926	Landers3@0.5g	Modified	4" spacer	Closed	Open
156	030519163549	Landers5H@0.5g	Modified	4" spacer	Closed	Open
157	030519164554	Landers5H@0.6g	Modified	4" spacer	Closed	Open

Dynamic Tests of Modified Switch Mounted on 4" Spacer; Blade open: 05/20/2003

	File Name	Signal name\Test	Switch Design	Mounting	Main Blade	Ground Switch
158	030520120634	Random in X direction	Modified	4" spacer	Open	Closed
159	030520120736	Random in Y direction	Modified	4" spacer	Open	Closed
160	030520120844	Random in Z direction	Modified	4" spacer	Open	Closed
161	030520123032	Landers5H@0.5g	Modified	4" spacer	Open	Closed
162	030520125337	Landers5H@0.85g	Modified	4" spacer	Open	Closed
163	030520132259	Landers5H@1.0g	Modified	4" spacer	Open	Closed
164	030520141531	Landers5H@1.17g	Modified	4" spacer	Open	Closed
165	030520143037	Random in X direction	Modified	4" spacer	Open	Closed
166	030520143143	Random in Y direction	Modified	4" spacer	Open	Closed
167	030520143252	Random in Z direction	Modified	4" spacer	Open	Closed
168	030520143714	Sweep24 in X direction	Modified	4" spacer	Open	Closed
169	030520144001	Sweep24 in Y direction	Modified	4" spacer	Open	Closed
170	030520144239	Sweep24 in Z direction	Modified	4" spacer	Open	Closed

Table B.1 ***(continued)***

Static and Free-Vibration Tests for Full-Length Support without Leveling Bolts (West): 05/23/2003

	File Name	Signal name\Test	Strain gages	Gage Location
171	030523105635	Pull-back test in X direction@300lbs	5–8	West 14' Support
172	030523111547	Manual excitation in X direction	5–8	West 14' Support

Free-Vibration and Fragility Tests for Rotating Insulator Post: 05/27/2003

	File Name	Signal name\Test	Strain gages	Gage Location
173	030527130701	Manual excitation in X direction	13–16	Rotating Insulator Post
174	030527130739	Manual excitation in Y direction	13–16	Rotating Insulator Post
175	030527152716	Fragility test in X direction	13–16	Rotating Insulator Post

Free-Vibration and Fragility Tests for Rigid and Jaw Insulator Posts: 05/28/2003

	File Name	Signal name\Test	Strain gages	Gage Location
176	030528104849	Manual excitation in X direction	9–12, 25–28, 29–34	Rigid Insulator Post
177	030528105049	Manual excitation in Y direction	9–12, 25–28, 29–34	Rigid Insulator Post
178	030528311501	Fragility test in X direction	9–12, 25–28, 29–34	Rigid Insulator Post
179	030528145353	Manual excitation in X direction	17–20, 21–24	Jaw Insulator Post
180	030528145507	Manual excitation in Y direction	17–20, 21–24	Jaw Insulator Post
181	030528152311	Fragility test in X direction	17–20, 21–24	Jaw Insulator Post

Appendix C Resonance Search for Support- and Spacer-Mounted Configurations Used in Qualification Study

The appendix presents plots for resonance search conducted for the support-mounted and spacer-mounted modified switch used in the qualification study.

The resonance search was conducted with a sine-sweep signal, and a typical power spectral density (PSD) of the acceleration data recorded at the table level is presented in Figure C.1.

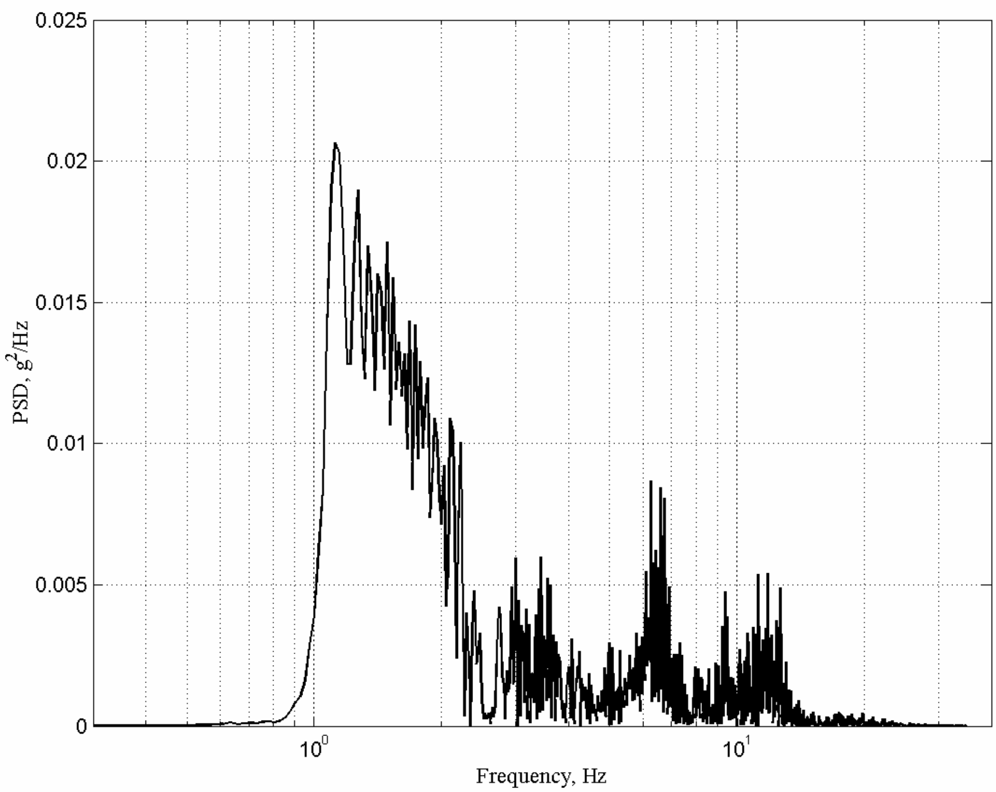

Fig. C.1 Typical PSD of acceleration data recorded at table level

The resonance-search results for the support-mounted switch with the main blade closed and the grounding blade open are presented in Figures C.2–C.4. The plots present acceleration PSD at two levels: at the level corresponding to the top of the support legs and at the top of insulator posts. Figures C.5–C.7 show the resonance-search results for the spacer-mounted switch with the main blade open and the grounding blade closed. The plots present acceleration PSD at the tops of insulator posts and at the tip of the main blade. The PSDs in the low-frequency range for the vertical direction (Figs. C.4 and C.7) repeat the trend of the PSD at the table level (Fig. C.1) that reflects the high stiffness of the switch in the vertical direction.

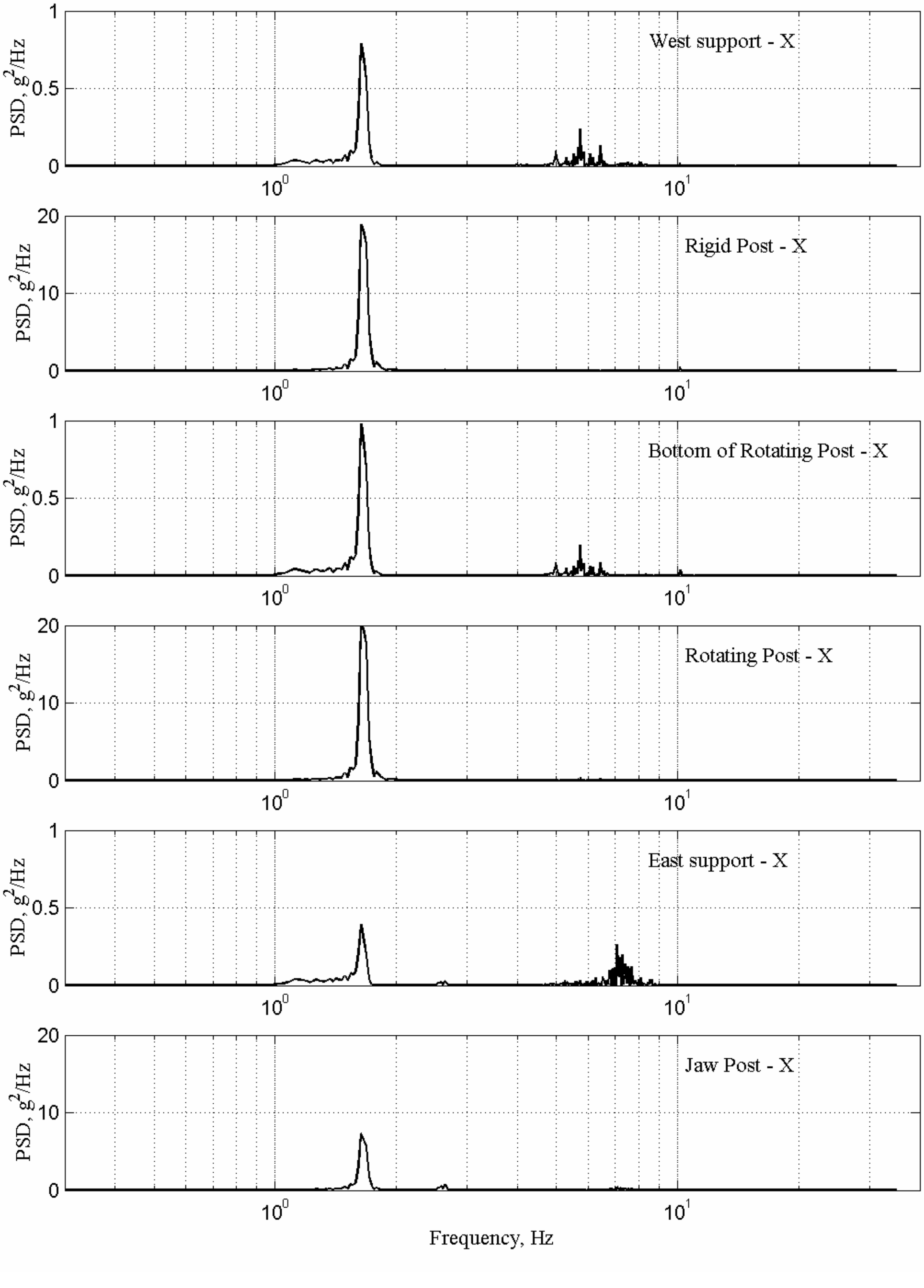

Fig. C.2 Resonance-search results for support-mounted switch in X direction

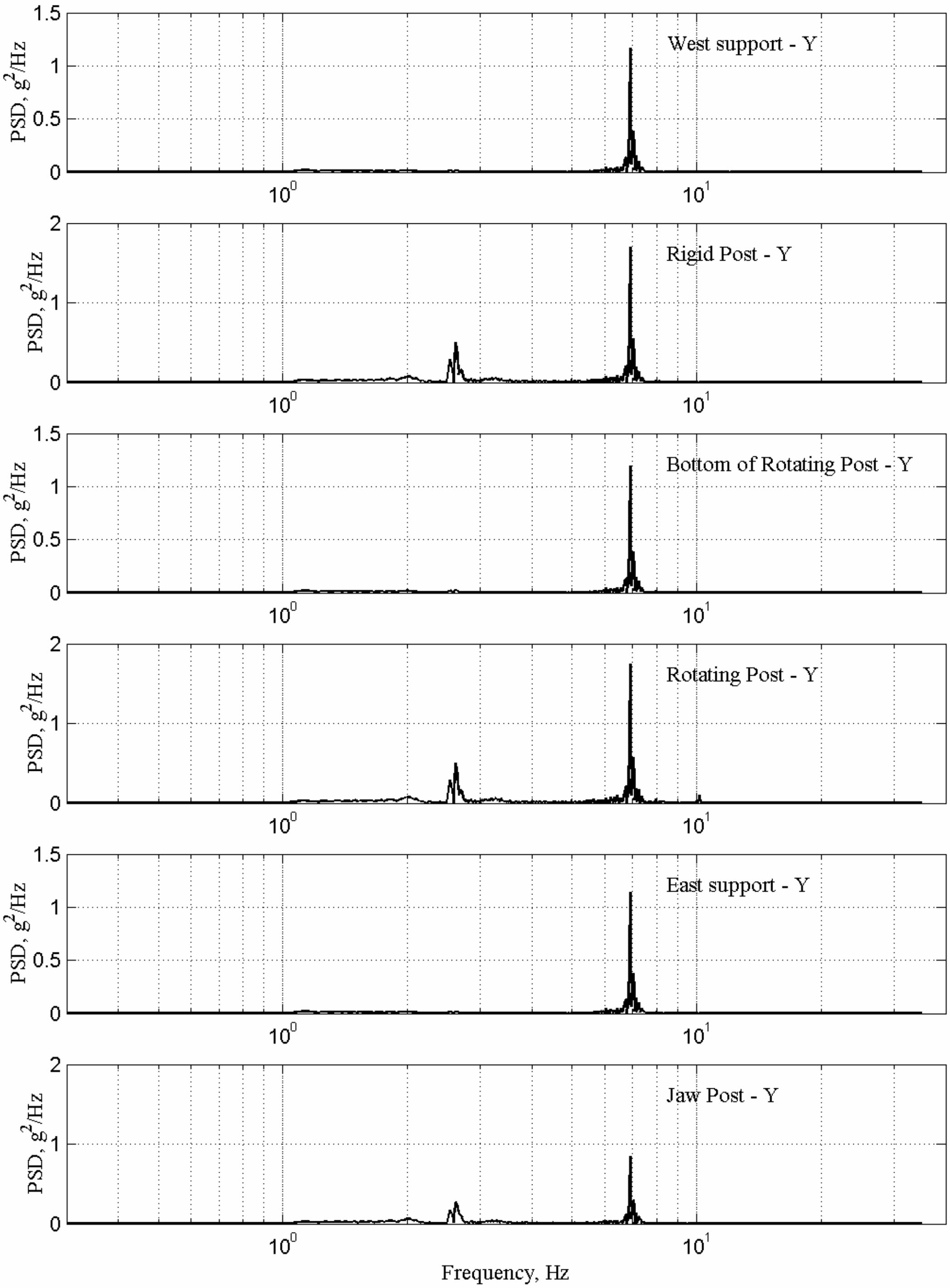

Fig. C.3 Resonance-search results for support-mounted switch in Y direction

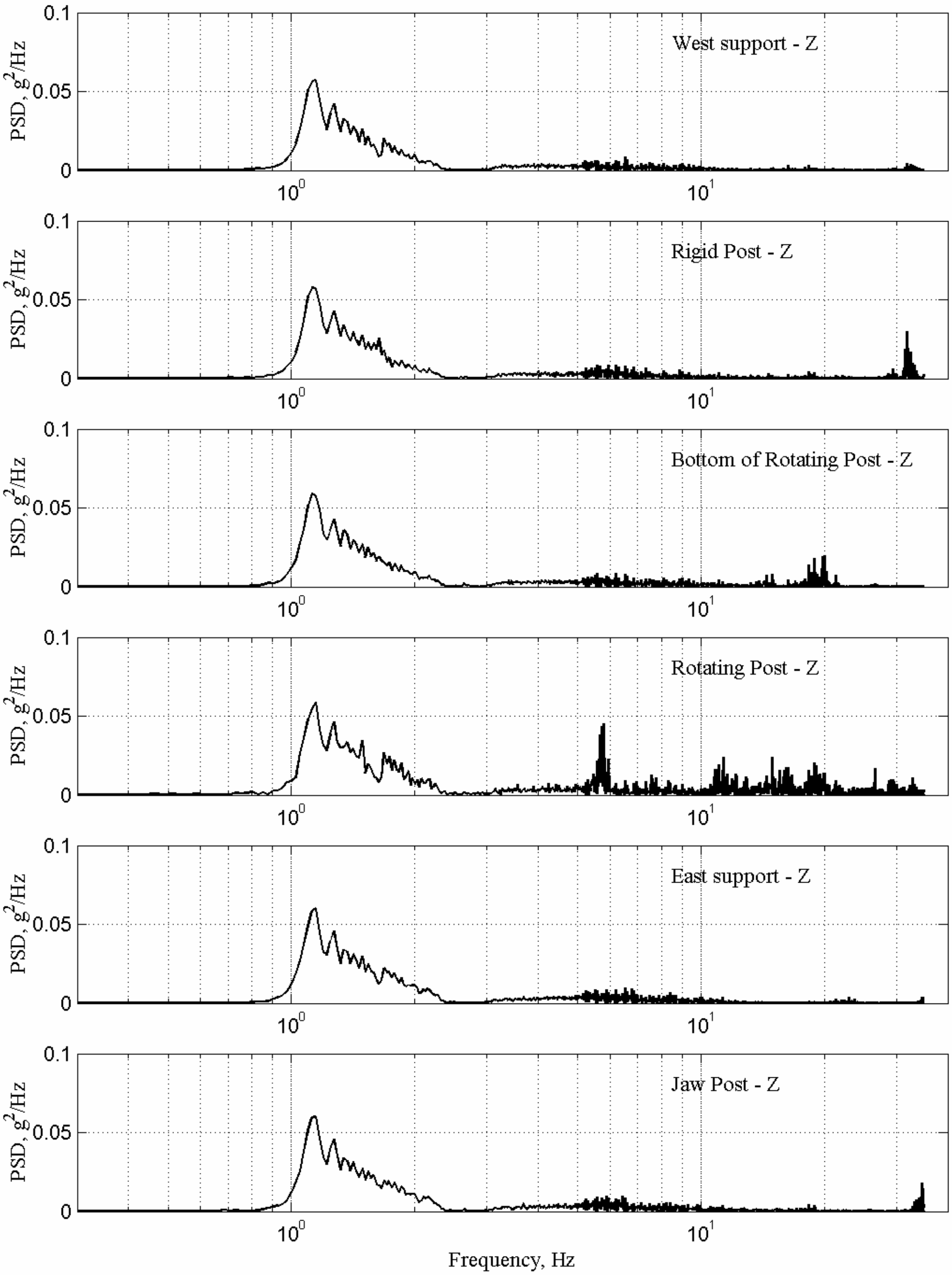

Fig. C.4 Resonance-search results for support-mounted switch in Z direction

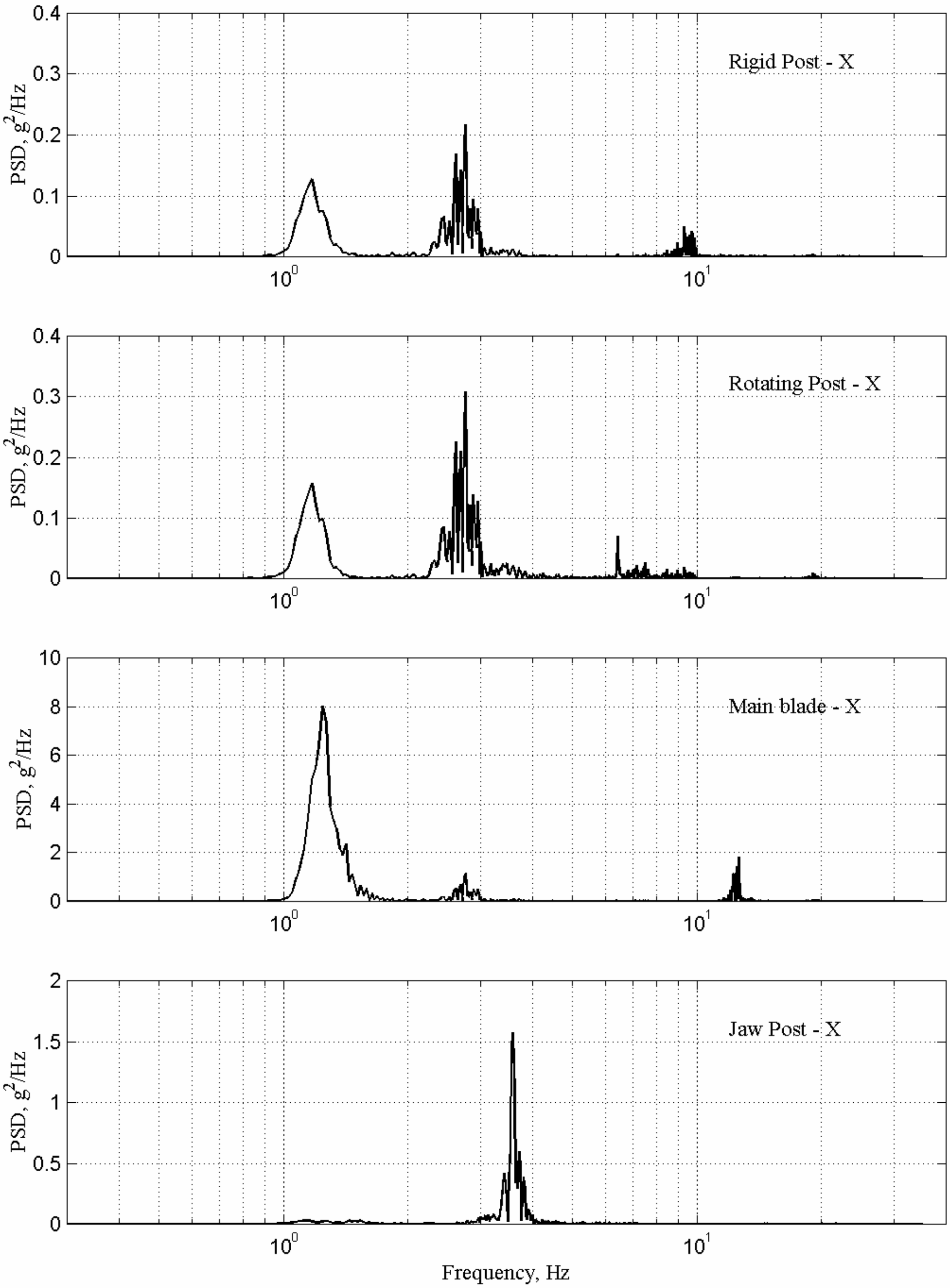

Fig. C.5 Resonance-search results for spacer-mounted switch in X direction

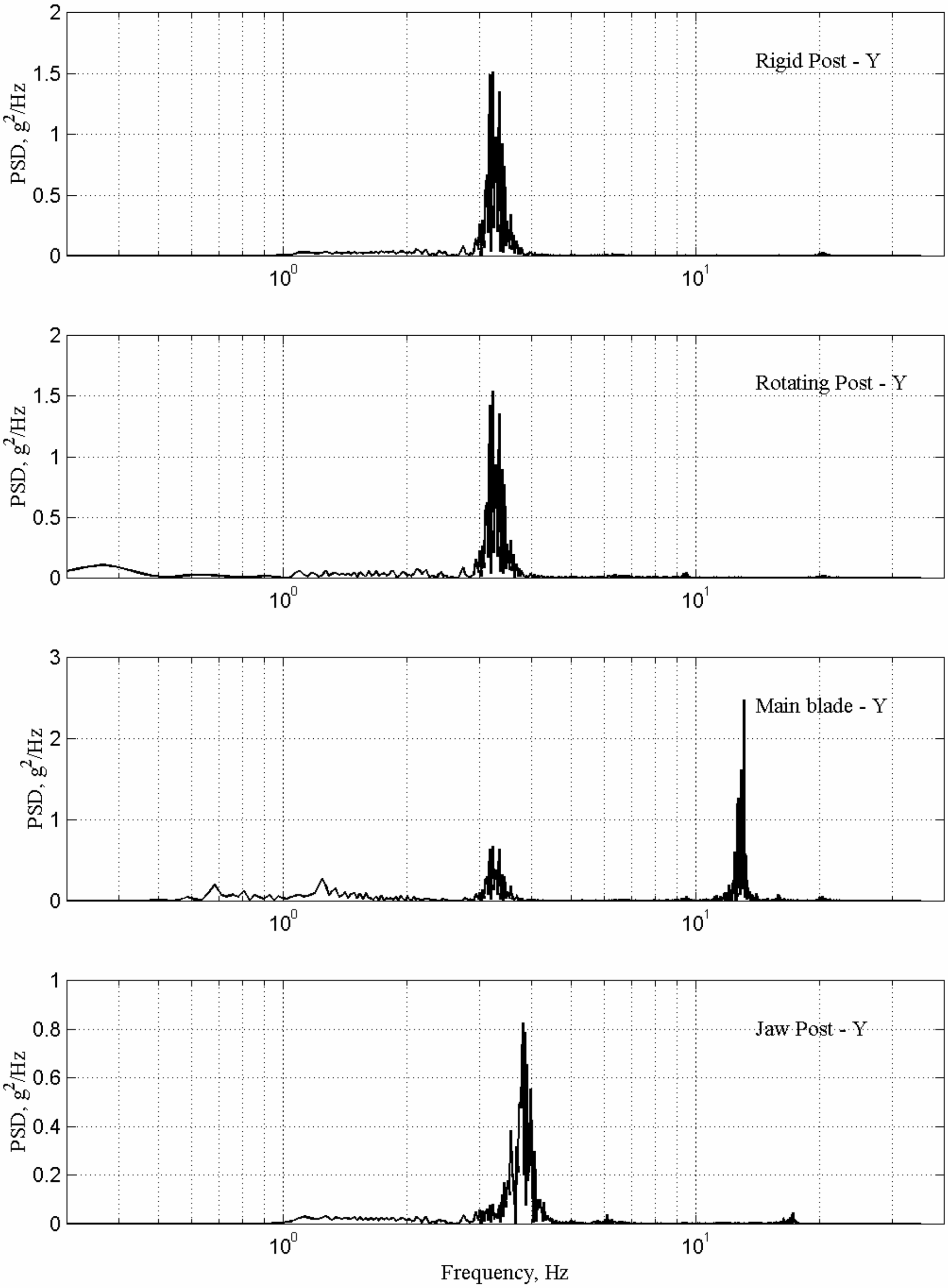

Fig. C.6 Resonance-search results for spacer-mounted switch in Y direction

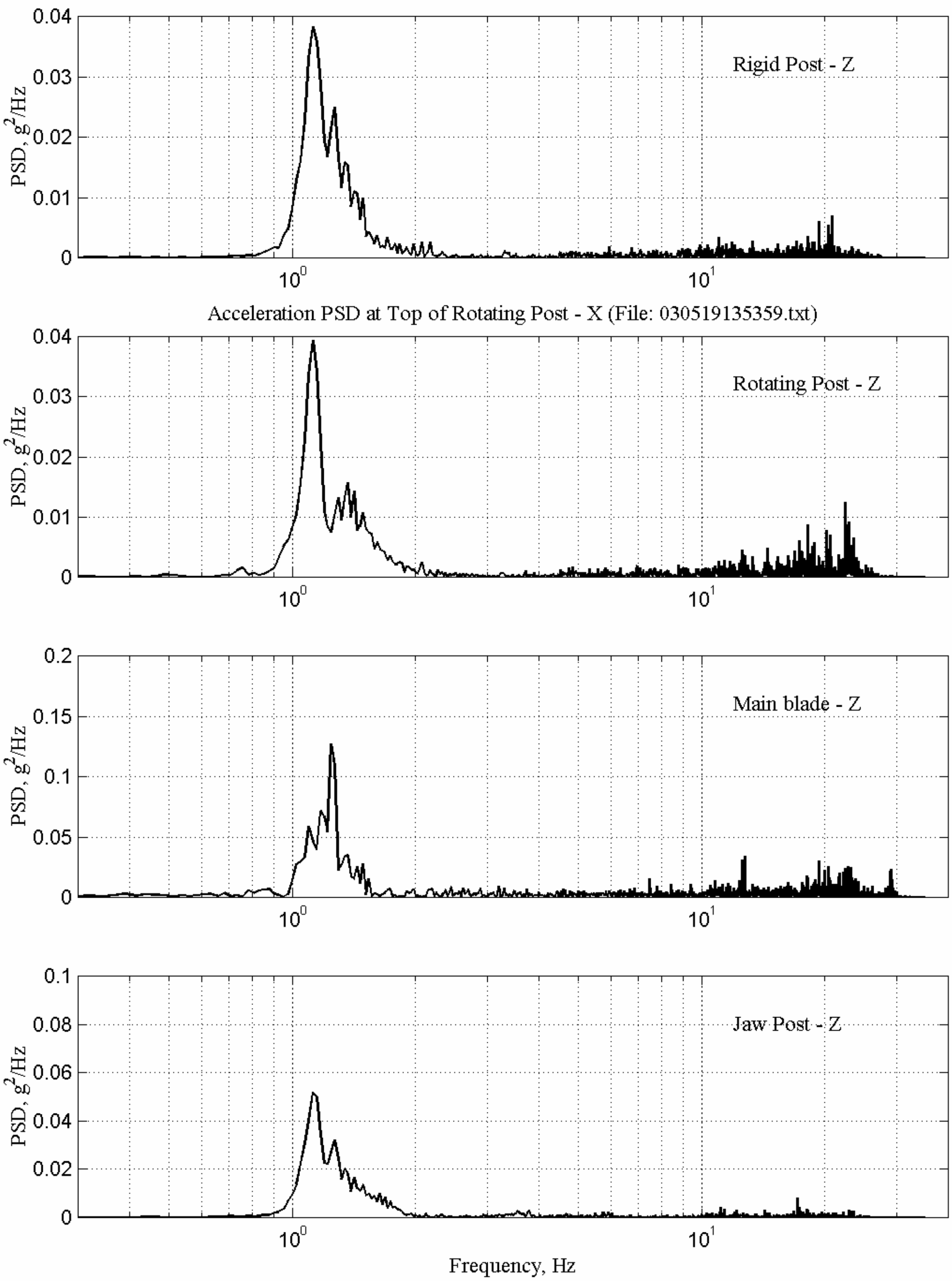

Fig. C.7 Resonance-search results for spacer-mounted switch in Z direction

PEER REPORTS

PEER reports are available from the National Information Service for Earthquake Engineering (NISEE). To order PEER reports, please contact the Pacific Earthquake Engineering Research Center, 1301 South 46th Street, Richmond, California 94804-4698. Tel.: (510) 231-9468; Fax: (510) 231-9461.

PEER 2004/08 *Seismic Qualification and Fragility Testing of Line Break 550-kV Disconnect Switches.* Shakhzod M. Takhirov, Gregory L. Fenves, and Eric Fujisaki. February 2005.

PEER 2004/07 *Ground Motions for Earthquake Simulator Qualification of Electrical Substation Equipment.* Shakhzod M. Takhirov, Gregory L. Fenves, Eric Fujisaki, and Don Clyde. January 2005.

PEER 2004/06 *Performance-Based Regulation and Regulatory Regimes.* Peter J. May and Chris Koski. September 2004.

PEER 2004/05 *Performance-Based Seismic Design Concepts and Implementation: Proceedings of an International Workshop.* Peter Fajfar and Helmut Krawinkler, editors. September 2004.

PEER 2004/03 *Evaluation and Application of Concrete Tilt-up Assessment Methodologies.* Timothy Graf and James O. Malley. October 2004.

PEER 2004/02 *Analytical Investigations of New Methods for Reducing Residual Displacements of Reinforced Concrete Bridge Columns.* Junichi Sakai and Stephen A. Mahin. August 2004.

PEER 2004/01 *Seismic Performance of Masonry Buildings and Design Implications.* Kerri Anne Taeko Tokoro, James C. Anderson, and Vitelmo V. Bertero. February 2004.

PEER 2003/18 *Performance Models for Flexural Damage in Reinforced Concrete Columns.* Michael Berry and Marc Eberhard. August 2003.

PEER 2003/17 *Predicting Earthquake Damage in Older Reinforced Concrete Beam-Column Joints.* Catherine Pagni and Laura Lowes. October 2004.

PEER 2003/16 *Seismic Demands for Performance-Based Design of Bridges.* Kevin Mackie and Božidar Stojadinović. August 2003.

PEER 2003/15 *Seismic Demands for Nondeteriorating Frame Structures and Their Dependence on Ground Motions.* Ricardo Antonio Medina and Helmut Krawinkler. May 2004.

PEER 2003/14 *Finite Element Reliability and Sensitivity Methods for Performance-Based Earthquake Engineering.* Terje Haukaas and Armen Der Kiureghian. April 2004.

PEER 2003/13 *Effects of Connection Hysteretic Degradation on the Seismic Behavior of Steel Moment-Resisting Frames.* Janise E. Rodgers and Stephen A. Mahin. March 2004.

PEER 2003/12 *Implementation Manual for the Seismic Protection of Laboratory Contents: Format and Case Studies.* William T. Holmes and Mary C. Comerio. October 2003.

PEER 2003/11 *Fifth U.S.-Japan Workshop on Performance-Based Earthquake Engineering Methodology for Reinforced Concrete Building Structures.* February 2004.

PEER 2003/10 *A Beam-Column Joint Model for Simulating the Earthquake Response of Reinforced Concrete Frames.* Laura N. Lowes, Nilanjan Mitra, and Arash Altoontash. February 2004.

PEER 2003/09 *Sequencing Repairs after an Earthquake: An Economic Approach.* Marco Casari and Simon J. Wilkie. April 2004.

PEER 2003/08 *A Technical Framework for Probability-Based Demand and Capacity Factor Design (DCFD) Seismic Formats.* Fatemeh Jalayer and C. Allin Cornell. November 2003.

PEER 2003/07 *Uncertainty Specification and Propagation for Loss Estimation Using FOSM Methods.* Jack W. Baker and C. Allin Cornell. September 2003.

PEER 2003/06 *Performance of Circular Reinforced Concrete Bridge Columns under Bidirectional Earthquake Loading*. Mahmoud M. Hachem, Stephen A. Mahin, and Jack P. Moehle. February 2003.

PEER 2003/05 *Response Assessment for Building-Specific Loss Estimation.* Eduardo Miranda and Shahram Taghavi. September 2003.

PEER 2003/04 *Experimental Assessment of Columns with Short Lap Splices Subjected to Cyclic Loads*. Murat Melek, John W. Wallace, and Joel Conte. April 2003.

PEER 2003/03 *Probabilistic Response Assessment for Building-Specific Loss Estimation.* Eduardo Miranda and Hesameddin Aslani. September 2003.

PEER 2003/02 *Software Framework for Collaborative Development of Nonlinear Dynamic Analysis Program.* Jun Peng and Kincho H. Law. September 2003.

PEER 2003/01 *Shake Table Tests and Analytical Studies on the Gravity Load Collapse of Reinforced Concrete Frames*. Kenneth John Elwood and Jack P. Moehle. November 2003.

PEER 2002/24 *Performance of Beam to Column Bridge Joints Subjected to a Large Velocity Pulse.* Natalie Gibson, André Filiatrault, and Scott A. Ashford. April 2002.

PEER 2002/23 *Effects of Large Velocity Pulses on Reinforced Concrete Bridge Columns.* Greg L. Orozco and Scott A. Ashford. April 2002.

PEER 2002/22 *Characterization of Large Velocity Pulses for Laboratory Testing.* Kenneth E. Cox and Scott A. Ashford. April 2002.

PEER 2002/21 *Fourth U.S.-Japan Workshop on Performance-Based Earthquake Engineering Methodology for Reinforced Concrete Building Structures*. December 2002.

PEER 2002/20 *Barriers to Adoption and Implementation of PBEE Innovations.* Peter J. May. August 2002.

PEER 2002/19 *Economic-Engineered Integrated Models for Earthquakes: Socioeconomic Impacts.* Peter Gordon, James E. Moore II, and Harry W. Richardson. July 2002.

PEER 2002/18 *Assessment of Reinforced Concrete Building Exterior Joints with Substandard Details.* Chris P. Pantelides, Jon Hansen, Justin Nadauld, and Lawrence D. Reaveley. May 2002.

PEER 2002/17 *Structural Characterization and Seismic Response Analysis of a Highway Overcrossing Equipped with Elastomeric Bearings and Fluid Dampers: A Case Study.* Nicos Makris and Jian Zhang. November 2002.

PEER 2002/16 *Estimation of Uncertainty in Geotechnical Properties for Performance-Based Earthquake Engineering.* Allen L. Jones, Steven L. Kramer, and Pedro Arduino. December 2002.

PEER 2002/15 *Seismic Behavior of Bridge Columns Subjected to Various Loading Patterns.* Asadollah Esmaeily-Gh. and Yan Xiao. December 2002.

PEER 2002/14 *Inelastic Seismic Response of Extended Pile Shaft Supported Bridge Structures.* T.C. Hutchinson, R.W. Boulanger, Y.H. Chai, and I.M. Idriss. December 2002.

PEER 2002/13 *Probabilistic Models and Fragility Estimates for Bridge Components and Systems.* Paolo Gardoni, Armen Der Kiureghian, and Khalid M. Mosalam. June 2002.

PEER 2002/12 *Effects of Fault Dip and Slip Rake on Near-Source Ground Motions: Why Chi-Chi Was a Relatively Mild M7.6 Earthquake.* Brad T. Aagaard, John F. Hall, and Thomas H. Heaton. December 2002.

PEER 2002/11 *Analytical and Experimental Study of Fiber-Reinforced Strip Isolators*. James M. Kelly and Shakhzod M. Takhirov. September 2002.

PEER 2002/10 *Centrifuge Modeling of Settlement and Lateral Spreading with Comparisons to Numerical Analyses***.** Sivapalan Gajan and Bruce L. Kutter. January 2003.

PEER 2002/09 *Documentation and Analysis of Field Case Histories of Seismic Compression during the 1994 Northridge, California, Earthquake.* Jonathan P. Stewart, Patrick M. Smith, Daniel H. Whang, and Jonathan D. Bray. October 2002.

PEER 2002/08 *Component Testing, Stability Analysis and Characterization of Buckling-Restrained Unbonded Braces™.* Cameron Black, Nicos Makris, and Ian Aiken. September 2002.

PEER 2002/07 *Seismic Performance of Pile-Wharf Connections.* Charles W. Roeder, Robert Graff, Jennifer Soderstrom, and Jun Han Yoo. December 2001.

PEER 2002/06 *The Use of Benefit-Cost Analysis for Evaluation of Performance-Based Earthquake Engineering Decisions*. Richard O. Zerbe and Anthony Falit-Baiamonte. September 2001.

PEER 2002/05 *Guidelines, Specifications, and Seismic Performance Characterization of Nonstructural Building Components and Equipment*. André Filiatrault, Constantin Christopoulos, and Christopher Stearns. September 2001.

PEER 2002/04 *Consortium of Organizations for Strong-Motion Observation Systems and the Pacific Earthquake Engineering Research Center Lifelines Program: Invited Workshop on Archiving and Web Dissemination of Geotechnical Data, 4–5 October 2001*. September 2002.

PEER 2002/03 *Investigation of Sensitivity of Building Loss Estimates to Major Uncertain Variables for the Van Nuys Testbed.* Keith A. Porter, James L. Beck, and Rustem V. Shaikhutdinov. August 2002.

PEER 2002/02 *The Third U.S.-Japan Workshop on Performance-Based Earthquake Engineering Methodology for Reinforced Concrete Building Structures*. July 2002.

PEER 2002/01 *Nonstructural Loss Estimation: The UC Berkeley Case Study.* Mary C. Comerio and John C. Stallmeyer. December 2001.

PEER 2001/16 *Statistics of SDF-System Estimate of Roof Displacement for Pushover Analysis of Buildings.* Anil K. Chopra, Rakesh K. Goel, and Chatpan Chintanapakdee. December 2001.

PEER 2001/15 *Damage to Bridges during the 2001 Nisqually Earthquake.* R. Tyler Ranf, Marc O. Eberhard, and Michael P. Berry. November 2001.

PEER 2001/14 *Rocking Response of Equipment Anchored to a Base Foundation.* Nicos Makris and Cameron J. Black. September 2001.

PEER 2001/13 *Modeling Soil Liquefaction Hazards for Performance-Based Earthquake Engineering.* Steven L. Kramer and Ahmed-W. Elgamal. February 2001.

PEER 2001/12 *Development of Geotechnical Capabilities in OpenSees.* Boris Jeremić. September 2001.

PEER 2001/11 *Analytical and Experimental Study of Fiber-Reinforced Elastomeric Isolators*. James M. Kelly and Shakhzod M. Takhirov. September 2001.

PEER 2001/10 *Amplification Factors for Spectral Acceleration in Active Regions.* Jonathan P. Stewart, Andrew H. Liu, Yoojoong Choi, and Mehmet B. Baturay. December 2001.

PEER 2001/09 *Ground Motion Evaluation Procedures for Performance-Based Design.* Jonathan P. Stewart, Shyh-Jeng Chiou, Jonathan D. Bray, Robert W. Graves, Paul G. Somerville, and Norman A. Abrahamson. September 2001.

PEER 2001/08 *Experimental and Computational Evaluation of Reinforced Concrete Bridge Beam-Column Connections for Seismic Performance*. Clay J. Naito, Jack P. Moehle, and Khalid M. Mosalam. November 2001.

PEER 2001/07 *The Rocking Spectrum and the Shortcomings of Design Guidelines.* Nicos Makris and Dimitrios Konstantinidis. August 2001.

PEER 2001/06 *Development of an Electrical Substation Equipment Performance Database for Evaluation of Equipment Fragilities*. Thalia Agnanos. April 1999.

PEER 2001/05 *Stiffness Analysis of Fiber-Reinforced Elastomeric Isolators.* Hsiang-Chuan Tsai and James M. Kelly. May 2001.

PEER 2001/04 *Organizational and Societal Considerations for Performance-Based Earthquake Engineering.* Peter J. May. April 2001.

PEER 2001/03 *A Modal Pushover Analysis Procedure to Estimate Seismic Demands for Buildings: Theory and Preliminary Evaluation.* Anil K. Chopra and Rakesh K. Goel. January 2001.

PEER 2001/02 *Seismic Response Analysis of Highway Overcrossings Including Soil-Structure Interaction.* Jian Zhang and Nicos Makris. March 2001.

PEER 2001/01 *Experimental Study of Large Seismic Steel Beam-to-Column Connections.* Egor P. Popov and Shakhzod M. Takhirov. November 2000.

PEER 2000/10 *The Second U.S.-Japan Workshop on Performance-Based Earthquake Engineering Methodology for Reinforced Concrete Building Structures.* March 2000.

PEER 2000/09 *Structural Engineering Reconnaissance of the August 17, 1999 Earthquake: Kocaeli (Izmit), Turkey.* Halil Sezen, Kenneth J. Elwood, Andrew S. Whittaker, Khalid Mosalam, John J. Wallace, and John F. Stanton. December 2000.

PEER 2000/08 *Behavior of Reinforced Concrete Bridge Columns Having Varying Aspect Ratios and Varying Lengths of Confinement.* Anthony J. Calderone, Dawn E. Lehman, and Jack P. Moehle. January 2001.

PEER 2000/07 *Cover-Plate and Flange-Plate Reinforced Steel Moment-Resisting Connections.* Taejin Kim, Andrew S. Whittaker, Amir S. Gilani, Vitelmo V. Bertero, and Shakhzod M. Takhirov. September 2000.

PEER 2000/06 *Seismic Evaluation and Analysis of 230-kV Disconnect Switches.* Amir S. J. Gilani, Andrew S. Whittaker, Gregory L. Fenves, Chun-Hao Chen, Henry Ho, and Eric Fujisaki. July 2000.

PEER 2000/05 *Performance-Based Evaluation of Exterior Reinforced Concrete Building Joints for Seismic Excitation.* Chandra Clyde, Chris P. Pantelides, and Lawrence D. Reaveley. July 2000.

PEER 2000/04 *An Evaluation of Seismic Energy Demand: An Attenuation Approach.* Chung-Che Chou and Chia-Ming Uang. July 1999.

PEER 2000/03 *Framing Earthquake Retrofitting Decisions: The Case of Hillside Homes in Los Angeles.* Detlof von Winterfeldt, Nels Roselund, and Alicia Kitsuse. March 2000.

PEER 2000/02 *U.S.-Japan Workshop on the Effects of Near-Field Earthquake Shaking.* Andrew Whittaker, ed. July 2000.

PEER 2000/01 *Further Studies on Seismic Interaction in Interconnected Electrical Substation Equipment.* Armen Der Kiureghian, Kee-Jeung Hong, and Jerome L. Sackman. November 1999.

PEER 1999/14 *Seismic Evaluation and Retrofit of 230-kV Porcelain Transformer Bushings*. Amir S. Gilani, Andrew S. Whittaker, Gregory L. Fenves, and Eric Fujisaki. December 1999.

PEER 1999/13 *Building Vulnerability Studies: Modeling and Evaluation of Tilt-up and Steel Reinforced Concrete Buildings.* John W. Wallace, Jonathan P. Stewart, and Andrew S. Whittaker, editors. December 1999.

PEER 1999/12 *Rehabilitation of Nonductile RC Frame Building Using Encasement Plates and Energy-Dissipating Devices.* Mehrdad Sasani, Vitelmo V. Bertero, James C. Anderson. December 1999.

PEER 1999/11 *Performance Evaluation Database for Concrete Bridge Components and Systems under Simulated Seismic Loads.* Yael D. Hose and Frieder Seible. November 1999.

PEER 1999/10 *U.S.-Japan Workshop on Performance-Based Earthquake Engineering Methodology for Reinforced Concrete Building Structures.* December 1999.

PEER 1999/09 *Performance Improvement of Long Period Building Structures Subjected to Severe Pulse-Type Ground Motions*. James C. Anderson, Vitelmo V. Bertero, and Raul Bertero. October 1999.

PEER 1999/08 *Envelopes for Seismic Response Vectors.* Charles Menun and Armen Der Kiureghian. July 1999.

PEER 1999/07 *Documentation of Strengths and Weaknesses of Current Computer Analysis Methods for Seismic Performance of Reinforced Concrete Members.* William F. Cofer. November 1999.

PEER 1999/06 *Rocking Response and Overturning of Anchored Equipment under Seismic Excitations.* Nicos Makris and Jian Zhang. November 1999.

PEER 1999/05 *Seismic Evaluation of 550 kV Porcelain Transformer Bushings.* Amir S. Gilani, Andrew S. Whittaker, Gregory L. Fenves, and Eric Fujisaki. October 1999.

PEER 1999/04 *Adoption and Enforcement of Earthquake Risk-Reduction Measures.* Peter J. May, Raymond J. Burby, T. Jens Feeley, and Robert Wood.

PEER 1999/03 *Task 3 Characterization of Site Response General Site Categories*. Adrian Rodriguez-Marek, Jonathan D. Bray, and Norman Abrahamson. February 1999.

PEER 1999/02 *Capacity-Demand-Diagram Methods for Estimating Seismic Deformation of Inelastic Structures: SDF Systems*. Anil K. Chopra and Rakesh Goel. April 1999.

PEER 1999/01 *Interaction in Interconnected Electrical Substation Equipment Subjected to Earthquake Ground Motions.* Armen Der Kiureghian, Jerome L. Sackman, and Kee-Jeung Hong. February 1999.

PEER 1998/08 *Behavior and Failure Analysis of a Multiple-Frame Highway Bridge in the 1994 Northridge Earthquake.* Gregory L. Fenves and Michael Ellery. December 1998.

PEER 1998/07 *Empirical Evaluation of Inertial Soil-Structure Interaction Effects.* Jonathan P. Stewart, Raymond B. Seed, and Gregory L. Fenves. November 1998.

PEER 1998/06 *Effect of Damping Mechanisms on the Response of Seismic Isolated Structures.* Nicos Makris and Shih-Po Chang. November 1998.

PEER 1998/05 *Rocking Response and Overturning of Equipment under Horizontal Pulse-Type Motions.* Nicos Makris and Yiannis Roussos. October 1998.

PEER 1998/04 *Pacific Earthquake Engineering Research Invitational Workshop Proceedings, May 14–15, 1998: Defining the Links between Planning, Policy Analysis, Economics and Earthquake Engineering.* Mary Comerio and Peter Gordon. September 1998.

PEER 1998/03 *Repair/Upgrade Procedures for Welded Beam to Column Connections.* James C. Anderson and Xiaojing Duan. May 1998.

PEER 1998/02 *Seismic Evaluation of 196 kV Porcelain Transformer Bushings.* Amir S. Gilani, Juan W. Chavez, Gregory L. Fenves, and Andrew S. Whittaker. May 1998.

PEER 1998/01 *Seismic Performance of Well-Confined Concrete Bridge Columns.* Dawn E. Lehman and Jack P. Moehle. December 2000.